ABSTRACT

AMARAL, AMANDA FIGUEIREDO. The Pig as a Model to Study Vaccine Development for Genital *Chlamydia trachomatis* Infection in Women (Under the direction of Dr. Tobias Käser and Dr. Scott Laster)

C. trachomatis infections are the most frequently reported bacterial sexually transmitted disease in the world, with an estimated yearly number of 131 million new cases worldwide. Although infection can be easily treated, about 70-90% of the women infected with *C. trachomatis* remain asymptomatic, and therefore do not seek treatment. Untreated infection can then ascend to the upper genital tract and infect Fallopian tube epithelial cells and cause reproductive problems such as ectopic pregnancy and infertility. Therefore, a vaccine would be extremely beneficial to prevent *C. trachomatis* infections. Pigs are great animals to be used as research models for vaccine development due to their physiological and immunological similarities to human. Although the pig has being used as an animal model for genital chlamydia vaccine development, they are still under-utilized in both *in vivo* and *in vitro* studies on host-pathogen interactions. Thus, the aim of this dissertation was to optimize the use of outbred *C. suis* pre-exposed pigs as an animal model for genital *C. trachomatis* vaccine development research. In section III, we performed an in vivo proof-of-principle *C. suis* vaccination and challenge study in *C. suis* pre-exposed outbred pigs to study vaccine immunogenicity and efficacy. The vaccine candidates consisted of UV-inactivated *C. suis* particles in the presence or absence of an adjuvant (TriAdj) and was administrated intranasally. Both groups of vaccinated pigs had lower *C. suis* burden post challenge compared with non-vaccinated group. Additionally, specially the TriAdj group induced $CD4^+$ T-cell differentiation into both lymph node homing central memory T cells and tissue homing effector memory T cells. These results indicate that mucosa *C. suis* vaccination of pre-exposed pigs primes for a stronger IFN-γ response of CD4 T

cells, suggesting that a similar approach could be applied to human vaccine trials. In section IV, we performed *in vitro* studies with *C. trachomatis* and porcine oviduct epithelial cells (pOECs) to study the *C. trachomatis* life cycle, and the induced immune response. Our results indicate that, similar to what is observed in human genital tract cells, *C. trachomatis* completes its life cycle in pOECs within 48 hours and that infection induced an increased mRNA expression of the chemokines CXCL10, CXCL11, CCL20 and RANTES, and the interferon-regulated genes MX1, MX2 and CMPK2. These similarities support that primary pOECs represent an excellent cell culture model to study the pathogenesis and innate immune response of genital *C. trachomatis* infections. In section V, we used our *in vitro* model of pOECs and *C. trachomatis* to study potential mechanisms of pathogenesis. Since it is known that chlamydia infections can induce an alteration in expression of claudins (1-4) in epithelial cells and decrease cell barrier function, in this study, we hypothesized that the *C. trachomatis* infection leads to a decrease in claudin-4 expression in pOECs. Our results demonstrate that, while the *C. trachomatis* infection does not interfere with the overall claudin-4 RNA expression and protein production, the infection reduces the claudin-4 expression in the pOECs membrane; and this reduction in claudin-4 cell membrane expression is likely induced by the internalization of this protein to the *C. trachomatis* inclusion. This chlamydia-induced reduction of cell membrane claudin-4 expression can represent a relevant pathway by which *C. trachomatis* decreases the genital tract epithelial barrier function and, in turn, contribute to the increased susceptibility of *C. trachomatis* patients to HIV infection. These experiments collectively provide new knowledge to support the use of pigs for *in vivo* and *in vitro* research that can contribute to the vaccine development for genital *C. trachomatis* infection in women.

The Pig as a Model to Study Vaccine Development for Genital *Chlamydia trachomatis* Infection in Women

by
Amanda Figueiredo Amaral

A dissertation submitted to the Graduate Faculty of
North Carolina State University
in partial fulfillment of the
requirements for the degree of
Doctor of Philosophy

Comparative Biomedical Sciences

Raleigh, North Carolina

2020

APPROVED BY:

_____	_____
Dr. Tobias Käser Committee Co-Chair	Dr. Scott Laster Committee Co-Chair
_____	_____
Dr. Glen Almond	Dr. Jonathan Fogle
_____	
Dr. Judy Gookin	

DEDICATION

I dedicate this dissertation to my parents: Wilson (in memory) and Elisa Amaral. Thanks Dad, for being my guardian angel. Thanks Mom, for being the best Mom! You are my example of a person of courage, faith, and determination. Thanks for your constant support and encouragement, especially during my PhD. I love you both so very much!

(Dedication in Portuguese)

Eu dedico essa dissertação aos meus pais: Wilson (em memória) e Elisa Amaral. Obrigada pai, por ser meu anjo da guarda. Obrigada mãe, por ser a melhor mãe! A senhora é meu example de pessoa corajosa, de fé, e determinada. Obrigada pelo seu apoio e incentivo constante, especialmente durante meu doutorado. Eu amo muito vocês!

BIOGRAPHY

Amanda Figueiredo Amaral was born and raised in Guapé, Minas Gerais, Brazil. She graduated with a degree in Veterinary Science from Federal University of Lavras (Lavras, Minas Gerais, Brazil) in 2013. During vet school, Amanda had the opportunity to work at her university's swine group (NESUI) under the supervision of Dr. Vinicius Cantarelli. That was when she fell in love with pigs. Sponsored by a Brazilian educational program ("Sciences without borders"), she completed one year of internship at the Animal Science/USDA department at Purdue University (West Lafayette, IN, USA) under the supervision of the excellent scientist Dr. Marcos Rostagno. It was during this time that she had the opportunity to work with swine research and decided she would pursue the research path. After that, from 2014 to 2016, Amanda obtained her Master of Science in Swine production, Reproduction and Health from Federal University of Rio Grande do Sul (Porto Alegre, Rio Grande do Sul, Brazil) with Dr. David Barcellos and studied the antimicrobial resistance profiles of the porcine respiratory bacteria *Pasteurella multocida.* In 2017, Amanda was accepted into the Comparative Biomedical Sciences program at NCSU College of Veterinary Medicine with a concentration in immunology. She has been an associate member of the Comparative Medicine Institute since 2017 and of the American Association of Veterinary Immunologists since 2018.

ACKNOWLEDGMENTS

My adviser Dr. Käser: Toby, you are such an exceptional scientist! I am incredibly grateful for having you as my adviser. I cannot thank you enough for all the time you spent commenting my work, for your advice, guidance, and support. Thank you for all the opportunities you gave me and for letting me learn from my mistakes.

The members and former members of my lab, the Käser lab, especially Liz and Andy for their friendship and help with my experiments. I could not have done this PhD without you!

Dr. Glen Almond, you are an excellent professor! Thanks for all your support and for showing how much you care about me. You made my PhD so much better! I will miss talking with you.

My committee members: Dr. Glen Almond, Dr. Jonathan Fogle, Dr. Jody Gookin, Dr. Scott Laster. Thank you so much for accepting to be part of my PhD journey as my research advisers. I learned so much with each one of you! I also would like to thank Stephanie Ward, my graduate school representative, for being available for my committee meetings.

All the professors and their team members that helped me during my PhD: Dr. Toni Darville and Bryan Mcqueen (University of North Carolina at Chapel Hill - UNC), for sharing so much knowledge about chlamydia with me. I feel very privileged to have worked with you; Dr. Caroline Laplante and Kim Bellingham (NCSU), for their mentorship, support, and great confocal microscope pictures; Dr. John Gadsby (NCSU), for assisting me during pig's oviduct collections; Dr. Bernhard Kaltenboeck and Dr. Shamsur Rahman (Auburn University), for their support and for testing our serum samples; Dr. Piedrahita (NCSU), for showing me how important it is to make interdisciplinary collaborations throw the Comparative Medicine Institute; Dr. Gonzalez, Dr. Amy Stewart, and Cecilia Schaaf (NCSU), for their collaboration,

advice, and support; Dr. Crisci and Alba Frias (NCSU), for their help and support; Dr. Sam Jones (NCSU), for his mentorship and support.

My immunology journal club professors, especially Dr. Susan Tonkonogy, Dr. Scott Laster, Dr. Jonathan Fogle, Dr. Paul Hess, D. Jeffrey Yoder, and Dr. Crisci: Thank you all so much for teaching me immunology and for being my examples of great immunologist scientist to me.

Pig trial support group: Patty Routh, Laura Edwards, Dr. Juliana Bonin Ferreira, Abhilasha Jindal, Elizabeth Noblett, Bruno Muro, and Amanda Sautner. Thank you all so much for helping me during my pig animal trial. I could not have done it without you!

NCSU staff: Laboratory Animal Resources (LAR) and Teaching Animal Unit (TAU) teams for taking such a great care of the pigs; Jenny (Dr. Paul Hess lab), for all her help and support and for being THE best lab neighbor I could ever have asked for; Katie Sapko, for being so helpful and supportive; Javid Mohammed, for all his help with the flow cytometry; the necropsy team, especially Ryan Walker, for their outstanding support and help during necropsy; Fanta, for her smile and “Good mornings!”.

NCSU IMM journal club peers: Paige Nemec, Alix Berglund, Jessica Gilbertie, Kathryn Polkoff, Paul Cray, Stephanie Johnstone, David Brodsky, Drake Phelps, Rosemary Bayless. I learned so much from each one of them! Special thanks to Jocsa Cortes, for all her help and support.

Undergraduate students: Abhilasha Jindal, Jack Schultz, Anna Beam-Mitchell, Luisa Schmidt, Amber Hazzard, and Seth Kodikara. I am incredibly grateful for the opportunity to mentor them and for learning so much with each one of them!

City Packing Plant (Neese's Sausage) of Burlington, NC, USA, especially Cecil and the plant inspector, for allowing and assisting me with the collection of the pig's oviducts.

Dr. Käser, Dr. Glen Almond, North Carolina Translational and Clinical Sciences Institute (UNC), and Comparative Medicine Institute (NCSU), for providing funding to conduct my PhD research. I would also like to thank Dr. Käser for providing the funding for my salary and tuition during this PhD.

Dr. Volker Gerdts and Stacy Strom (VIDO-InterVac), for providing the TriAdj adjuvant for my pig trial. Pedro Alonso and TECNOVET S.L. - IMPORT-VET, for providing the gilt post cervical artificial insemination (PCAI) catheters for my pig trial. BEI Resources, for proving monoclonal antibodies for my research.

The pigs, for helping with the advance of science for us all, animals and humans. I am sincerely thankful for working with them.

My Fitzpatrick family: Annemarie, Larry, Jimmy, Marykate, Annie, Grandma Judy, and Aunt Zuzana. I feel so blessed to be part of this family! Thank you for all your prayers and encouragement during my PhD.

My Figueiredo Amaral family: my mom Elisa, for talking with me when I wanted to give up, for reminding me that God has a plan for me and that I need to trust Him; my sweet sister Juliana, for talking with me so many times over the phone during my walks and for encouraging me to keeping moving forward; my brother Diogo, my niece Maria Eduarda and my sister in law Talia, for reminding me the value of family and for showing me the farm I grow up: it brings me so many beautiful memories; all my aunts, ancles, and cousins, for encouraging me to pursue my dreams and for believing I could do my PhD.

Jonathan, my sweet husband. I could not have made to the end of this PhD without you. Thanks for always being there for me and for encouraging me on my decisions. I love you!

TABLE OF CONTENTS

LIST OF TABLES

II. BACKGROUND AND LITERATURE REVIEW

III. MUCOSAL VACCINATION WITH UV-INACTIVATED *CHLAMYDIA SUIS* IN PRE-EXPOSED OUTBRED PIGS DECREASES PATHOGEN LOAD AND INDUCES CD4 T-CELL MATURATION INTO IFN-γ^+ EFFECTOR MEMORY CELLS

IV. *CHLAMYDIA TRACHOMATIS* LIFE CYCLE AND INNATE IMMUNE RESPONSE DURING INFECTION IN PORCINE OVIDUCT EPITHELIAL CELLS

LIST OF FIGURES

I. INTRODUCTION

Chlamydia (C.) trachomatis infection is the most reported bacterial sexually transmitted disease (STD) in the world [1]. According to the latest USA Centers for Disease Control and Prevention STD surveillance report (year of 2018), there was a total of more than 1.7 million cases in the USA; in North Carolina alone, it was reported that there were more than 66 thousands cases [2]. Initial infection can lead to endocervical discharge and bleeding [3], which can be easily treated with antimicrobials such as azithromycin and doxycycline [4]. However, about 70-90% of the women infected with *C. trachomatis* remain asymptomatic, which contributes to why we see the majority of women not seeking treatment [5]. Untreated infection can reach the upper genital tract and infect Fallopian tube epithelial cells, leading to increased probability of ectopic pregnancy and infertility [6]. Furthermore, genital *C. trachomatis* infection in women does not prevent re-infection, and re-infection can still occur post-antimicrobial treatment [6]. In this context, a vaccine is a great alternative to prevent *C. trachomatis* infections.

Vaccines for chlamydia infection have been studied for more than 70 years [7]. The first studies were based on Pasteurian principles of isolation, inactivation and inoculation, and vaccine formulations [8]. After these initial studies, researchers focused on the study of chlamydia specific antigen candidates, tested in different animal models, such as the mice, non-human primates (NHPs), and pigs [8]. While no single animal model can perfectly mimic all of the host-pathogen interactions in genital chlamydia diseases in humans, understanding the advantages and disadvantages of each model will ensure their best use to drive chlamydia research including vaccine development.

The murine model is the most commonly used animal model to study genital chlamydia infection due to its various advantages, such as: low experiment costs, ease of handling, and

many knockout strains and laboratory reagents availability [9]. However, important differences between mice and humans limit its use as a translational animal model, especially regarding immune genes [5] and the mechanism of interferon gamma (IFN-γ) inhibitory effects on *C. trachomatis* [10-12]. Since IFN-γ is a key immune modulator in the response against *C. trachomatis*, this difference can limit the use of mice in *C. trachomatis* research [6]. NHPs mimic the genital chlamydia disease in humans most closely and therefore it is the best translational animal model. However, studies with these animals are expensive and involve ethical concerns, resulting in a limited use of this animal model in research [9]. Consequently, alternative animal models such as pigs started to be explored. Pigs are easier to handle and have less ethical concerns when compared with NHPs, and they are the natural host to *C. suis*, a close relative to *C. trachomatis* [13]. Additionally, compared to humans, the pig has a similar hormonal reproductive cycle, physiology, and immune system [14-16], making them a suitable translational animal model.

Although pigs have been used previously to study *C. trachomatis* vaccine development, this animal model can still be considered under-utilized in both *in vivo* and *in vitro* studies on host-pathogen interactions in *C. trachomatis*. Regarding *in vivo* studies, because *C. suis* is highly prevalent in outbred pig populations and the cross-reactivity between *C. suis* and *C. trachomatis*, outbred *C. suis* pre-exposed pigs can serve as a model to mimic a genetically diverse *C. trachomatis* pre-exposed human population used in phase III clinical trial. Therefore, due to the similarities between humans and pigs, a vaccine candidate that shows immunogenicity and efficacy in this *C. suis* pre-exposed animal model may also be immunogenic and efficacious in *C. trachomatis* pre-exposed humans. Furthermore, the little amount of *C. trachomatis in vitro* studies in pigs represents an under-utilization of another advantage of pigs: The vast access to

porcine genital tract tissue enables the isolation of a plethora of porcine oviduct epithelial cells (pOECs) – the counterparts of human Fallopian tube epithelial cells and the main target cell of *C. trachomatis*. The pig is used as a food animal and genital tracts are by-products of meat production. Therefore, these tissues can be collected at slaughterhouses for nearly no cost, and without the need to sacrifice the animals for research, which is a great advantage according to the 3R principle: replacement, refinement, and reduction [17].

The overall purpose of this PhD project was to optimize the outbred *C. suis* pre-exposed pig model of human genital *C. trachomatis* infection and we did that by: i) performing an *in vivo* proof-of-principle *C. suis* vaccination and challenge study in *C. suis* pre-exposed outbred pigs to study vaccine immunogenicity and efficacy (section III); ii) performing *in vitro* studies with *C. trachomatis* and pOECs to study a) the *C. trachomatis* life cycle and the induced immune response (section IV), and b) a potential mechanisms of pathogenesis – the *C. trachomatis* induced downregulation of the tight junction protein claudin-4 (section V).

II. BACKGROUND AND LITERATURE REVIEW

1. *Chlamydia trachomatis* and its life cycle

C. trachomatis is an obligate intracellular Gram-negative bacterium that has a spherical or ovoid shape and is a member of the *Chlamydiaceae* family and *Chlamydia* genus [13]. This bacterium has different serological variants (serovars), and each serovar has different clinical manifestations, as described in Table 1 [4,18].

Table 1. *Chlamydia trachomatis* serovars and their associated diseases in humans. Table modified from [18].

Serovars	**Human disease**	**Method of spread**	**Pathology**
A, B, Ba and C	Ocular trachoma	Hand to eye, fomites, and eye-seeking flies	Conjunctivitis and conjunctival/corneal scarring
D, Da, E, F, G, H, I, Ia, J, Ja and K	Urogenital disease	Sexual and perinatal	Cervicitis, urethritis, endometritis, pelvic inflammatory disease, tubal infertility, ectopic pregnancy, neonatal conjunctivitis, and infant pneumonia
L1, L2 and L3	Lymphogranuloma venereum	Sexual	Submucosa and lymph-node invasion, with necrotizing granulomas and fibrosis

Chlamydia's membrane is composed mainly by lipopolysaccharides (LPS) and several proteins such as polymorphic membrane proteins (Pmps) and major outer membrane protein (MOMP) [19-21]. Many of these membrane components are highly immunogenic and serve as

targets for vaccine antigens [22,23]. *C. trachomatis* does not produce tryptophan, and since this amino acid is essential for this bacteria, chlamydia has to obtain it from the host [18]. This dependency on tryptophan explains the high sensitivity of C. trachomatis for interferon-γ (IFN-γ): IFN-γ can downregulate the cell-intrinsic tryptophan concentrations; this capacity makes it one of the most potent immune molecules in the anti-*C. trachomatis* response [18]. This response will be discussed in the innate immune response section.

This bacterium has a biphasic developmental cycle with two distinct forms: the extracellular infectious elementary bodies (EBs), and the intracellular non-infectious reticulate bodies (RBs) [13,18]. The *C. trachomatis* developmental cycle has been well-described in mice [24,25] and humans cells [26-30] and it has been nicely summarized over the years [18,31-33]: the cycle starts when EBs attach and invade their target cells – mainly columnar epithelial cells [18]. EBs first bind to heparin sulfate proteoglycans on cells and then interact with their cell surface receptors [33]. It has been demonstrated for example that *C. trachomatis* serovar D binds to ephrin type A receptor 2 (EphA2) in Hela cells [34]. Within the first 2 hours following internalization into the cells, EBs form intracytoplasmic inclusions (Figure 1). Between 2 and 6 hours post-internalization, EBs within the inclusion begin to differentiate into RBs. By 12 hours post-infection (hpi), RBs can be observed dividing by binary fission, and between 18 and 24 hpi, they peak in numbers. After 24 to 48 hours, non-infectious RBs convert back to metabolically inactive, infectious EBs, which are released by lysis or extrusion [35] around 48 to 72 hpi [32].

Figure 1. *Chlamydia trachomatis* infection in porcine oviduct epithelial cells. Transmission electronic microscope image showing intracellular chlamydia inclusions (black arrows).

2. The role of claudin-4 in genital chlamydia infection

Epithelial cells provide a physical barrier between the inside and the outside of the body, contributing to the protection against pathogens [36]. In the genital tract, epithelial cells are essential to prevent pathogens inducing STD, such as chlamydia, from entering the host [36]. These cells adhere to each other at their lateral membranes by intercellular junctions such as the tight junction [37]. Tight junctions are composed by a complex of proteins, including claudins, which play a key role in the permeability of epithelial cells [38].

In vitro studies have shown that chlamydia infection can alter tight junction formation and disturb epithelial integrity. For example, Prozialeck et al [39] showed that infection of primary

human cervical epithelial cells with *C. trachomatis* disturbed cell-cell contact, as indicated by a marked loss of cell membrane N-cadherin protein, a component of the adherens intercellular junctions in epithelial cells [37]. Furthermore, *Chlamydia muridarum* infection was shown to alter the composition of tight junction proteins such as claudins 1-4 in mouse oviduct epithelial cells [40]. It has also been demonstrated that *C. trachomatis* can decrease claudin-4 RNA expression in human uterine epithelial cell line and that this decrease in tight junction protein expression is associated with a decrease in the barrier function of tight junction, as demonstrated by a decrease in transepithelial electrical resistance [41].

Moreover, studies have shown that chlamydia infections are associated with an increased HIV shedding in the female reproductive tract and may facilitate HIV transmission [42-45]. It is not fully understood how chlamydia infection can lead to this increase in HIV infection. A possible mechanism of pathogenesis of chlamydia that could contribute to the increased susceptibility of *C. trachomatis* patients to HIV infection will be explored in section v of this dissertation.

3. Genital *Chlamydia trachomatis* epidemiology, pathogenesis, and treatment in women

C. trachomatis infections are the most frequently reported bacterial sexually transmitted disease in the world, with an estimated yearly number of 131 million new cases worldwide [1]. In addition, according to the latest USA Centers for Disease Control and Prevention sexually transmitted disease (STD) surveillance report (2018), there was a total of 1,758,668 cases (about 540 cases per 100,000 people) reported in the USA, with North Carolina alone reporting a total of 66,553 cases (about 648 cases per 100,000 people) [2]. *C. trachomatis* genital infection is most common among young people and it has been estimated that, in the United States, 1 in 20 sexually active 14 to 24 years old women have chlamydia [46].

C. trachomatis EBs initially infect the columnar epithelial cells of cervix [3]. This initial infection can lead to symptoms of cervicitis such as mucopurulent endocervical discharge and induced endocervical bleeding [3]. Although there is missing information on the timing of infection acquisition and *C. trachomatis* strain identification, studies have reported that about half of the uncomplicated and untreated genital *C. trachomatis* infections resolve in ~1 year after initial chlamydia testing [47,48]. However, *C. trachomatis* genital infection can also ascend from the cervix to the uterus and the Fallopian tubes, causing chronic complications such as pelvic inflammatory disease and Fallopian tube inflammation (salpingitis) [6,18].

This inflammation of the Fallopian tubes can cause scarring and occlusion, which leads to infertility or ectopic pregnancy [6]. Even though the mechanism of chlamydia pathogenesis is not completely understood [6], a "cellular paradigm" hypothesis has been presented [49]. According to this hypothesis, the host response against chlamydia is initiated and sustained by *C. trachomatis* infected epithelial cells. These cells release matrix metalloproteases (MMPs), which are involved with both: i) facilitation of immune response, by increasing lymphocyte adhesion in the tissue [50], and ii) tissue damage, by lysing the extracellular matrix [6]. Infected cells also release cytokines and chemokines that recruit inflammatory cells; while these immune modulators are crucial in the response against *C. trachomatis*, they also induce more infiltration of immune cells such as neutrophils that produce MMPs, leading to tissue damage and thereby driving immunopathology [51].

C. trachomatis genital infection can be treated with antibiotics such as azithromycin and doxycycline [5] and some high-income countries have created screening programs to diagnose and treat chlamydia. However, about 70 to 90% of infected women remain asymptomatic, and

therefore do not seek treatment [5]; and screening programs are costly and difficult to bring to scale [52].

In conclusion, genital chlamydia infection remains a problem worldwide, including in the USA. Therefore, it is essential to keep investing in the development of an effective chlamydia vaccine that induces a protective immune response against *C. trachomatis.*

4. Immune response against *Chlamydia trachomatis* infection in the female genital tract

4.1. Innate immune response

The epithelial cells in the female genital tract with their interconnecting tight junctions play an important role in the innate immune protection against chlamydia by providing a strong physical barrier and by recruiting immune cells to the site of infection [53]. These immune cells can be recruited by epithelial cells after sensing pathogens using pattern recognition receptors (PRRs), such as Toll-like receptors (TLRs), including TLR2 and TLR4 [54,55]; PRRs will recognize pathogen-associated molecular patterns (PAMPs) on the surface of pathogens such as chlamydia EBs. Thereafter, the innate immune machinery in epithelial cells is activated.

The recognition of chlamydia PAMPs by PRRs in cervical epithelial cells initiates the release of proinflammatory cytokines, such as interleukin-1 (IL-1), IL-6, IL-8, and tumor necrosis factor (TNF) [56-58]; these cytokines will then induce an increase of vascular permeability and the expression of VCAM-1 on endothelial cells [57]. This increased permeability facilitates the infiltration of immune cells into the infected genital tract. Epithelial cells will also produce chemokines, such as CCL20, CCL5 (also known as RANTES), CXCL10, and CXCL11, which can then attract immune cells, including neutrophils, natural killer (NK) cells, dendritic cells (DCs), macrophages, and T cells. Together, the increased permeability of

the blood vessels and the produced chemokines will induce an influx of immune cells to the submucosa of the site of infection, called immune inductive sites [18].

Neutrophils and NK cells are the first cells recruited to the site of chlamydial infection [5]; they can also recognize chlamydia PAMPs via their PRRs. Neutrophils are recruited in large numbers and are capable of phagocytizing and killing accessible EBs at the site of infection [6]. NK cells can control the chlamydia infection in two ways: i) by killing infected cells via the release of perforin and granzymes, ii) by producing IFN-γ, which can control chlamydial growth by altering the availability of tryptophan, an essential amino acid for chlamydia [18,59,60]. *In vitro* studies show that human IFN-γ induces the production of indoleamine-2,3-dioxygenase 1 (IDO1), an enzyme that degrades tryptophan, resulting in the inhibition of chlamydia growth by tryptophan starvation [59]. As a result, chlamydia may die, and the infection is cleared; alternatively, the RBs may enter into a persistent state, slowing down the infection [18].

Antigen presenting cells (APCs), such as epithelial cells and DCs, also express PRRs, which recognize PAMPs, process the bacteria and present their antigens via their major histocompatibility complex class I (MHC-I) to $CD8^+$ T cells and via MHC-II to $CD4^+$ T cells [61]. Because the majority of chlamydia proteins are located inside an inclusion, they are considered exogenous and, therefore, will be typically processed for recognition via MHC-II (expressed in DCs and epithelial cells) by $CD4^+$ T cells [61,62]. However, there are some exceptions. For example, DCs can do cross-presentation and present exogenous antigens via MHC-I to $CD8^+$ T cells [61]. In fact, it has been demonstrated that DCs pulsed with heat-killed *C. muridarum* and adoptively transferred to mice induced chlamydia-specific $CD4^+$ T cell immune response and protection against chlamydia infection [63]. In addition, during chlamydia replication in epithelial cells there appears to be a limited subset of chlamydia proteins that do

have access to the cytoplasm, subjecting them to recognition by CD8+ T cells [64]. These include membrane proteins that lie at the interface between the *Chlamydia* vacuole and the host cytosol, such as Cap1 and CrpA [65].

In conclusion, innate immune cells are the first responders to chlamydia infection and play an important role in controlling the infection by killing both chlamydia EBs and infected epithelial cells. Additionally, innate cells not only produce cytokines and chemokines that attract adaptative cells, but they can process and present chlamydia antigens to these adaptative cells.

4.2. T cells

The role of T cells in chlamydia genital infection immunity was first demonstrated when Rank et al. showed that athymic nude mice developed a chronic *C. muridarum* genital infection [66]. Afterwards, studies have demonstrated a role for different T cells, especially $CD8^+$ T cells, and $CD4^+$ T cells.

Activation of naïve $CD8^+$ T cells occurs in lymph nodes upon cross-presentation of chlamydial antigens by DCs via MHC-I [61]. Activated $CD8^+$ T cells, also known as cytotoxic T cells (CTL), can then migrate to the infected genital tract tissue and kill *C. trachomatis* infected epithelial cells. This killing involves the release of two types of preformed cytotoxic proteins – granzymes and the pore-forming protein perforin [64]. Studies in animal models support the role of $CD8^+$ T cells during chlamydia infection. For instance, studies in mice have demonstrated that *C. trachomatis*-specific $CD8^+$ T-cell are partially protective when adoptively transferred into *C. trachomatis* infected mice [67].

$CD4^+$ T cells play a predominant role in the protective immunity against chlamydia infections. As for CD8 T cells, naïve CD4+ T cells are activated in the lymph nodes after antigen

presentation by DCs – but this time via MHC-II- [61]. Activated $CD4^+$ T cells will then proliferate and differentiate to lymph node tracking central memory (T_{CM}) and tissue-tracking effector memory (T_{EM}) T cells, which goes to the site of infection and produce mainly INF-γ. This cytokine has been demonstrated to be of extreme importance against chlamydia infections [18,68]. While NK cells are the main IFN-γ responders in the early anti-*C. trachomatis* response, $CD4^+$ T cells are the main IFN-γ producers of the later, the adaptive immune response.

The importance of $CD4^+$ T cells in the immune response against chlamydia has been demonstrated in multiple studies. For example, studies in mice demonstrate that the immune inductive sites formed after genital chlamydia infection contain mainly $CD4^+$ T cells [69]. Furthermore, mice deficient in CD4 and MHC-II have shown to fail to resolve *C. trachomatis* infection [70]. The importance of $CD4^+$ T cells was recently confirmed in swine: The porcine T cell-mediated immune response to *C. trachomatis* mainly consisted of IFN-γ producing $CD4^+$ T cells [71].

Further highlighting the importance of IFN-γ producing $CD4^+$ T cells, it has also been demonstrated that IFN-γ receptor deficient mice exhibited an increase in bacterial shedding and a delay in clearance of infection compared with wild type mice [72]. Additionally, Helble et al. [73] recently showed that, although the production of IFN-γ by these cells are dispensable for T cell homing, IFN-γ producing $CD4^+$ T cells are required for chlamydia clearance in the murine genital tract.

Activated $CD4^+$ T cells can also become memory T cells, which are essential for protection against reinfection. In the case of chlamydia infections, *C. trachomatis*-specific memory $CD4^+$ T cells have been shown to be essential for protection against secondary chlamydia genital infection. For instance, it has been shown that the induction of two subsets of

IFN-γ producing $CD4^+$ T cells is crucial for protection against *C. trachomatis*: tissue-resident memory T cells (T_{RM}) and circulating memory T cells consisting of both lymph node tracking central memory (T_{CM}) and tissue-tracking effector memory (T_{EM}) T cells [74].

4.3. B cells and immunoglobulins

The role of B cells, plasma cells and immunoglobulins (Igs, also known as antibodies) is controversially discussed: While some studies reported a critical role for antibodies in the anti-*C. trachomatis* response and protection [75,76], other results indicate that antibody levels do not influence the disease outcome of *C. trachomatis* infections [77].

The role of antibodies against chlamydia infection have been demonstrated by many studies. For example, Morrison et al. demonstrated that mice that lack B cells and are depleted of $CD4^+$ T cells appear to be unable to control *C. trachomatis* secondary infection [78]. The same authors later showed that this B cell mediated immune protection is due to antibodies by performing a passive serum transfer into B cell deficient and $CD4^+$ T cell depleted mice: The transferred antibodies provided protective immunity to reinfection [79]. Moreover, Rank and Batteiger [80] showed that passive transfer of serum from previously infected animals significantly reduce bacterial shedding from the genital tract of naïve guinea pigs, demonstrating the role of antibodies in the chlamydia immune response [80]. In addition to serum-derived antibodies, mucosal antibodies, such as IgA and IgG, have also shown to play a role in the protection against chlamydia infection. For instance, it is known in women that cervical secretory IgA (sIgA) is inversely correlated with cervical chlamydia load [81]. It also has been demonstrated in mice that genital IgA is associated with protection against genital *C. muridarum* infection and pathology [82]. Studies in minipigs also show that infiltration of IgA^+ and IgG^+

plasma cells into the lower genital tract are associated with protection against genital chlamydia infection [75]. Additionally, the increase in the vaginal secretory IgA has been associated with the decrease in chlamydia load in the minipig model [76].

However, epidemiological studies in women indicate that *C. trachomatis*-specific serum antibody titers does not seem to correlate with infection resolution; on the contrary, it seems to correlate with increased severity of genital tract sequels, such as Fallopian tube damage [77]. Darville et al, 2019 also showed that although anti-chlamydia IgG and IgA correlates with reduction of cervical chlamydia burden, anti-chlamydia IgG are associated with increased risk of infection.

There are different possible mechanisms by which antibodies contribute to chlamydia protection, such as opsonization and neutralization. During opsonization, after binding to pathogens, the antibody's Fc region can bind to Fc receptors on immune cells such as neutrophils, helping these cells to ingest and kill the pathogen [83]. Antibodies can also bind to chlamydia EBs and inhibit their infection of epithelial cells, a process called neutralization [83]. For instance, mice lacking Fc receptors had more severe *C. muridarum* secondary infection compared with the wild mice, indicating that B cells and antibodies can contribute to the increase of protective response [84]. It has also been demonstrated *in vitro* that *C. trachomatis* MOMP-specific murine monoclonal antibodies can neutralize *C. trachomatis* [85].

In conclusion, B cells, plasma cells and antibodies are involved in the chlamydia response. The importance of these cells, however, is still controversial, and more studies in animal models and epidemiological analysis are necessary to understand their full contribution to chlamydia protection.

In summary, $CD4^+$ T cells, $CD8^+$ T cells and potentially B cells make effective contributions to the host defense against genital chlamydia infections: $CD4^+$ T cells are essential because they are necessary for B cell activation and are the main producers of IFN-γ, which induce chlamydia death due tryptophan starvation; $CD8^+$ T cells can kill infected cells and therefore control the spread of chlamydia; plasma cells can produce antibodies that eliminate EBs on the mucosa, which contributes to the decrease of chlamydia infection and the spread of chlamydia to other epithelial cells.

4.4. The effect of hormones in the immune response against chlamydia

It has been demonstrated that *C. trachomatis* infection and immune response can be influenced by the sexual hormones estrogen and progesterone [86,87]. Overall, *in vivo* studies show that, under the influence of estrogen, there is an increase in chlamydia infection in the genital tract [16]. For instance, mice inoculated with *C. muridarum* during estrus or under estrogen supplementation are in general more resistant to infection [18,87]. Additionally, Lorenzen et al. [88] showed that intrauterine inoculation with *C. trachomatis* in pigs during diestrus (progesterone dominant reproductive phase) resulted in a longer lasting infection (at least 10 days) compared to when inoculation was performed during estrus (estrogen predominant reproductive phase) (3 to 5 days). These findings are in line with earlier observations in pigs inoculated with *E. coli*: animals that received *E. coli* intrauterine inoculation during metestrus (progesterone dominant reproductive phase) had an acute purulent endometritis, while animals that were in estrus did not [89].

These results could be explained, at least in part, by the fact that the innate immune response is more active during estrogen predominant reproductive phase, as demonstrated by a

higher number of neutrophils in the endometrium of pigs after intrauterine inoculation with *C. trachomatis* during estrus [16]. Additionally, studies in mice show that progesterone affects primary human DCs by decreasing expression of CD80, CD86 and CD40 and therefore inhibited DCs ability to activate naïve T cells *in vitro* [90]. Furthermore, mice receiving progesterone and infected intranasally with *C. trachomatis* had significant fewer CD40-expression DCs in their cervical lymph nodes and were not able to clear infection from lungs compared with mice that did not received progesterone [90].

In conclusion, sex hormones can influence chlamydia infection by regulating both innate and adaptative immune response. Therefore, it is important to consider the role of sex hormones in the susceptibility to chlamydia infection and in the immune response analysis.

5. Animal models to study vaccine development for genital *Chlamydia trachomatis* infection in women

While emergency vaccines such as Ebola vaccine can be approved withing 5 years [91], vaccine development take many steps and in average over 10 years to complete [92]. These steps can be grouped into three main phases – preclinical, clinical (clinical phases I-III), and post-licensure (also known as phase IV). The preclinical stage includes the identification of vaccine candidates and *in vitro* and *in vivo* studies using animal models to assess parameters such as vaccine safety, formulation and dose, route of delivery, immunogenicity and efficacy [93].

Animal models are, therefore, an essential part of vaccine development and, because no single animal model can provide all necessary information for the development of a vaccine, it is important to identify the most appropriate animal for the study of specific aspects of a diseases.

Although multiple animal models have been developed to study genital *C. trachomatis* vaccine, this bibliography review will focus on the main relevant advantages and disadvantages of the mouse, non-human primate (NHP) and pig animal models.

5.1. Mouse

One of the main advantages of the mouse model are the low cost, small size, and simple handling [5,9]. Furthermore, besides the availability of many well-characterized inbred and knockout mouse strains, there are many commercially available laboratory's reagents for mouse, making this animal an attractive model [5,9]. Consequently, the mouse model is the most frequently used animal model for chlamydia vaccine studies, which reflects on the number of current chlamydia vaccine candidates studied in mice (Table 2).

Many genital chlamydia studies using the mouse model have been done over the years. For instance, in 2015, Karunakaran et al. [94] demonstrated that the chlamydia vaccine consisting of chlamydial Pmps and MOMP + adjuvant dimethyl dioctadecyl ammonium and monophosphoryl lipid A (DDA/MLP) significantly accelerates the clearance of *C. trachomatis* in the mouse genital tract. Although the authors did not investigate the induction of IFN-γ producing $CD4^+$ T cells, this acceleration on chlamydia clearance could be explained not only by the selection of molecularly defined and immunogenic antigens, but also by the use of an adjuvant known to induce a high frequency of IFN-γ producing $CD4^+$ T cells [94,95]. The mouse model was also used for possibly one of the most promising *C. trachomatis* vaccination studies. Stary et al. showed in 2015 [74] that mucosal administration of ultraviolet-inactivated *C. trachomatis* combined with charge-switching synthetic adjuvant particles (cSAP) resulted in long-lived protection against genital *C. trachomatis* challenge. In addition, as mentioned in the

previous T-cell section, the authors demonstrated that the induction of T_{RM}, $T_{CM,}$ and T_{EM} IFN-γ producing $CD4^+$ T cells are crucial for protection against *C. trachomatis* [74].

Furthermore, a strong chlamydia research group in Denmark [22,23,96] has contributed significantly to the development of a genital chlamydia vaccine using the pig and the mouse animal models (Table 2). Using the mouse model, they first demonstrated that chlamydia variable domain 4 of MOMP (MOMP-VD4) based vaccine adjuvanted with dimethyl dioctadecyl ammonium and trehalose-6,6-dibehenate (DDA/TDB) induce protection against *C. trachomatis* infection and upper genital tract pathology via stimulation of serum neutralizing antibodies [22,23]. More recently, this same research group [97] showed that protection against *C. trachomatis* genital infection in mice immunized with *C. trachomatis* vaccine formulated with CAF01 adjuvant was associated with tissue-resident memory $CD4^+$ T cell infiltration into the uterus [97]. The vaccine adjuvant DDA/TDB, also known as CAF01, is also known to induce a high frequency of IFN-γ producing $CD4^+$ T cells [94,95].

However, the mouse model also has some limitations. Different from women, the murine reproductive cycle is only 4-5 days [98], which will reflect in the hormone levels and therefore and immune response against chlamydia. Regarding the immune system cells, the composition of circulating leukocytes is different, with lower proportion of neutrophils and higher percentage of lymphocytes in mice, compared with pigs and humans [99,100]. Furthermore, a high number of 185 immune genes are not shared with humans [101] and the inhibitory effects of IFN-γ on *C. trachomatis* differ in humans and mice: in contrast with human, upon *in vitro* LPS and IFN-γ stimulation, murine cells produce iNOS, but not IDO [10-12]. All together, these difference can impair the use of mice for *C. trachomatis* research [11].

Table 2. Current *Chlamydia trachomatis* vaccine candidates. Table modified from [52,102].

Candidate name/identifier (sponsor)	**Pre-clinical trial/animal model**	**Phase I**	**Reference**
MOMP + Pmps (Pan-Provincial Vaccine Enterprise Inc. and British Columbia CDC)	Mouse		[94]
MOMP-VD4 (Statens Serum Institut)	Mouse		[22,23]
UV-killed *C. trachomatis* (Selecta Biosciences)	Mouse		[74]
MOMP-VD4 (Statens Serum Institut)	Pig		[96]
Live attenuated (plasmid-deficient) trachoma vaccine (NIH/NIAID)	NHP		[103]
MOMP-VD4 (Statens Serum Institut)		x	[104]

MOMP: major outer membrane protein; Pmps: polymorphic membrane proteins; MOMP-VD4: variable domain 4 (VD4) of MOMP; UV: ultraviolet; NIH: National Institutes of Health; NIAID: National Institute of Allergy and Infectious Diseases, NHP: non-human primate.

5.2. Non-human primate

NHPs are physiologically and genetically more similar to humans compared with mice, and it is a great animal model for chlamydia vaccine because it mimics the human disease the most [5,9,105]. Furthermore, NHPs reproductive cycle lasts for about 28-33 days [106-108], and, as

for women, they have a single ovulation per cycle [106,107]. When comparing anatomy, NHPs and humans show a similar overall conformation of the genital tract [109]. In addition, similar to what is observed in women, NHPs' endocervix and upper genital tract are formed by columnar epithelium (chlamydia target cells) [110]. The immune system components in NHPs and humans have shown to be very similar, especially the B cell dynamic and T cell composition [111]. Importantly for the chlamydia infection, NHPs also have the IDO/tryptophan pathway as observed in human cells [112,113].

Different NHPs species have been used to study genital *C. trachomatis* infection: chimpanzees, marmosets, macaques, grivets, and baboons [9,114]. But the most frequently used is the macaque, like pig-tailed macaque (*M. nemestrima*), rhesus macaques (*Macaca mulatta*), and cynomolgus macaques (*M. fascicularis*) [9,114]. The pig-tailed macaque model developed by Patton et al. [115] greatly contributed to our current knowledge on chlamydia genital infection. This model established a lower genital tract (vagina and cervix) chlamydia inoculation that resembles the establishment of human genital infection: absent to mild inflammatory responses, such as vaginal/cervical mucosa erythema/edema and vaginal discharge [114]. Furthermore, repeated direct inoculations of oviducts have induced salpingitis with tubal scarring and tubal obstructions [9], as observed in women following chronic genital infections and pelvic inflammatory disease [116]. These inoculations induce an increase in Th1 cytokines and both local and systemic antibodies. Furthermore, histological evaluations show signs of fibrosis and mononuclear cell infiltration [9]. Hence, experimental inoculations of macaques with *C. trachomatis* produce similar clinical symptoms as observed in women, varying from none to mild erythema to severe tubal obstructions.

Although the first chlamydia vaccine animal trials in NHPs using whole chlamydia particles demonstrated limited protection [7], recent whole cell antigen vaccines have shown promising results and it is listed as a current chlamydia vaccine candidate (Table 2). For example, Kari et al. [103,117] showed that ocular vaccination of cynomolgus macaques with plasmid deficient strain of *C. trachomatis* induces an increase in serum IgG, IgA, and antibody neutralization, as well as increase in IFN-γ production by PBMC. More importantly, the authors showed that five out of six animals demonstrated to be protected against chlamydia reinfection after vaccination [103,117].

Although NHPs have been proved to be a great animal model, they are much more expensive than mice, need special facilities and trained personal, and have high ethical issues [5,9,105]. These limitations have limited the use of NHPs in *C. trachomatis* vaccine development and lead researchers to explore the use of alternative animal models such as pigs.

5.3. Pig

The pig is a suitable animal model to study genital chlamydia vaccine development for many reasons: i) Pigs are the natural host for *C. suis*, which is very similar to *C. trachomatis*, highly prevalent in pig herds [13,118], and associated with reproductive disorders in sows [119]; ii) pigs are outbred animals and therefore more representative of human population heterogeneity, allowing for a more accurate assessment of vaccine efficacy [14]; iii) compared with mice, pigs are physiologically more similar to humans and provide more samples (e.g. blood and tissue) [14,16]; iv) in contrast with NHPs, pigs are widely available, are more affordable, and have more general public acceptance for their use in experiments [105]. Other pig's advantages, as well as limitations, relevant for the genital chlamydia vaccine development will be discussed below.

Regarding the reproductive cycle parameters, both pigs and women have spontaneous ovulations and continuous reproductive cycles [16]. The reproductive cycle length in pigs and women is slightly different: while in women the follicular and luteal phases are more rigorously separated and lasts about 28 days, porcine follicle growth occurs during luteal phase, which results in a shorter cycle of about 19-21 days [16]. But apart from these differences, the reproductive cycle hormonal fluctuations are similar between sows and women.

Regarding the reproductive tract anatomy, the cervix of pigs contains an anatomic structure, not found in women, called cervical pulvini, made of interdigitating prominent solid mucosal folds throughout the porcine cervix [120]. Therefore, transcervical inoculation of chlamydia and vaccine is easier done during estrus, when the cervical canal is open and allows catheterization [105]. Different from woman, the porcine uterus is bicornuate and elongated, creating a longer distance between the porcine vagina and the oviducts (the counterpart of Fallopian tubes in woman) [16]. Although this longer distance can represent an obstacle for the chlamydia to ascend to the oviducts, a study done in pigs have demonstrated that after intravaginal inoculation with *C. trachomatis*, pigs showed an ascending infection with chlamydia replication on oviducts [121]. Pigs have human-like, prominent, Fallopian tubes [16,120], making them an attractive animal to study chlamydia infection in this organ. Furthermore, in both women and pigs, simple columnar epithelial cells (the chlamydia cell target) are found in uterus and Fallopian tubes/oviducts epithelium [16,122] [122,123].

In terms of immunology, the pig immune system is well characterized and, overall, similar to that of humans [14]. For instance, compared with mice, pigs have more immunological genes shared with humans (230 genes) and have 4.5 times fewer genes (41 genes) which are not shared with humans [101]. One of the main immunological differences between pigs and humans

is the higher infiltration of neutrophils into uterine mucosa during estrus in pigs compared with humans [16], which should be considered for the development of inoculation and/or vaccine administration strategy. Furthermore, besides the fact pigs have a higher proportion of $CD4^+CD8^+$ double positive cells and γδ T cells in blood [124], the distribution of the other blood lymphocytes is similar between pigs and humans [16]. Important for the study of the immune response against chlamydia in the pig model, the immunological toolbox to investigate chlamydia infections in pigs has increased in the last years [14,71,105,125,126]. Käser et al. [71] provided a detailed view of the porcine T-cell immune response to *C. suis* and *C. trachomatis*: as in humans, pigs develop a strong $CD4^+$ T-cell response upon *C. trachomatis* or Cs infection consisting of mainly IFN-γ- single or IFN-γ/TNF- double-cytokine producing $CD4^+$ T cells; this response was heterologous, thus, *C. suis* infected pigs responded to *C. trachomatis* and vice versa. Additionally, there are indications that the IFN-γ /tryptophan pathway in pigs is similar to the one in humans: It has been shown that lipopolysaccharide (LPS) stimulation of pig blood cells induces indoleamine 2,3-dioxygenase (IDO) protein expression and activation, as characterized by an increase of tryptophan metabolites [127].

The pig has been used as an animal model for genital chlamydia infection and vaccine development since 2005, when Varompay et. [121] established the pig as model for genital *C. trachomatis* infection. In this study, the authors showed that the pig is susceptible to the human *C. trachomatis*. After that, as mentioned in the previous mouse model section, a strong chlamydia research group in Denmark has contributed significantly to the development of a genital chlamydia vaccine using the pig, and the mouse animal models. They first validated the use of pigs to study chlamydia infection by performing four *C. trachomatis/C. suis* studies in sexually mature conventionally bred female pigs. In their first study, the authors validated the pig

as a model for *C. trachomatis* genital challenge and for testing recombinant protein vaccines by showing that the pigs could be infected with *C. trachomatis* via vaginal inoculation [128]. In their second and third studies, the authors aimed to evaluate the protective role of a DNA vaccine based on the MOMP protein against genital *C. trachomatis* infection [129,130]. They found that, although pigs immunized with the DNA vaccine has significant less macroscopic legions and chlamydia replication in the genital tract compared with mock-vaccinated pigs, infection was not completely cleared. Finally, in their fourth study, it was demonstrated that pigs can also be infected with *C. suis* and elucidate humoral and cellular immune response [131], demonstrating that both *C. trachomatis* and *C. suis* can be used in the study of chlamydia vaccine in pigs.

This same group of Danish researchers also investigated chlamydia infection and vaccines using sexually mature female Göttingen minipigs. Lorenzen et al. [76] first demonstrated that intramuscular (systemic) priming and intranasal (mucosal) boosting induce strong genital immunity through secretory IgA in minipigs infected with *C. trachomatis.* This genital IgA response induced after animals received intra-nasal vaccine demonstrated the existence of the nasal-genital immunization route in pigs [76]. Two years later, Lorenzen et al. [88] demonstrated that intrauterine inoculation with *C. trachomatis* during diestrus establishes a longer infection compared to vaginal inoculation during estrus. Next, it was demonstrated that genital chlamydia infection induced an increase in neutrophils and plasma cells infiltration within the sub-epithelial stroma of the vagina [132]. Boje et al. [96] then showed that chlamydia MOMP-VD4 vaccine administered intramuscularly that induced serum neutralizing antibodies and IFN-γ responses was able to protect against a genital infection in minipigs. This study is listed as one of the current chlamydia vaccine candidates in Table 2. In their last study, these Danish researchers showed that protection against *C. trachomatis* genital infection in minipigs

intramuscularly immunized with UV-inactivated *C. trachomatis* vaccine formulated with CAF01 adjuvant was associated with cervical infiltration of $CD4^+$ T cells and tissue-resident memory $CD4^+$ T cell infiltration into the uterus [75].

In summary, as shown in Table 3, each animal model has its advantages as well as its limitations. The mouse is a great animal model, but they are not a great translational model. Therefore, it is important to verify murine results in an animal model that resemble more humans. NHPs offer the closest resemblance to humans, but they have some limitations that prevent their utilization in large scale: they are expensive and have high ethical concerns. In this context, pigs are a great alternative animal model, since they are less expensive, had less ethical concerns than NHPs, and are physiologically, immunologically, and genetically more similar to humans than mice. Therefore, pigs are an excellent animal model for the evaluation of genital *C. trachomatis* vaccine parameters such as efficacy and immunogenicity.

Table 3. Advantages (PRO) and disadvantages (CON) of mouse, Non-human primate (NHP) and pig models to study vaccine development of *Chlamydia trachomatis* infection in the female genital tract.

	Mouse	**NHP**	**Pig**
PRO	-Small size and easy to handle -Low cost -Abundant availability of laboratory reagents -Many well-characterized inbred and knockout mouse strains [5,9]	-Physiologically, immunologically, and genetically more similar to humans than mice and pigs -Mimics the human disease the most [5,9,105]	-Physiologically, immunologically, and genetically more similar to humans than mice -Outbred -Easier to handle and have less ethical concerns -Large availability of sample (e.g. blood and tissue) [5,9,14,16,93,105]
CON	-Limited amount of sample (e.g. blood, tissues) -Inbred -Different IFN-γ /tryptophan pathway [5,9,105]	-More expensive than mice and pigs -Need special facilities and trained personnel -High ethical issues [5,9,105]	-More expensive than mice -Need special facilities and trained personnel -Less available laboratory reagents compared to mice [5,9,14,16,93,105]

6. Clinical trial for *Chlamydia trachomatis* genital vaccine

Once a vaccine candidate proves to be safe and immunogenic during the preclinical stage, it can then move to the next stage of vaccine development, which is the clinical stage, where the vaccine candidate will be then tested in humans. The clinical stage involves three phases: phase I, which aims to investigate safety and immunogenicity and is done with a small group of volunteers (20 to 100); phase II, which also aims to investigate safety and immunogenicity, but

in a larger population (several hundred volunteers); and phase III, which involves a larger (hundreds of thousands) and often more diverse target population in order to demonstrate and confirm vaccine efficacy [92,133].

The first *C. trachomatis* genital vaccine phase I clinical trial was done last year by the strong chlamydia vaccine Danish group mention before (Table 2) [104]. Of note, this vaccine candidate was tested in both the mouse and the pig models during pre-clinical phase. In this trial, the authors tested a novel chlamydia vaccine based on a recombinant protein subunit CTH522 adjuvanted with CAF01 liposomes or aluminum hydroxide in a population of 35 healthy women aged 19 to 45 years. The vaccine was administered 3 times via intramuscular and 2 times via intranasal. The vaccine CTH522 adjuvanted with either CAF01 or aluminum hydroxide demonstrated to be safe (no serious adverse reaction) and immunogenic, as demonstrated by an increase in serum neutralizing antibodies, nasal and vaginal mucosa IgG/IgA, and IFN-γ production by PBMC [104]. However, CAF01 adjuvant seems to induce a higher antibody titer and cell-mediated response compared to aluminum hydroxide. These results are in accordance with previous studies in mice and pigs that demonstrated that CAF01 adjuvant is highly immunogenic in both mice and pigs by inducing neutralizing antibodies and IFN-γ producing $CD4^+$ T cells [22,23,96]. Furthermore, as expected and previously demonstrated in pigs [76], intranasal vaccination booster tend to increase IgA levels in nasal and genital tract secretions. Vaccination by mucosal routes are also known to induce antigen specific lymphocytes migration to mucosal surfaces upon re-encounter with antigen [134], which could also contribute to the protection observed in this clinical trial.

An ideal *C. trachomatis* vaccine should prevent infertility in women by preventing irreversible damage in the Fallopian tubes. Therefore, the immune response stimulated by this

vaccine should include both neutralizing antibodies, to inactivate extracellular chlamydia EBs, and IFN-γ producing $CD4^+$ T cells, to eliminate intracellular chlamydia RBs. Another important aspect of an effective genital chlamydia vaccine is the induction of both T_{RM}, which will stay in the tissue and act as sentinels to protect the mucosa, and circulating memory T cells, which will be trafficking between lymph node and blood (T_{CM}) and go to the tissue upon re-infection (T_{EM}).

In conclusion, although there is still a lot to be investigated, this first *C. trachomatis* genital vaccine phase I clinical trial established a major milestone for chlamydia vaccine development: the vaccine tested demonstrated to stimulate neutralizing antibodies and IFN-γ producing $CD4^+$ T cells. Therefore, these results give us more hope that we are getting closer to the first chlamydia vaccine that will improve the health of so many people around the world, including here in North Carolina.

III. MUCOSAL VACCINATION WITH UV-INACTIVATED *CHLAMYDIA SUIS* IN PRE-EXPOSED OUTBRED PIGS DECREASES PATHOGEN LOAD AND INDUCES CD4 T-CELL MATURATION INTO IFN-γ^+ EFFECTOR MEMORY CELLS

Amanda F. Amaral[1,7], Khondaker S. Rahman[2], Andrew R. Kick[1,7], Lizette M. Cortes[1], James Robertson[3], Bernhard Kaltenboeck[2], Volker Gerdts[4], Catherine M. O'Connell[5], Taylor B. Poston[5], Xiaojing Zheng[5,6], Chuwen Liu[6], Sam Y. Omesi[5], Toni Darville[5] and Tobias Käser[1,7]*

[1] Department of Population Health and Pathobiology, College of Veterinary Medicine, North Carolina State University, 1060 William Moore Drive, Raleigh, NC 27607, USA
[2] Department of Pathobiology, College of Veterinary Medicine, Auburn University, Auburn, AL 36849, USA
[3] College of Veterinary Medicine, North Carolina State University, 1060 William Moore Drive, Raleigh, NC 27607, USA
[4] Vaccine and Infectious Disease Organization - International Vaccine Centre (VIDO-InterVac), University of Saskatchewan, 120 Veterinary Road, S7N 5E3 Saskatoon, Saskatchewan, Canada
[5] Department of Pediatrics, University of North Carolina at Chapel Hill, Chapel Hill, NC 27599, USA
[6] Department of Biostatistics, University of North Carolina Gillings School of Global Public Health, Chapel Hill, NC 27599, USA
[7] Comparative Medicine Institute, North Carolina State University, 1060 William Moore Drive, Raleigh, NC 27607, USA

* Correspondence: tekaeser@ncsu.edu; +1-919-513-6352

Received: 29 May 2020; Accepted: 30 June 2020; Published: 2 July 2020
Vaccines 2020, 8, 353; doi:10.3390/vaccines8030353, www.mdpi.com/journal/vaccines

Abstract: *Chlamydia trachomatis* (*Ct*) infections are the most frequent bacterial sexually transmitted disease, and they can lead to ectopic pregnancy and infertility. Despite these detrimental long-term sequelae, a vaccine is not available. Success in preclinical animal studies is essential for vaccines to move to human clinical trials. Pigs are the natural host to *Chlamydia suis* (*Cs*) - a chlamydia species closely related to *Ct*, and are susceptible to Ct, making them a valuable animal model for *Ct* vaccine development. Before making it onto market, Ct vaccine candidates must show efficacy in a high-risk human population. The high prevalence of human Ct infection combined with the fact that natural infection does not result in sterilizing immunity,

results in people at risk likely having been pre-exposed, and thus having some level of underlying non-protective immunity. Like human Ct, Cs is highly prevalent in outbred pigs. Therefore, the goal of this study was to model a trial in pre-exposed humans, and to determine the immunogenicity and efficacy of intranasal Cs vaccination in pre-exposed outbred pigs. The vaccine candidates consisted of UV-inactivated Cs particles in the presence or absence of an adjuvant (TriAdj). In this study, both groups of vaccinated pigs had a lower Cs burden compared to the non-vaccinated group; especially the TriAdj group induced the differentiation of CD4+ cells into tissue-homing $CCR7^-$ IFN-γ-producing effector memory T cells. These results indicate that Cs vaccination of pre-exposed pigs effectively boosts a non-protective immune response induced by natural infection; moreover, they suggest that a similar approach could be applied to human vaccine trials.

Keywords: chlamydia trachomatis; chlamydia suis; large animal model; swine; translational research; vaccine development; TriAdj; vaccination; immunology; T cells; effector memory

1. Introduction

Chlamydia trachomatis (*Ct*) continues to be the most prevalent sexually transmitted disease worldwide [1,135]. Especially after repeated or long-term genital infections, *Ct* can lead to pelvic inflammatory disease [18]. Thereby, *Ct* contributes to relevant reproductive issues such as ectopic pregnancy and infertility. Despite these detrimental long-term sequelae and extensive research into *Ct* vaccine development, a *Ct* vaccine is not available.

The lack of a *Ct* vaccine can be partially explained by limitations of the currently used animal models (Figure 1). The advantages and disadvantages of different animal models for *Ct*

research has been recently reviewed [105]. The mouse model has advantages of low cost and a vast toolkit; but important differences between mice and humans limits its use as a translational animal model. A high number of 185 immune genes are not shared with humans [101] and IFN-γ's inhibitory effects on *Ct* differ in humans and mice. Since IFN-γ is a key immune modulator in the response against *Ct*, this difference impairs the use of mice for *Ct* research [11]. Nevertheless, the mouse model was used for possibly one of the most promising *Ct* vaccination studies. Stary et al. showed in 2015 that mucosal administration of UV-inactivated *Ct* combined with charge-switching synthetic adjuvant particles (cSAP) resulted in long-lived protection against genital *Ct* challenge. In addition, they demonstrated that the induction of two subsets of IFN-γ-producing $CD4^+$ T cells is crucial for protection against *Ct* – tissue-resident memory T cells (T_{RM}) and circulating memory T cells consisting of both lymph node-homing central memory (T_{CM}) and tissue-homing effector memory (T_{EM}) T cells [74].

Non-human primates are very similar to humans, but NHPs studies are expensive and involve ethical concerns. As a result, NHPs were only used in six *Ct* vaccine development studies which makes NHPs only the fourth frequently used animal model [136]. The limitations of these two animal models have led to a bottleneck for *Ct* vaccine development (Figure 1). Consequently, *Ct* vaccine researchers are exploring the use of alternative animal models such as guinea pigs, koalas, and pigs.

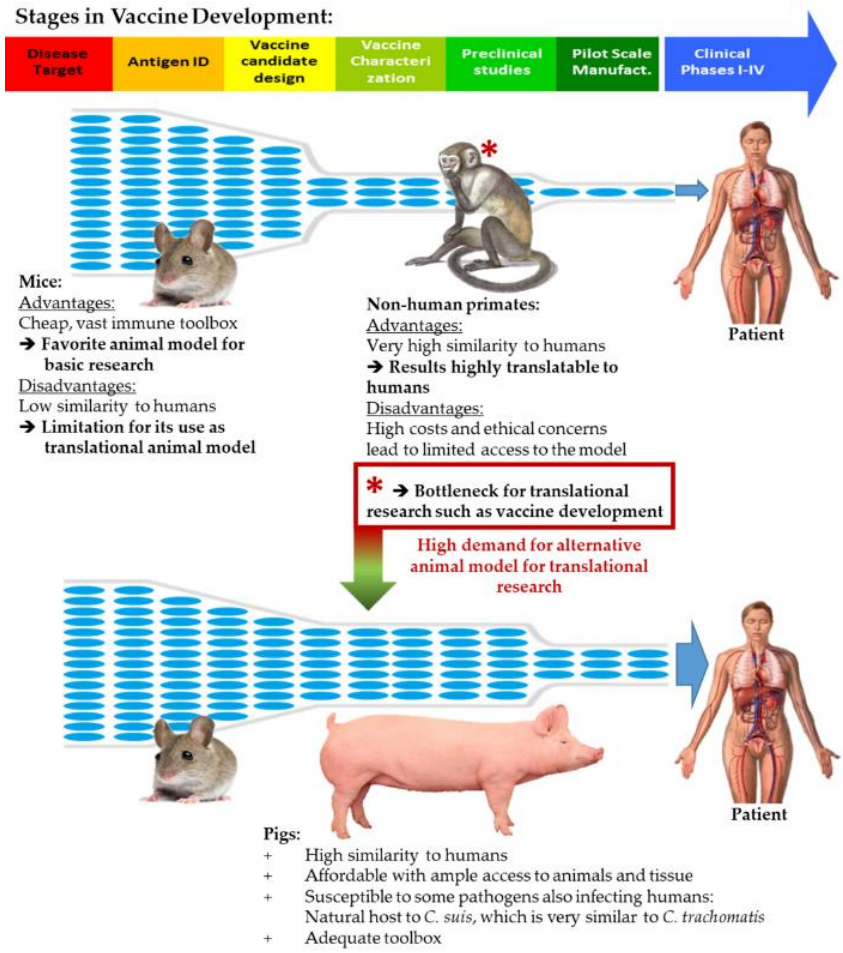

Figure 1. Animal models for vaccine development. The various animal models have advantages and disadvantages during the process of vaccine development. While the associated costs and vast immune toolbox of mice make them an excellent model for basic research, non-human primates are an excellent choice for translational research. Due to high costs and ethical concerns, access to non-human primates is limited, creating a bottleneck for vaccine development. The pig has several advantages as a biomedical translational animal model and can open the bottleneck to advance promising vaccine candidates into clinical trials. The stages in vaccine development were adapted from https://www.niaid.nih.gov/research/vaccine-development-pipeline.

With eight *Ct* vaccine studies, koalas are the second most frequently used animal model. But these studies are concentrated on *C. pecorum*, which naturally infect koalas and lead to devastating reproductive issues. Thus, the end goal for many koala vaccine studies is protection of this iconic Australian marsupial.

The third most frequently used animal model for *Ct* vaccine development is the pig– both, commercial and minipig breeds. The pig has several advantages as a biomedical translational animal model [9,105] and it significantly contributed to the study of sexually transmitted diseases including *Ct* vaccine development [71,96,121,128-130]. Pigs have a similar size, physiology, and hormonal reproductive cycle to humans [16]. Pigs are not only susceptible to common *Ct* strains but they are also the natural host for *Chlamydia suis* [137] – a chlamydia species very close to *Ct* [13,138]. Finally, pigs have an immune system that is very similar to humans. Compared to mice, pigs have more immunological genes shared with humans (230 genes); and 4.5 times fewer genes (41 genes) which are not shared with humans [101].

Although ethical concerns for any animal trial exist, the pig has the big advantage that it is used as a food animal. Porcine genital tracts, blood and lymph nodes are by-products of meat production. Thereby, primary cells used for biomedical *Ct* research can be collected at nearly no cost and without sacrificing animals – a strong advantage in accordance with the 3R principle – replacement, refinement, and reduction. Furthermore, *Ct* vaccine trials in pigs cost substantially less than comparable trials in NHPs [105].

Pigs have been used to study *Ct* infections and vaccine development since 2005 [121]. The Vanrompay group showed that *Ct* can successfully infect specific-pathogen-free (SPF) pigs [121], and then tested vaccine candidates in SPF pigs [128-130]. They were also able to isolate *Cs* out of humans – a sign for a zoonotic potential of the pig pathogen *Cs* [138]. A strong Danish collaboration of the Agerholm, Anderson, Follmann and Jungersen research groups used Goettingen minipigs for their *Ct* research. This collaboration studied not only basic characteristics of the pig model relevant for translational *Ct* research; but they also used their combined expertise for *Ct* vaccine development and demonstrated *Ct* vaccine efficacy and

immunogenicity in naïve minipigs [96]. In their latest studies, the authors showed that protection against *Ct* genital infection in minipigs immunized with *Ct* vaccine formulated with CAF01 adjuvant was associated with cervical infiltration of $CD4^+$ T cells [75] and tissue-resident memory $CD4^+$ T cell infiltration into the uterus [97]. Käser et al. provided a detailed view of the porcine T-cell immune response to *Cs* and *Ct*. As in humans, pigs develop a strong $CD4^+$ T-cell response upon *Ct* or *Cs* infection consisting of mainly IFN-γ single- or IFN-γ/TNF-α- double-cytokine producing $CD4^+$ T cells; and this response was heterologous – so *Cs* infected pigs responded to *Ct* and vice versa [71].

This heterologous response provides a great advantage for the pig model, since *Cs* is highly prevalent in outbred pigs. Vaccination of *Cs*-pre-exposed outbred pigs can simulate *Ct* vaccination of pre-exposed humans. This gives this animal model the ability to predict the outcome of phase III clinical vaccine trials in pre-exposed humans. This last pre-licensing phase is the most time-consuming, extensive, and costly vaccine development phase. To facilitate timely completion for STIs, phase III trials will require completion in high-risk populations. So, any successful *Ct* vaccine candidate must show safety, immunogenicity, and efficacy in pre-exposed humans of high genetic diversity. A vaccine candidate that shows immunogenicity and efficacy in this *Cs* pre-exposed animal model may also be immunogenic and efficacious in *Ct* pre-exposed humans. Furthermore, once a *Ct* vaccine successfully completes the clinical trial phases and makes it to market, it should be administered to as many individuals as possible. Wide coverage will optimize herd immunity against *Ct*. Due to the high prevalence of *Ct*, it would be detrimental to vaccinate only naïve patients. However, a model for testing *Ct* vaccines in pre-exposed outbred animals to closely resemble the situation in humans is currently not available. To overcome that limitation and to provide essential information on the effect of *Ct*

vaccines in pre-exposed patients, the goal of this study was to establish a model for testing vaccine immunogenicity and efficacy in outbred, pre-exposed pigs.

Therefore, we performed a proof-of-principle *Cs* vaccine study in outbred commercial high-health pigs with documented pre-exposure to *Cs*. Before vaccination, these pigs received antibiotic treatment to eliminate genital *Cs* infection. Pigs received two intranasal vaccinations of either MOCK or UV-inactivated *Cs* particles with or without the TriAdj adjuvant [2]. Sixteen days post-vaccination, pigs were challenged post-cervically with *Cs*. Throughout the study, *Cs* load was evaluated via qPCR, and the induced immune response was monitored by ELISA and multi-color flow cytometry. We determined that prime/ boost intranasal administration of a killed whole-cell *Cs* vaccine is both immunogenic and effective. This vaccine strategy induced the differentiation of IFN-γ-producing $CD4^+$ cells into tissue-homing T-effector memory cells; and compared to MOCK-vaccinated pigs, it effectively limited genital *Cs* infection. This study demonstrates that outbred pre-exposed pigs can serve as a valuable animal model for *Ct* vaccine development.

2. Materials and Methods

2.1. Chlamydia suis

The *Chamydia suis* strain S45 (ATCC VR-1474 strain 545 lot 1171210) was propagated in HeLa cells using standard technique [139] and purified as previously described [140]. Bacteria were titrated on HeLa cells as previously described [141].

2.2. Vaccine and adjuvant preparation

The vaccine used in this study consists of ultraviolet light (UV) inactivated *Chlamydia suis* only or in association with the triple adjuvant combination (TriAdj [135]), Vaccine and Infectious Disease Organization – International Vaccine Center (VIDO-InterVac), Saskatchewan, Canada). Each vaccine dose includes 1 x 10^9 *Cs* inclusion-forming units (IFU) in 1 ml of sucrose phosphate glutamic acid buffer (SPG, [139]) and exposed to 8 watts UV light at 30 cm distance for 1 hour (adapted from [74]). The TriAdj was prepared according to the manufacturer's instructions (VIDO-InterVac) to have the following composition per pig: 150 µg of poly I:C; 300 µg of host defense peptide; and 150 µg of polyphosphazene.

2.3. Pigs and experimental design

Twenty-four 25-week-old sexually mature female *Cs* pre-exposed pigs were selected from a commercial high-health farm. Their *Cs* exposure status was determined by qPCR of vaginal swabs as described below. The setup and timeline of this study is shown in Figure 2. Upon arrival, pigs were randomly distributed into four groups with six pigs each. To treat the *Cs* infection, each pig was treated daily by oral administration of 1.44 g of doxycycline (Doxycycline Hyclate, West-Ward, Eatontown, NJ) for four days and additionally with 3 g of tylosin (Tylan soluble, Elanco^{TM}, Indianapolis, IN) twice a day for 3.5 days.

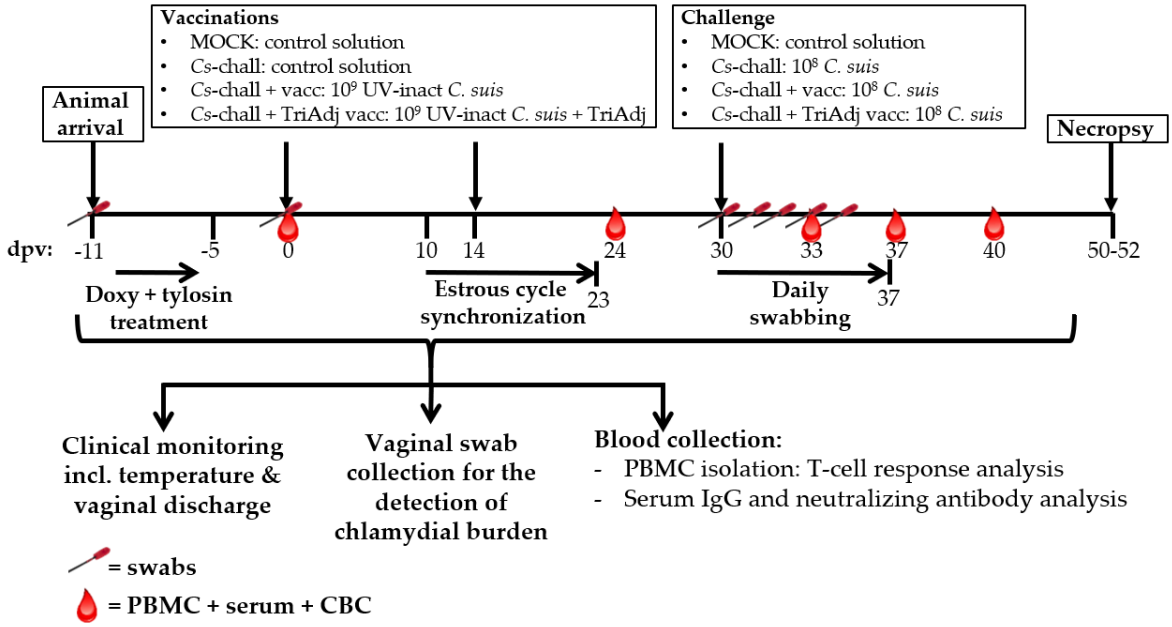

Figure 2. Setup of the *in vivo C. suis* vaccination experiment. Twenty-four sexually mature female *C. suis* pre-exposed pigs were randomly distributed into four groups with six pigs each. Pigs were treated with doxycycline and tylosin from -11 to -5 days post vaccination (dpv). At 0 and 14 dpv, pigs were vaccinated intranasally with: control solution (MOCK and *Cs*-chall), 10^9 UV-inactivated *C. suis* IFU (*Cs*-chall + vacc), or 10^9 UV-inactivated *C. suis* IFU + Tri Adjuvant (*Cs*-chall + TriAdj vacc). From 10-23 dpv, the estrus cycle of pigs was synchronized with synthetic progesterone. At 30 dpv, pigs were challenged trans-cervically with control solution (MOCK) or 10^8 *C. suis* IFU (*Cs*-chall, *Cs*-chall + vacc and *Cs*-chall + TriAdj vacc). Pigs were clinically monitored every day throughout the study and swab/blood collection was performed on the stated dpv. Necropsy was performed on 50–52 dpv. *C. suis* were detected in vaginal swabs via qPCR. Both IgG and neutralizing antibody levels were determined in serum. PBMC were used for analysis of T-cell mediated immune responses.

Pigs were vaccinated intranasally with 1.5ml/nostril of either a control solution (SPG; groups "MOCK" and "*Cs-chall*") or with 10^9 UV-inactivated *Cs* particles without adjuvant (group "*Cs*-chall + vacc") or with adjuvant (group "*Cs*-chall + TriAdj vacc") in SPG at 0- and 14-days post first vaccination (dpv). Intra-nasal vaccination was performed using an intranasal mucosal atomization device (MAD Nasal™ Mist, Teleflex medical, Research Triangle Park, NC).

From 10-23 dpv, the estrus cycle of pigs was synchronized with synthetic progesterone (MATRIX®, Merck, Madison, NJ) according to manufacturer instructions. At 30 dpv, pigs were

challenged trans-cervically with SPG (group MOCK) or SPG with 10^8 *Cs* particles (all "*Cs*-chall" groups). Transcervical challenge was performed in a total volume of 20 ml using gilt post cervical artificial insemination (PCAI) catheters (kindly provided by IMPORT-VET, Centelles, Spain) connected to a 50 ml syringe.

Animals were clinically monitored throughout the study, including for hyperthermia and vaginal discharge. Pigs were considered to have hyperthermia if their rectal temperature was ≥39.5°C [142]. Blood was collected at 0, 24, 33, 37 and 40 dpv, while swabs were collected at -11, 0 and 30-34 dpv. Pigs were sacrificed at 50, 51 and 52 dpv using captive bolt gun followed by exsanguination. Thereafter, genital tracts were collected at necropsy for monitoring of gross pathological changes. These procedures are in accordance with and approved by the North Carolina State University Institutional Animal Care and Use Committee (IACUC #17-029-B).

2.4. Sampling

Swab samples were collected using 4NG FLOQ swabs (Copan flock technologies, Murrieta, CA) as described previously [12]. Blood samples for serum and peripheral blood mononuclear cell (PBMC) isolation were collected from the external jugular vein into SST or heparin tubes, respectively. Serum was incubated at room temperature for 2 hours and spun at 2,000 *g* for 20 minutes at 23°C. Isolation of PBMC was performed using lymphocyte separation medium (Ficoll-Paque Premim, density 1.077g/ml, GE Healthcare, Uppsala, Sweden).

2.5. Detection of chlamydia via qPCR

Chlamydia DNA from vaginal swab was used to measure the chlamydia infection load via Taqman qPCR assay with primers and probe targeting the 23S rRNA gene of *Cs* as previously described including primer and probe design [140]: Fwd primer:

CCTAAGTTGAGGCGTAACTG, Rv primer: GCCTACTAACCGTTCTCATC, Probe: FAM-TTAAGCACGCGGACGATTGGAAGA-TAMRA. The Taqman qPCR was run on a qTOWER3G qPCR machine (AnalytikJena, Jena, Germany). A standard curve of *Cs* gBlocks (IDT® Integrated DNA Technologies, Coralville, IA) was included on every plate to determine the number of chlamydia particles per swab.

2.6. Serum anti-Chlamydia suis Immunoglobulin G detection

Primary IgG antibodies were detected with horseradish peroxidase (HRP)-conjugated goat anti-pig IgG-h+l cross-adsorbed antibody (A100-205P) (Bethyl Laboratories, Inc., Montgomery, TX) by colorimetric enzyme-linked immunosorbent assay (ELISA) as described previously [126], with two modifications: (A) wash buffer contained 200 mM NaCl, 0.1% Tween-20, 0.005% Benzalkonium chloride, 20 mM Tris-HCl, and a pH of 7.4; (B) assay diluent and blocking buffer contained 10% chicken sera, 1% polyethylene glycol, 200 mM NaCl, 0.1% Tween-20, 0.005% Benzalkonium chloride, 50 mM Tris-HCl, and a pH of 7.4.

Streptavidin coated clear 96-well microtiter plates (Thermo-Fisher Scientific, Waltham, MA, Nunc # 436014) were coated with two mixtures of *Cs*-specific biotinylated peptide antigens: 1) *Cs*-specific peptide mixture contained 18 peptides from CT442, CT529, CT618, OmcB, OmpA, PmpD proteins of *Cs*; and 2) *Cs*-specific peptide mixture contained 18 peptides from IncG, IncA, and two IncA family proteins.

For determination of assay background, each serum was tested in wells not coated with any antigen (only solvent dimethyl-sulfoxide in assay diluent). Background-corrected colorimetric signals (OD values) of each individual serum was calculated by subtracting 120% serum background (mean + 2×SD) produced in non-coated well from the signals produced in

wells coated with the two *Cs*-specific peptide mixtures. Average OD of two background-corrected signals for these *Cs*-specific peptide mixtures was used in the analysis to determine IgG level in the serum.

2.7. Neutralizing antibody detection

Neutralizing antibody detection was performed as previously described [71]. Shortly, serum was heat-inactivated at 56°C for 45 minutes and incubated with *Cs* (MOI of 0.5) at 37˚C for 30 minutes in a 1:10 final serum dilution. Next, confluent HeLa cells were infected with this serum-*Cs* mix by centrifugation at 900 g for 1 hour at 37˚C. After an additional hour of incubation, cells were washed and incubated for 30 h. Then, cells were harvested and stained for flow cytometry evaluation of infection using the anti-chlamydia antibody clone ACI (LSBio, Seattle, USA) and the secondary anti-mouse IgG3-Alexa 488 antibody (Southern Biotech, Birmingham, USA). Cells were recorded on a Cytoflex flow cytometer using the CytExpert software (Beckman Coulter, Brea, CA). Data analysis was performed with FlowJo version 10.5.3 (FLOWJO LLC) as previously described [141]. Percent suppression was calculated for each animal using the following formula:

$$\% \text{ suppression} = 100 - \left(\frac{\% \text{ infection [x dpc]}}{\% \text{ infection [-2 dpc]}} \right) \text{x } 100$$

In which "x dpc" (days post challenge) is the day of the calculated percent of suppression.

2.8. Chlamydia suis-specific CD4 T-cell proliferation

Thawed PBMCs were stained with CellTrace™ Violet and seeded in 96-well round-bottom plate (Sarstedt) in quadruplicate at a density of $2x10^5$ cells/well in RPMI-1640 (Corning) supplemented with 10% FBS (VWR) and 1x antibiotic-antimycotic (Corning). Cells were co-

cultured for 4 days with *Cs* lysate at 1µg/ml. After cultivation, quadruplicates were pooled and stained according to Table 1. Cells were recorded and data was analyzed as described in the previous section. The gating hierarchy used for this analysis is shown in Supplementary Figure S1. In addition to a standard percentage analysis of cell subsets, we are introducing two novel ways of numerical and statistical evaluation of the immune response to a pathogen/vaccination: I) The "Differentiation value": To facilitate the statistical comparison of the differentiation status of each group, we first gave $T_{naïve}$ cells a value of zero, T_{CM} a one and T_{EM} a two, based on their differentiation status: $T_{naïve}$ are undifferentiated ($T_{naïve} = 0$), then they first differentiate into T_{CM} ($T_{CM} = 1$), and then into T_{EM} cells ($T_{EM} = 2$). Then, we multiplied the frequency of each of the three differentiation statuses with the respective value: For example, if 20% of the proliferating CD4 T cells in an animal are naïve, 30% are T_{CM} and 50% are T_{EM}, the differentiation value for these proliferating CD4 T cells is calculated as follows – ($T_{naïve}$) 0.2 x 0 + (T_{CM}) 0.3 x 1 + (T_{EM}) 0.5 x 2 = 1.3. And II), the "Response value": Here, we are introducing a method for combined analysis of the cellular response (e.g. proliferation or IFN-γ production) with the cell differentiation status ($T_{naïve}$, T_{CM}, and T_{EM}) – the *Cs* "response value". To provide this combinatorial value, we multiply the response value (e.g. 15% proliferation) with the differentiation value of this cell subset (e.g. 0.6) and 100. So, for this example the response value is 0.15 x 0.6 x 100 = 9.

Table 1. Flow cytometry antibody panels.

Antigen	Clone	Isotype	Fluorochrome	Labeling strategy	Primary Ab source	2nd Ab source
PBMC proliferation staining panel						
CD3	PPT3	IgG1	FITC	Directly conjugated	Southern Biotech	-
CD4	74-12-4	IgG2b	Brilliant Violet 480	Secondary antibody	BEI Resources	Jackson Immunoresearch
CD8α	76-2-11	IgG2a	Brilliant Violet 605	Biotin-streptavidin	Southern Biotech	Biolegend
CCR7	3D12	rIgG2a	Brilliant Blue 700	Directly conjugated	BD Biosciences	-
Live / Dead	-	-	Near Infra-red	-	Invitrogen	-
Proliferation	-	-	CellTrace™ Violet	-	Invitrogen	-
PBMC Intracellular cytokine staining panel						
CD3	PPT3	IgG1	FITC	Directly conjugated	Southern Biotech	-
CD4	74-12-4	IgG2b	Brilliant Violet 421	Secondary antibody	BEI Resources	Jackson Immunoresearch
CD8α	76-2-11	IgG2a	PE-Cy5.5	Biotin-streptavidin	Southern Biotech	Southern Biotech
CCR7	3D12	rIgG2a	Brilliant Violet 480	Directly conjugated	BD Biosciences	-
IFN-γ	P2G10	IgG1	PE	Directly conjugated	BD Biosciences	-
Live / Dead	-	-	Near Infra-red	-	Invitrogen	-
PBMC MACS reanalysis staining panel						
CD4	74-12-4	IgG2b	PE	Secondary antibody	BEI Resources	Southern Biotech
CD172a	74-22-15	IgG1	Alexa Flour 647	Secondary antibody	BEI Resources	Southern Biotech
Live / Dead	-	-	Near Infra-red	-	Invitrogen	-

2.9. Chlamydia suis-specific IFN-γ production by CD4 T cells

Frozen PBMCs were thawed and stimulated as above but at a density of $5x10^5$ cells/well and only for 18 h. Monensin (5µg/ml, Alfa Aesar) was added for the last 4 h of cultivation to block the cellular Golgi export system. Cultured cells were pooled and stained for flow cytometry as mentioned above and as stated in Table 1. Recording and analysis of the flow cytometry data was performed as described above. The gating hierarchy used for this analysis is

shown in Supplementary Figure S2. “Differentiation value” and “response value” at 37 dpv were calculated for each animal as described in the previous section.

2.10. Blood CD4 T-cell mRNA data acquisition, processing, and analysis

Frozen PBMC were thawed and stimulated with *Cs* lysate overnight as above; only the addition of the Golgi inhibitor was omitted. At the end of the culture, PBMC were harvested; then, CD4 T cells were isolated by magnetic activated cell sorting (MACS) using positive cell sorting on $CD4^+$ cells (Miltenyi Biotech), according to manufacturer’s protocol. The purity of the MACS sorts was confirmed by flow cytometry reanalysis of the sorted fractions using antibodies according to Table 1. The sort purity was consistently over 90% in the $CD4^+$ cell fraction (Supplementary Figure S3).

Transcriptional responses of purified CD4 T cells were then profiled using RNA-seq. Cells were stored at -80°C in preservative solution (RNA/DNA Shield, Zymo Research, Irvine, CA) prior to extraction. Total RNA was extracted using a Quick RNA™ nucleic acid isolation kit (Zymo Research) with on-column DNAse I treatment of the RNA. Library preparation and sequencing was conducted by the High-Throughput Sequencing Facility at the University of North Carolina at Chapel Hill. cDNA libraries were generated from rRNA-depleted template using the NuGen Ovation SoLo RNA-Seq System (NuGen, San Carlos, CA, USA). Following library cDNA quantification, the pooled libraries were sequenced using a SI flow cell on the Illumina Novaseq sequencing platform (50 bp, paired ends). Base calling and quality filtering were performed per the manufacturer’s instructions.

Quality control and trimming were performed using Fastqc [143] and fastq-mcf [144], respectively. The QC report was first applied to the raw sequence data followed by application of the sequence Trimmer. As a result, sequences were trimmed based on a phred quality score of

more than 20 and cycle removal at an 'N' (bad read) of 0.5%. The filtered sequences were mapped onto the white pig gene ensemble (Ensembl build 11.1), using STAR [145]. For comparing the levels of gene expression across all samples, the read counts per gene were normalized using DESeq2 [146], which rescaled the counts using the relative effective library sizes. Genes with normalized counts greater than or equal to 25 in at least 5 samples were used for analysis. The differential gene expression between the non-challenged MOCK group and challenged groups (*Cs* challenged, *Cs* challenged + vaccinated and *Cs* challenged + Tri Adjuvant vaccinated) was assessed using DESeq2. DESeq2 estimated variance-mean dependence in count data from high-throughput sequencing and tested for differential expression based on a model using the negative binomial distribution. Multiple testing was adjusted by Benjamini-Hochberg.

2.11. Statistical analysis

Statistical analyses were performed using GraphPad Prism (GraphPad Software, Inc., La Jolla, CA). Data comparisons at specific time points were analyzed using one-way ANOVA with *in vivo* infection as the one factor. Data comparisons throughout the study were performed using repeated-measures two-way ANOVA with *in vivo* infection and time as the two factors; post hoc multiple comparisons were performed using the Dunnett's test. Differences were defined significant (*) for $p < 0.05$.

3. Results

The goal of this study was to determine the efficacy and immunogenicity of *Cs* vaccination in pre-exposed outbred pigs. Pre-exposed gilts received antibiotic treatment to clear

the *Cs* infection; then pigs were used to investigate the effect of vaccination on A) chlamydial burden and B) the induction of humoral and cellular immune responses.

3.1. Chlamydia load in vaginal swabs

Pre-exposure and the efficacy of the antibiotic treatment: Prior to and after antibiotic treatment, rectal and genital *Cs* loads were determined from rectal and vaginal swabs to confirm that the antibiotic treatment was successful in clearing ongoing *Cs* infections. Prior to antibiotic treatment, all animals (24/24) were *Cs* positive in the rectum with a median *Cs* load of 1,647 *Cs* particles per swab (=*Cs*/swab). In the genital tract, one third of the animals (8/24) were *Cs* positive; within these, the median *Cs* load was 49 *Cs*/swab. In contrast, post antibiotic treatment, pigs had either cleared (12/24) or vastly reduced (12/24) the gastrointestinal tract *Cs* infection (Median of *Cs*-infected pigs: 5 *Cs* /swab). Most importantly, all pigs had cleared the genital tract *Cs* infection (Supplementary Figure S4).

Effect of vaccination on the genital *Cs* load: After clearance of prior genital *Cs* infections, pigs were vaccinated at 0 and 14 dpv. At 40 dpv (equaling 0 dpc), pigs were challenged post-cervically with 10^8 *Cs* particles. Vaginal Cs shedding assessed by qPCR was used to determine vaccine efficacy. The effect of vaccination on the genital *Cs* load is shown in Figure 3. Prior to challenge, pigs from all groups were negative for *Cs*: MOCK (gray), *Cs* challenged (*Cs*-chall, blue), *Cs* challenged + vaccinated (*Cs*-chall + vacc, orange) and *Cs* challenged + Tri Adjuvant vaccinated (*Cs*-chall + TriAdj vacc, red). In addition, all MOCK challenged animals stayed negative throughout the study. All but one of the *Cs*-challenged pigs developed an active genital infection starting at 1 dpc, peaking at 2 dpc and declining by 4 dpc. Non-vaccinated animals (blue) showed the strongest *Cs* propagation with a peak median

abundance of 8,685 *Cs*/swab. Both vaccinated groups had a significantly decreased genital chlamydial burden compared to *Cs* challenged: The non-adjuvanted group (orange) peaked at 1,661 *Cs*/swab; the TriAdj-adjuvanted group peaked at 2,228 *Cs*/swab. This vaccine-induced reduction shows the efficacy of both vaccines in reducing the genital *Cs* burden.

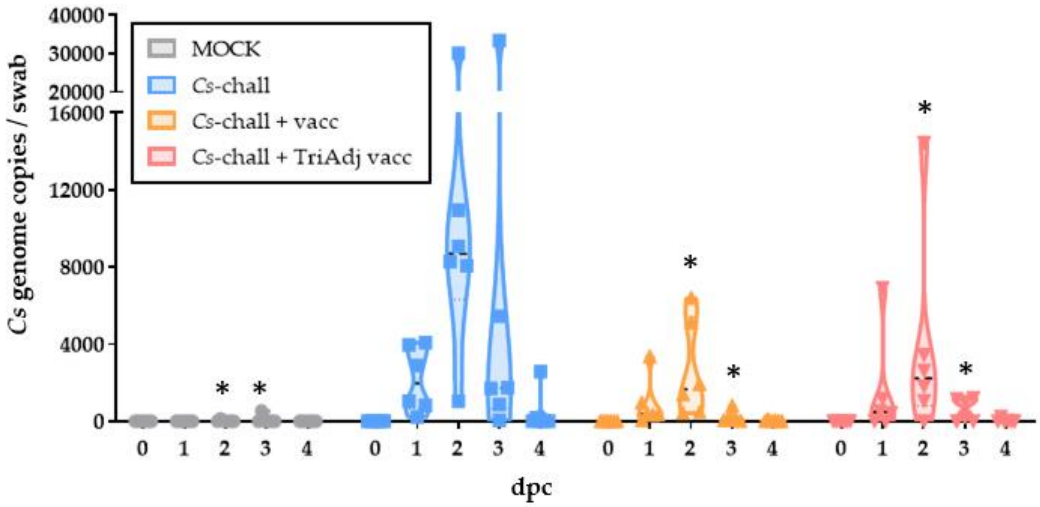

Figure 3. *C. suis* load is reduced in vaccinated pigs post challenge. *C. suis* load was analyzed via qPCR in vaginal swabs from MOCK (gray), *C. suis* challenged (*Cs*-chall, blue), *C. suis* challenged + vaccinated (*Cs*-chall + vacc, orange) and *C. suis* challenged + Tri Adjuvant vaccinated (*Cs*-chall + TriAdj vacc, red) pigs prior to challenge (0 days post challenge, dpc) and after challenge (1-4 dpc). Values for individual pigs, medians, and 25/75 percentiles are shown. Data were analyzed using a repeated-measures 2-way ANOVA in comparison to *Cs*-chall animals and corrected for multiple comparisons with Dunnett's multiple comparisons test. *$p < 0.05$.

3.2. The humoral immune response to Chlamydia suis vaccination and challenge

After showing that both vaccines reduced the post-challenge *Cs* burden, we investigated the mechanisms involved in the anti-chlamydia immune response. The *Cs* humoral immune response was evaluated in serum in two ways – by determining the anti-*Cs* IgG levels using *Cs*-specific multi peptide ELISAs (Figure 4A), and the effect of neutralizing antibodies on suppression of *Cs* infection rate in HeLa cells (Figure 4B). Except for a trend to higher serum IgG levels at 40 dpv in the vaccinated animals, no statistical

differences were observed for the humoral immune response upon *Cs* vaccination and/ or challenge. In addition, day 0 sera already showed high IgG titers (O.D. ~1.0) and neutralizing antibody levels that suppressed on average ~90% of *Ct* (Supplementary Figure S5). These data document pre-existing humoral anti-*Cs* immunity in commercial high-health farm raised pigs.

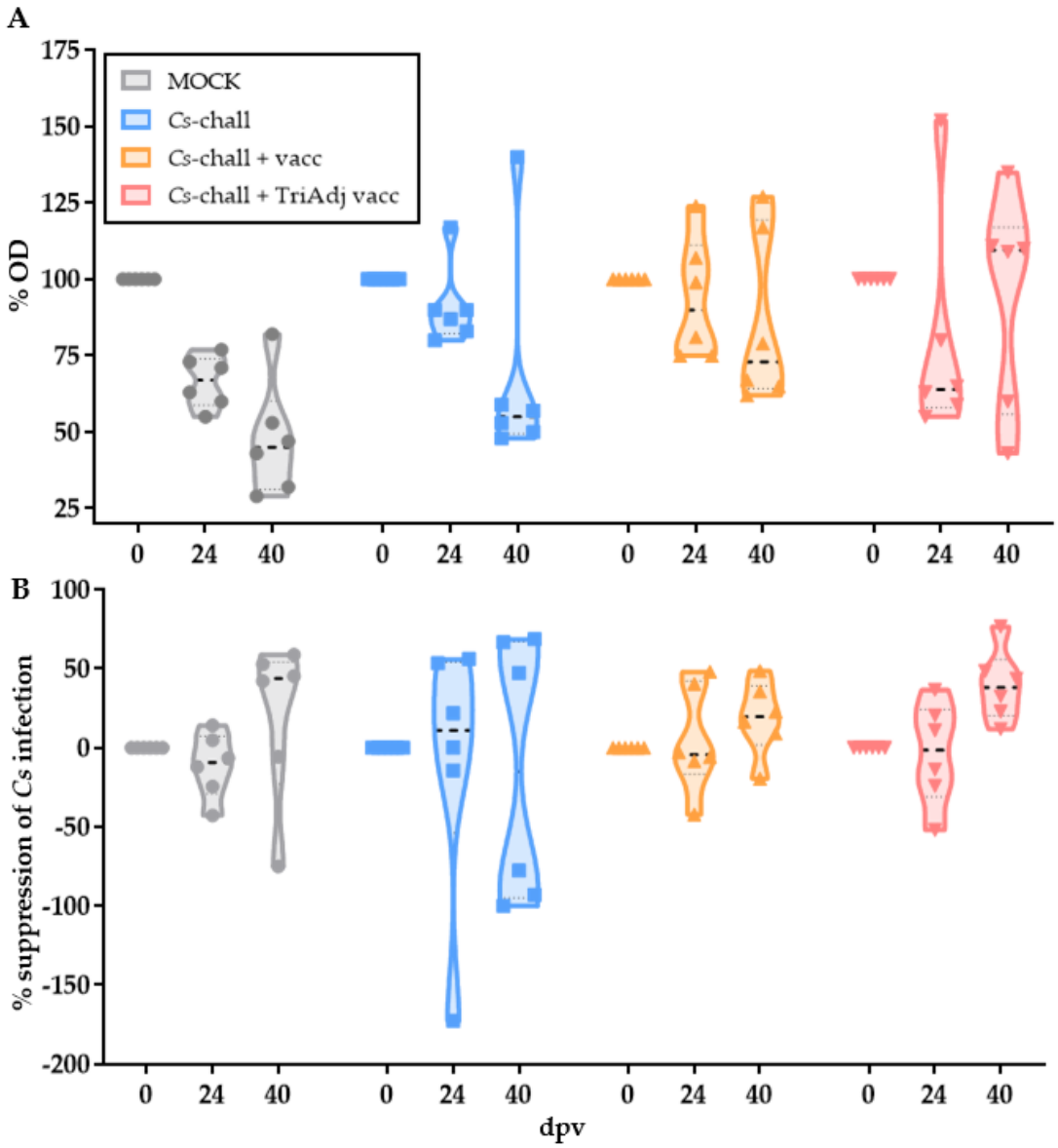

Figure 4. The systemic anti-*Cs* humoral immune response is equivalent in pre-exposed, challenged and vaccinated/challenged pigs. The humoral immune response for each individual pig was analyzed in MOCK (gray), *C. suis* challenged (*Cs*-chall, blue), *C. suis* challenged + vaccinated (*Cs*-chall + vacc, orange) and *C. suis* challenged + Tri Adjuvant vaccinated (*Cs*-chall + TriAdj vacc, red) pigs. (A) Anti-*C. suis* serum IgG levels at stated days post first vaccination (dpv, x-axis) were analyzed via peptide ELISA. While no significant differences were obtained, serum anti-*Cs* IgG levels were elevated by number at 40 days post vaccination (10 days post challenge) in the TriAdj vaccinated pigs. (B) Neutralizing antibodies in serum were analyzed by infecting HeLa cells with *Cs* in the presence of serum (1:10 dilution). The % suppression of infection (y axis) was calculated via flow cytometry by dividing the infection rate at the day post first vaccination (dpv, x-axis) by the infection rate before challenge within the same animal. No between-group differences were obtained. Values for individual pigs, medians, and 25/75 percentiles are shown.

3.3. The CD4 T-cell response to Chlamydia suis vaccination and challenge

In addition to the humoral immune response, we analyzed the $CD4^+$ T-cell response, which is the most important adaptive immune response against chlamydia. PBMC were re-stimulated in vitro with Cs lysate to determine the anti-Cs CD4 T cell response via multicolor flow cytometry. The proliferative response and IFN-γ production of CD4 T cells as well as the differentiation of these responding cells from naïve ($T_{naïve}$) into lymph node homing central memory (T_{CM}) and tissue-homing effector memory (T_{EM}) cells is shown in Figure 5. At the time points with the highest CD4 T cell proliferation (40 dpv) and IFN-γ production (37 dpv), we performed two novel analyses in addition to the standard percentage analysis of the cellular response (Proliferation, Figure 5A; IFN-γ production, Figure 5E): As described in the materials and methods (section 2.8), we calculated a "differentiation value" (Figure 5C, 5G) and a "response value" (Figure 5D, 5H). The "differentiation value" assesses the differentiation status of the responding cells. The "response value" represents a combined analysis of the percentage of responding cells (proliferating or IFN-γ^+ CD4 T cells) and the differentiation value of the responding cells.

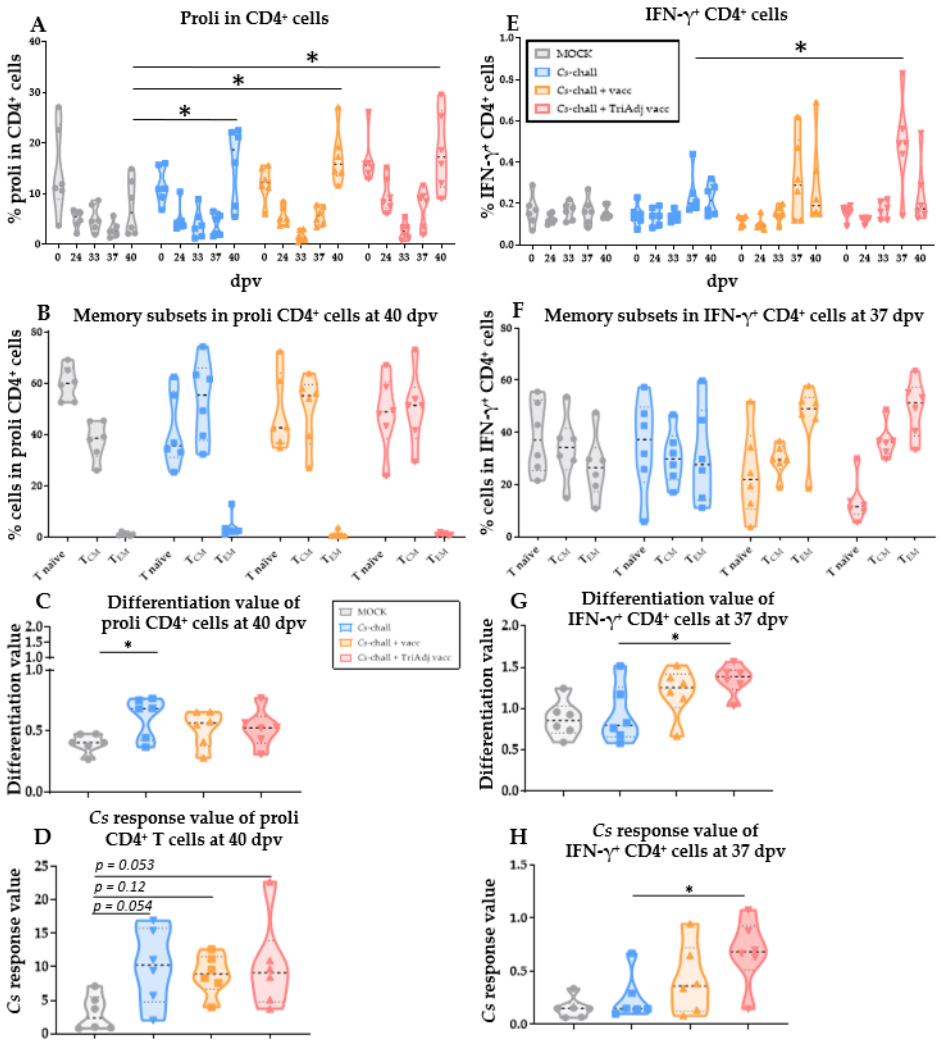

Figure 5. The CD4 T-cell response to *C. suis*: While *C. suis* infection induces CD4 T-cell proliferation, intranasal vaccination drives $CD4^+$ T-cell maturation and primes for a stronger IFN-γ response and post-challenge. PBMC from the stated days post first vaccination (dpv) were isolated from MOCK (gray), *C. suis* challenged (*Cs*-chall, blue), *C. suis* challenged + vaccinated (*Cs*-chall + vacc, orange) and *C. suis* challenged + Tri Adjuvant vaccinated (*Cs*-chall + TriAdj vacc, red) pigs. For *C. suis*-specific proliferative response analysis (A to D), PBMC were stained with CellTrace™ Violet and cultured with *C. suis* lysate for four days. For *C. suis*-specific IFN-γ production analysis (E to H), PBMC were cultured with *C. suis* lysate for 18 h in the presence of a Golgi inhibitor for the last 4 hours. Cells were then harvested and stained as indicated in Table 1. Proliferating $CD4^+$ (proli $CD4^+$) or IFN-γ^+ $CD4^+$ cells were further differentiated as $T_{naïve}$, T central memory (T_{CM}) and T effector memory (T_{EM}) at specific dpv (B and F). Differentiation and response values were calculated for proliferating $CD4^+$ cells (C and D, respectively) and for IFN-γ^+ $CD4^+$ cells (G and H, respectively). Values for individual pigs, medians, and 25/75 percentiles are shown. Data were analyzed using repeated measures; two-way ANOVA in comparison to MOCK (A and B) and *Cs*-inf animals (E and F) with Dunnett's multiple comparisons test; and one-way ANOVA in comparison to MOCK (C and D) and *Cs*-inf animals (G and H). *$p < 0.05$.

The proliferative response of $CD4^+$ T cells to *Cs* is shown in Figure 5 A-D. Even before vaccination at 0 dpv, CD4 T cells from these pre-exposed pigs showed a strong proliferative response to *Cs*. This response dropped until 33 dpv. While T cells from pigs from both non-vaccinated groups (MOCK and *Cs*-chall) exhibited low responses at 37 dpv (= 7dpc), both vaccinated groups showed an increase in their T-cell proliferative response at this time point. At 40 dpv, or 10 dpc, T cells from all challenged pigs proliferated more strongly to *Cs* than T cells from MOCK animals (Figure 5A). These data show that *Cs* infection leads to a strong proliferative CD4 T-cell response. However, there was no significant difference in the proliferative response between the *Cs*-chall and the vaccinated groups.

The differentiation of the CD4 T cells that proliferate upon *Cs*-restimulation at 40 dpv is shown in Figure 5B. While in MOCK pigs the majority (~60%) of proliferating CD4 T cells were naïve, only 38% of these cells belonged to the T_{CM} fraction. In contrast, in all three *Cs*-challenged groups there was an even distribution between naïve and T_{CM} proliferating CD4 T cells (50-53%). Interestingly, *Cs*-specific $CD4^+$ T_{EM} cells did not show a significant proliferative response in any of the groups.

Differentiation analyses using the differentiation value calculation at 40 dpv revealed that, compared with MOCK animals, proliferating CD4 T cells from *Cs*-chall were more differentiated (Figure 5C, $p=0.04$). While the response value did not reach a significant difference between the MOCK and either of the challenged groups, all challenged groups had by number a higher response value (Figure 5D). In summary, *Cs* infection, either by pre-exposure to *Cs* or *Cs* challenge during the trial, induced a strong proliferative response in

CD4 T cells; and by trend, it primed for a higher frequency of differentiated proliferating CD4 T cells.

To provide more details on the systemic anti-chlamydia response of CD4 T-cells induced by *Cs* infection, we performed an in-depth analysis of their transcriptional profile using RNAseq. PBMC were restimulated overnight with *Cs* and their transcriptional profile was compared between MOCK and *Cs*-chall pigs at 37 dpv – based on the peak IFN-γ response at this time point (Figure 5). The data are summarized in Supplementary Table S1: Compared to MOCK controls, 89 transcripts were significantly ($p<0.05$) upregulated in CD4 T cells isolated from the blood of pigs trans-cervically challenged with *Cs*. These genes are primarily involved in T-cell growth, proliferation, adhesion, migration, inflammation, and immunity: We observed the upregulation of key genes involved in T-cell receptor (TCR) signaling and activation, including *PKD2 [147,148]*, *VDR [149]*, *PFDN1 [150]* and *TRAF3 [151]*, along with genes important for T cell survival, growth, and proliferation mediated via the AKT signaling pathway like *IGF1 [152]*, *TNFSF11 [153,154]* and *PINK1 [155]*. We also observed upregulation of *RORA* and *DAPK1*, which are critical for T cell differentiation and effector function [156-159]. These transcriptional profiling data can provide valuable insight into the details of the systemic anti-chlamydia CD4 T-cell response; and they will be used as the basis for future more in-depth analyses on this crucial immune response in the highly relevant pig model.

In this study, we focused our analysis on the CD4 T-cell response that has been shown to be most crucial for protection against chlamydia – their IFN-γ response and their ability to migrate to the genital tract tissue. Studying the IFN-γ response of CD4 T cells revealed a contrast to the above-described proliferation data: Despite pre-exposure to *Cs*,

IFN-γ production by CD4 T cells was low in all groups at the start of the trial (0 dpv). Within all groups, the median frequency of IFN-γ^+ CD4 T cells stayed below 0.2% at 0 dpv (Figure 5E); and this response stayed low through 33 dpv. But at 37 dpv (7 dpc), compared to *Cs*-chall animals, the IFN-γ response from CD4 T cells of both vaccinated groups increased, with T cells from the the TriAdj vaccinated animals having a significantly increased IFN-γ response (Figure 5E, $p < 0.0001$). Figures 5F, 5G, and 5H show the differentiation of these IFN-γ-producing CD4 T cells at their peak response (37 dpv): Compared with *Cs*-chall animals, IFN-γ^+ CD4 T cells from the TriAdj vaccinated animals had more memory cells with the majority of them being tissue-homing T_{EM} cells (Figure 5F). As a result, these cells also had a higher differentiation value in TriAdj vaccinated pigs compared to *Cs*-chall pigs (Figure 5G, p=0.03). Compared to the *Cs*-chall group, the combinatorial response value was also significantly increased in the *Cs*-chall + TriAdj vacc group (Figure 5H, $p = 0.02$). This comparison shows the effect of the adjuvanted vaccine on both IFN-γ production and differentiation of the responding CD4 T cells. In summary, intranasal *Cs* vaccination, especially if adjuvanted with the TriAdj adjuvant, primed for a stronger IFN-γ response post challenge; and it induced the differentiation of CD4 T cells into tissue-homing T_{EM} cells.

4. Discussion

Due to the high prevalence of *Ct* in humans, vaccination of pre-exposed patients would benefit a timely establishment of herd immunity. Therefore, the goal of this study was to provide an animal model to test future *Ct* vaccine candidates in outbred pigs naturally pre-exposed to *Cs* – the close relative of *Ct*. This model has the strong potential to predict *Ct* vaccine safety and

efficacy for both critical Phase III clinical trials in a high-risk population and pre-exposed *Ct* patients.

To establish this model, we performed a proof-of-principle experiment studying *Cs* vaccine efficacy and immunogenicity in *Cs* pre-exposed pigs. At arrival, all pigs were pre-exposed to *Cs* as demonstrated by anti-*Cs* serum IgG levels. In addition, 100% of pigs had an ongoing infection in the gastrointestinal tract; and 33% were *Cs*-positive in the genital tract. Antibiotic treatment with doxycycline and tylosin cleared the *Cs* infection in 50% of the GI tracts and vastly reduced the *Cs* burden in the remaining 50%. This treatment also cleared 100% of genital tract *Cs* infections (Supplementary Figure S4). This demonstrates the efficacy of this combinatorial treatment plan for *Cs* in pigs. And in turn, this substantial reduction of *Cs* from these pigs explains a peculiarity of the observed immune response – the drop in antibody levels and CD4 proliferation from 0 dpv to 24 dpv even in vaccinated pigs. While the antibiotic treatment nearly eliminated *Cs* from these pigs, it is unlikely that the humoral and T-cell response vanishes within 5 days. This is reflected by the substantial serum antibody levels (Supplementary Figure S5) and the high frequency of proliferating CD4 T cells (Figure 5A) at 0 dpv (= 5 days post antibiotic treatment). However, this antibody and proliferative response dropped substantially by 24 dpv (= 29 days post antibiotic treatment). This drop shows that the humoral and T-cell response to natural *Cs* infection strongly declined within one month of antibiotic treatment. This drop was present in all groups, so neither of the vaccines could overcome the effect of *Cs* clearance on the systemic antibody levels and CD4 T-cell proliferation. In summary, these data show that in contrast to our vaccine candidates, natural *Cs* infection induces a strong systemic humoral immune response and CD4 T cell proliferation which declines within one month after antibiotic treatment.

While natural infection led to high serum antibody levels and a strong proliferative CD4 response, it did not induce a notable IFN-γ response (Figure 5). Since genital infections with both *Cs* and *Ct* induce an IFN-γ response [71,75,96], the observed lack of IFN-γ production despite a clear proliferative response can potentially be explained by the fact that all pre-exposed pigs were mainly infected in the GI tract; however, chlamydia infections of the GI tract have been shown to be rather homeostatic [160]. Since IFN-γ production by CD4 T cells is a central immune mechanism in the clearance of both *Cs* and *Ct*, this result indicates that GI *Cs* and *Ct* infections are not likely to be cleared by the natural immune response and require antibiotic treatment.

The final question that needs to be addressed is: Which immune mechanism did the vaccines induce to significantly lower the genital *Cs* load on days 2 and 3 post challenge (Figure 3)? To answer that question, we studied the humoral and CD4 T-cell response pre-vaccination (= 0 dpv), at ten days post boost vaccination (=24 dpv), and at 3, 7, and 10 days post challenge (=33, 37, and 40 dpv). Neither of the vaccines induced a significant systemic humoral immune response (Figure 4). This lack of induction of a systemic humoral response to *Cs* is in line with our results from a previous *Cs* and *Ct* infection study [71]. Nevertheless, this result does not rule out a contribution of the local humoral immune response in the protection against genital *Ct* infection as shown by Erneholm et al. [161].

While the humoral immune response was not altered significantly by *Cs* vaccination, both vaccinations primed for a stronger and arguably more efficient CD4 T-cell response. Intranasal administration of UV-inactivated *Cs* particles with and without TriAdj adjuvant improved the CD4 T cell response in three ways: First, although only by number, compared to the MOCK group, both vaccinated groups primed for a faster proliferative response of CD4 T

cells (Figure 5A, 37 dpv). Second, compared with the *Cs*-chall group, the TriAdj-adjuvanted vaccine induced a significantly stronger post-challenge IFN-γ response (Figure 5E, 37 dpv). And third, both vaccines but mainly the TriAdj vaccine induced the differentiation of IFN-γ-producing CD4 T cells into memory cells, especially into tissue-homing T_{EM} cells (Figures 5F-H). In pigs, IFN-γ-producing CD4 T_{EM} cells have been shown to have a crucial role in protection of genital *Ct* infections. First, we showed that pigs develop a strong IFN-γ $CD4^+$ T-cell response upon *Ct* or *Cs* infection [71]; and second, the influx of CD4 T cells into the genital tract tissue has previously been shown to represent a good correlate of protection: Erneholm et al. showed in minipigs that cervical infiltration of CD4 T cells upon immunization with inactivated *Ct* + CAF01 adjuvant was associated with protection against genital *Ct* infection [75]. The importance of these IFN-γ-producing $CD4^+$ T cells is demonstrated by their association with reduced risk of *Ct* re-infection in humans [162]. Furthermore, these cells have been shown to correlate with protection [163]; and they are essential for pathogen clearance [6,74,164]. During chlamydia infection in mice, naïve T cells differentiate into effector T cells in uterus-homing lymph nodes and these effector cells are then recruited to the mucosa of the genital tract to establish tissue-resident memory cells (T_{RM}) [97,165,166]. And in 2015, Stary et al. showed that the generation of "two waves of protective memory T cells", tissue-resident CD4 T_{RM} and circulating T_{CM} and T_{EM} cells, is required for optimal clearance of genital *Ct* infections [74]. Based on the combination of i) the protective effect of our vaccines on the genital chlamydial burden, and ii) the induction of CD4 T-cell differentiation into tissue-homing IFN-γ-producing CD4 T_{EM} cells our data support two main conclusions of these studies: First, IFN-γ-producing tissue-homing CD4 T_{EM} cells, that can further differentiate into T_{RM} cells, could serve as a promising blood biomarker for

protection against genital *Ct* infections; and second, mucosal delivery of adjuvanted UV-inactivated chlamydia particles is a promising strategy for *Ct* vaccine development.

5. Conclusions

This proof-of-principle study demonstrates that intranasal vaccination with UV-inactivated *Cs* particles +/- TriAdj is immunogenic; and it lowers genital *Cs* burden even in pre-exposed outbred pigs. This vaccination primes for a stronger IFN-γ response of CD4 T cells; and it drives CD4 T-cell differentiation into both lymph node homing central memory T cells and tissue homing effector memory T cells. Thus, this vaccination induces both waves of CD4 T-cell memory – the immune mechanisms previously reported to be required for protection against *Ct* [74,75]. Thereby, this study provides the first insight to our knowledge into the performance of a chlamydia vaccine candidate in pre-exposed outbred animals. This insight supports that mucosal *Ct* vaccination can help generate herd immunity in humans by vaccinating both, naïve and pre-exposed patients; and it further supports the relevance of the pig model for translational research on *Ct*.

Supplementary figures and table:

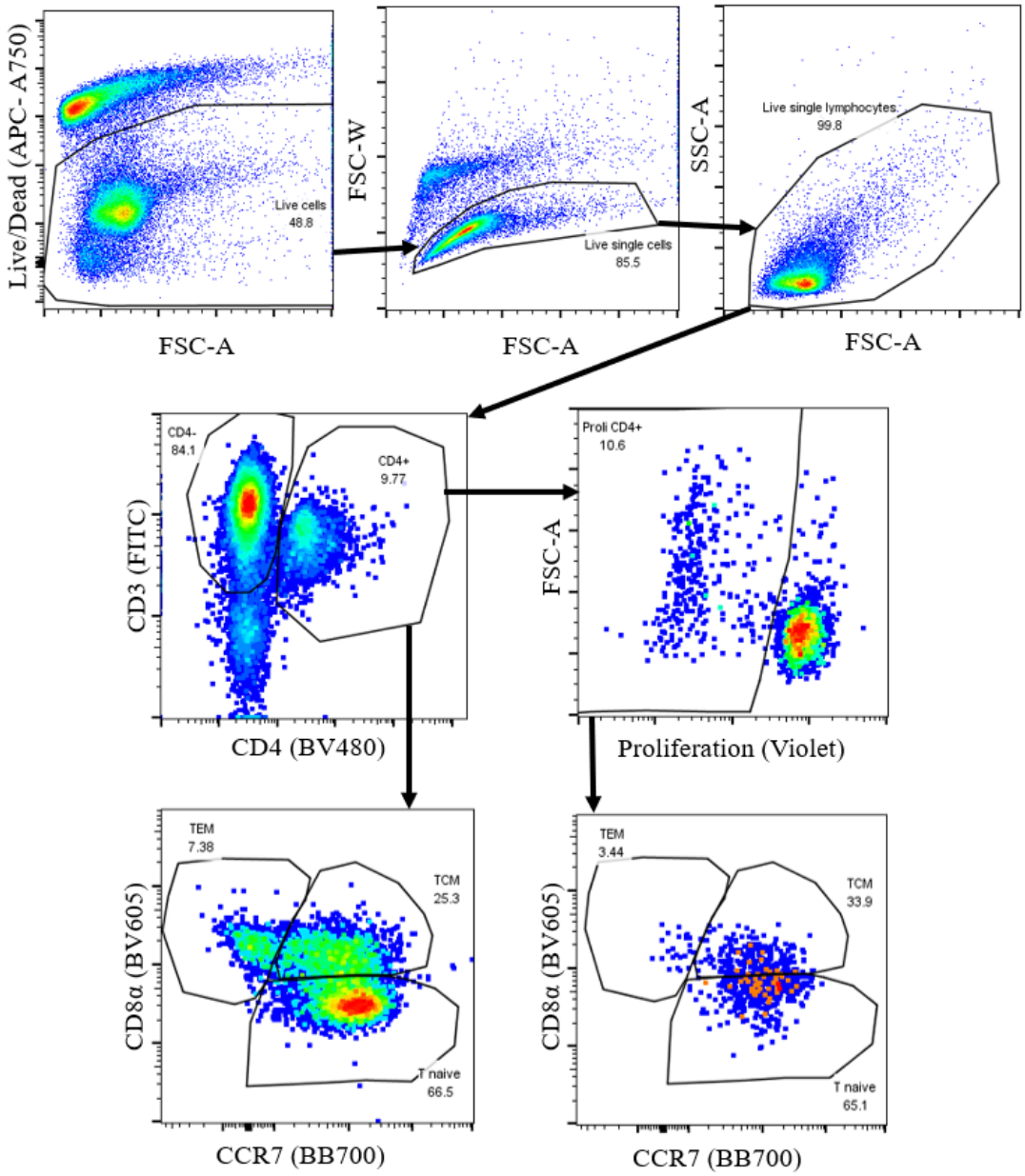

Supplementary Figure S1. Gating hierarchy for PBMC proliferation analysis via flow cytometry. Proliferation of $CD4^+$ T cells was analyzed by CellTrace™ Violet in combination with FCM stainings for immune markers. Live cells were identified by a gate on Live/Dead Near infra red staining. Next, doublets were excluded by an FSC-A (area)/FSC-W (width) gate. Lymphocytes were then identified by cell size (FSC-A) and granularity (SSC-A). $CD4^+$ T cells were identified via their CD3 and CD4 expression. Within these $CD4^+$ T cells, proliferation was analyzed using a CellTrace™ Violet/FSC-A gate. $CD4^+$ and proliferating $CD4^+$ cells were further differentiated into naïve (T naïve), central (T_{CM}) and effector memory cells (T_{EM}) via CCR7 and CD8α markers: T_{CM} is $CCR7^+CD8\alpha^+$ and T_{EM} is $CCR7^-CD8\alpha^+$. Gating is based on relevant fluorescent minus one (FMO) controls.

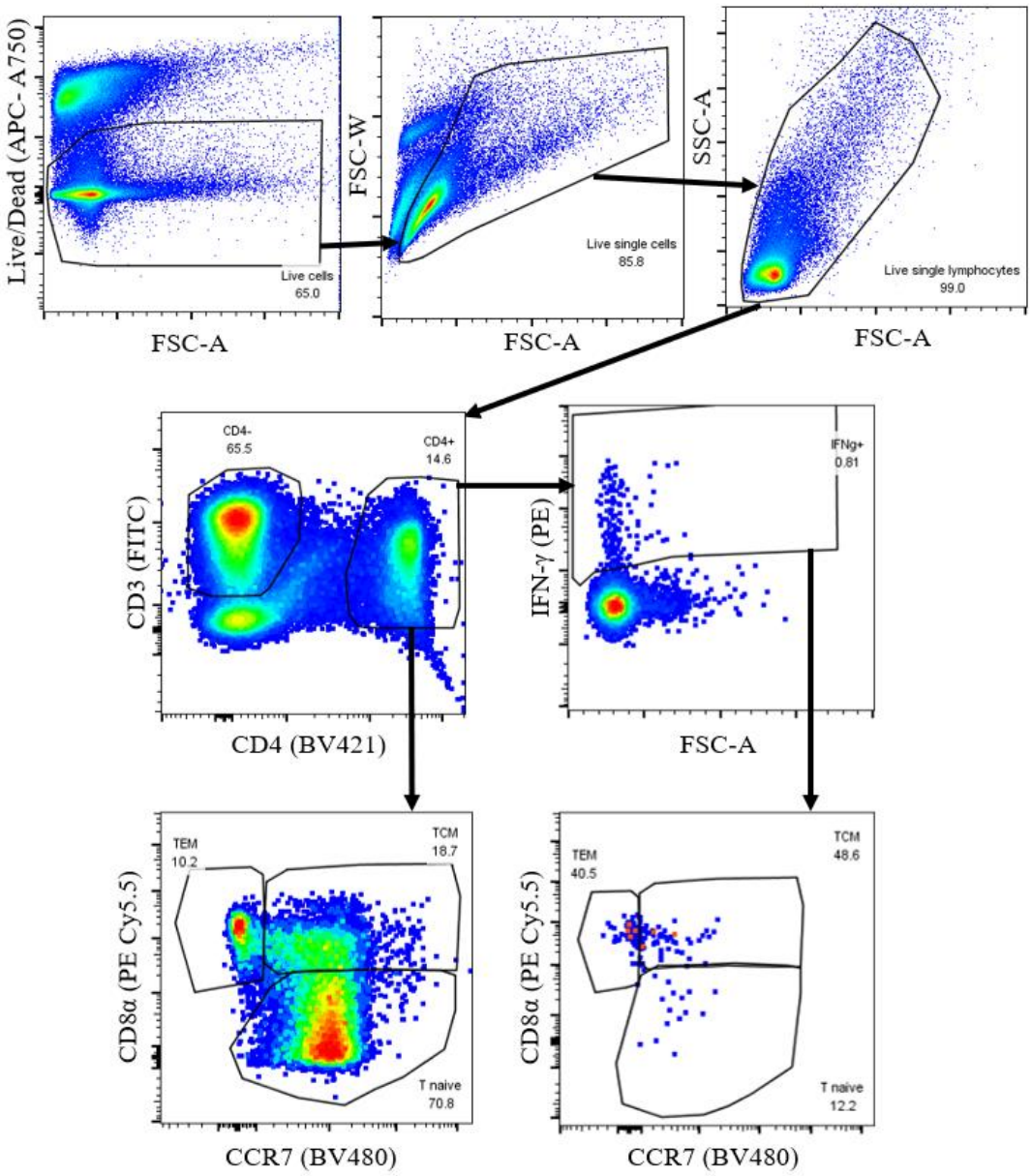

Supplementary Figure S2. Gating hierarchy for PBMC intracellular cytokine analysis via flow cytometry. Cytokine production in $CD4^+$ T-cells was analyzed via polychromatic flow cytometry. Live cells were identified by a gate on Live/Dead Near infra-red staining. Next, doublets were excluded by an FSC-A (area)/FSC-W (width) gate. Lymphocytes were then identified by cell size (FSC-A) and granularity (SSC-A). $CD4^+$ T-cells were identified via CD3 and CD4 markers and IFN-γ production was analyzed in live single $CD4^+$ T cells. $CD4^+$ and IFN-γ^+ $CD4^+$ cells were further differentiated into naïve, central and effector memory cells (T naïve, T_{CM}, T_{EM}, respectively) via CCR7 and CD8α markers. T_{CM} is $CCR7^+CD8\alpha^+$ and T_{EM} is $CCR7^-CD8\alpha^+$. Gating is based on the relevant fluorescent minus one (FMO) controls.

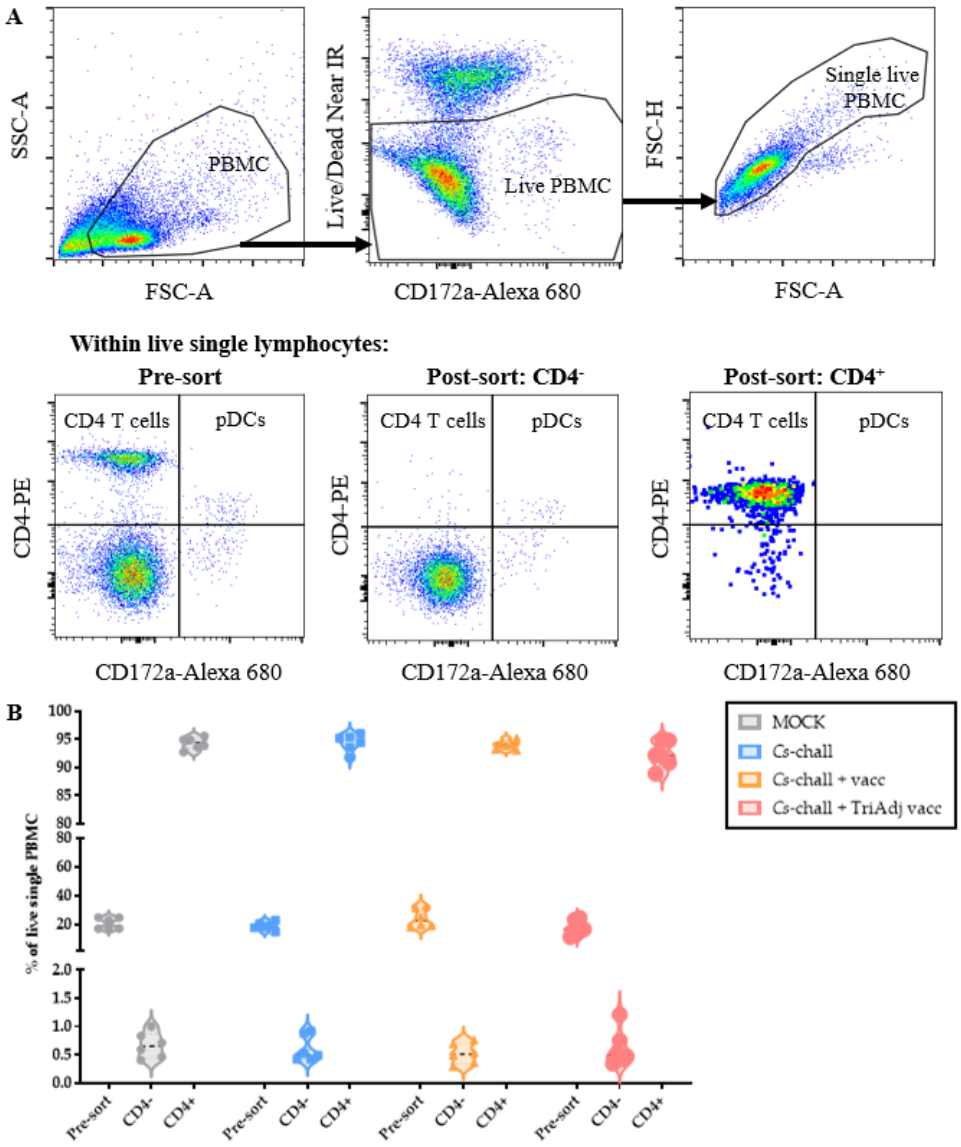

Supplementary Figure S3. Reanalysis of blood CD4 T cells isolated by magnetic activated cell sorting via flow cytometry. PBMC from 37 days post first vaccination were isolated from MOCK (gray), *C. suis* challenged (*Cs*-chall, blue), *C. suis* challenged + vaccinated (*Cs*-chall + vacc, orange) and *C. suis* challenged + Tri Adjuvant vaccinated (*Cs*-chall + TriAdj vacc, red) pigs. PBMC were cultured with *C. suis* lysate overnight and CD4 T cells were isolated by magnetic activated cell sorting (MACS) using positive cell sorting on $CD4^+$ cells (Miltenyi Biotech), according to manufacturer's protocol. MACS sorts were then identified via flow cytometry. (A) Gating hierarchy of $CD4^+$ cells: Lymphocytes were identified by cell size (FSC-A) and granularity (SSC-A); live cells were then identified by Live/Dead Near infra-red and CD172a staining; next, doublets were excluded by an FSC-A (area)/FSC-H (height) gate; CD4 T-cells were identified as $CD4^+CD172a^-$ cells, as oppose to plasmacytoid dendritic cells (pDC) which are $CD4^+CD172a^+$ cells. Gating is based on the relevant fluorescent minus one (FMO) controls. (B) The purity of the MACS sorts was confirmed by flow cytometry reanalysis of the sorted fractions. Values for individual pigs, medians, and 25/75 percentiles are shown.

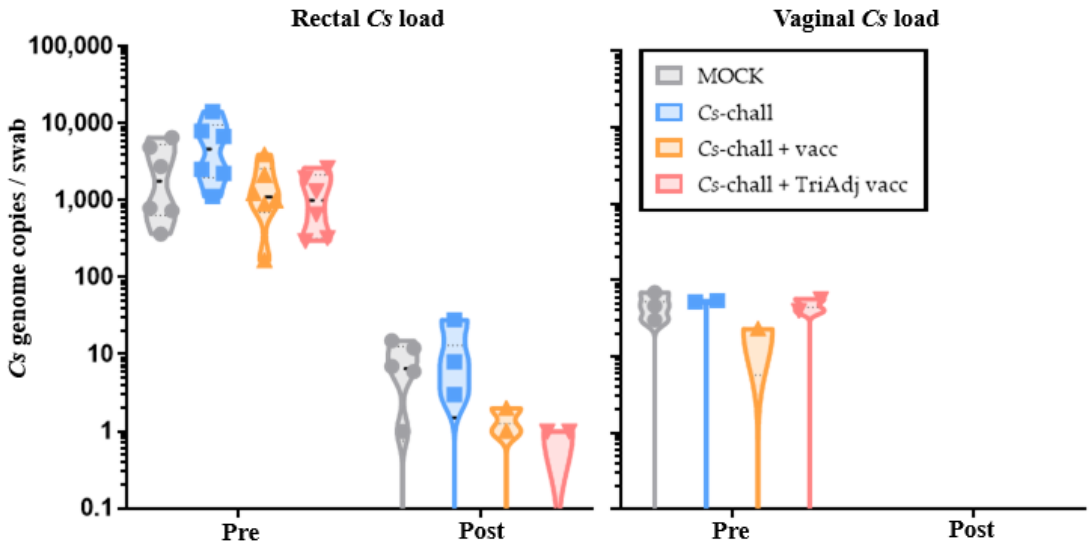

Supplementary Figure S4. Antibiotic treatment eliminates vaginal *C. suis* load and decreases rectal *C. suis* load. The *C. suis* load in rectal and vaginal swabs from MOCK (gray), *C. suis* challenged (*Cs*-chall, blue), *C. suis* challenged + vaccinated (*Cs*-chall + vacc, orange) and *C. suis* challenged + Tri Adjuvant vaccinated (*Cs*-chall + TriAdj vacc, red) pigs were analyzed via qPCR prior to challenge (Pre, x-axis) and post challenge (Post, x-axis). Chlamydia levels below the standard curve were considered negative and are not represented in the graph. Values for individual pigs, medians, and 25/75 percentiles are shown.

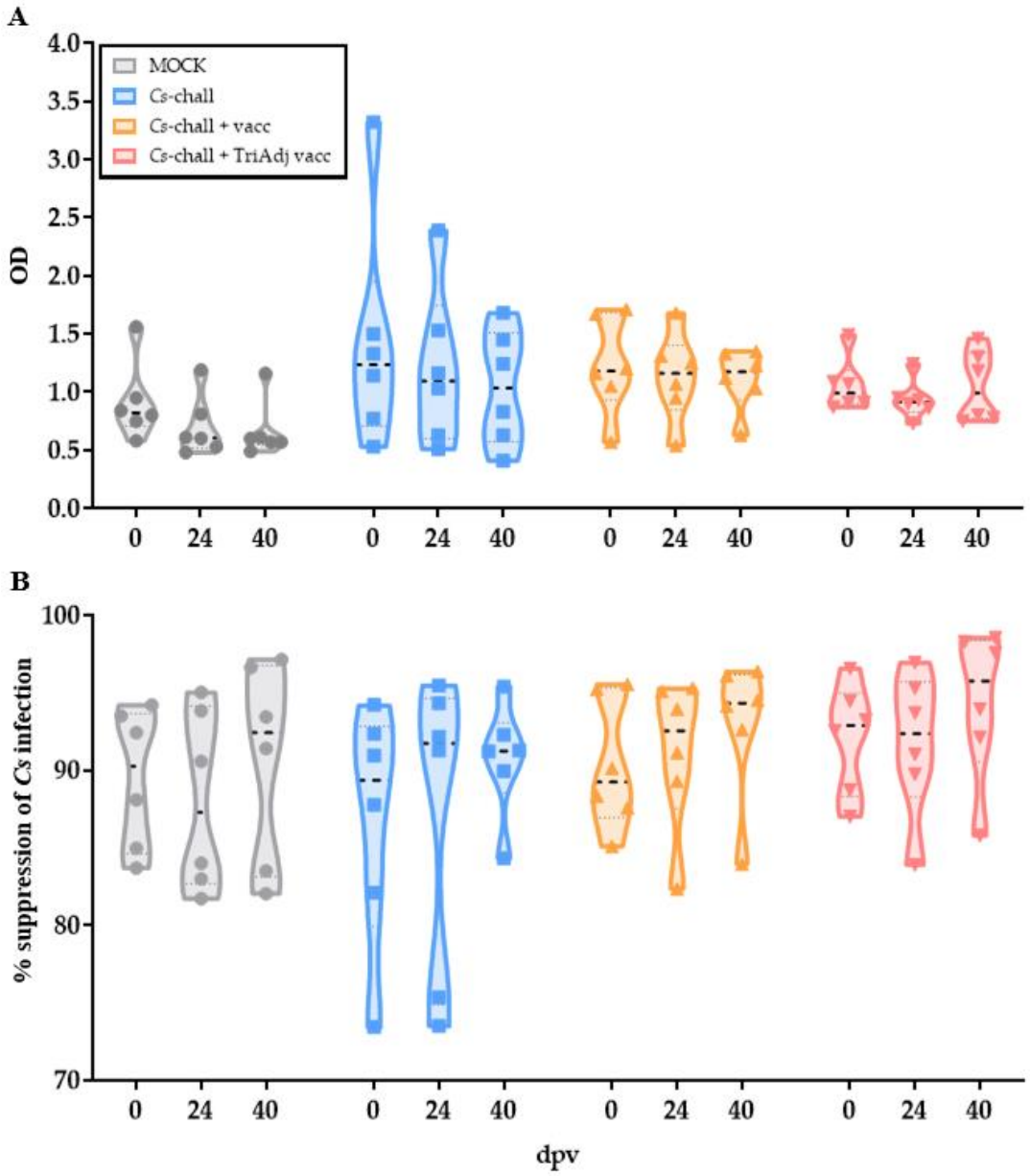

Supplementary Figure S5. Serum anti-*C. suis* antibody levels in commercial pigs from high-health farms. The humoral immune response was analyzed in MOCK (gray), *C. suis* challenged (*Cs*-chall, blue), *C. suis* challenged + vaccinated (*Cs*-chall + vacc, orange) and *C. suis* challenged + Tri Adjuvant vaccinated (*Cs*-chall + TriAdj vacc, red) pigs. (A) Anti-*C. suis* serum IgG levels at stated days post first vaccination (dpv, x-axis) were analyzed via peptide ELISA. (B) Neutralizing antibodies in serum were analyzed by infecting HeLa cells with *Cs* in the presence of serum (1:10 dilution). The % suppression of infection (y axis) was calculated via flow cytometry by dividing the infection rate at the day post first vaccination (dpv, x-axis) by the infection rate of serum from specific pathogen free (SPF) pigs. Values for individual pigs, medians, and 25/75 percentiles are shown.

Supplementary Table S1. Blood $CD4^+$ T cell total mRNAs profiled using RNA-seq. The pairwise differential gene expression analysis between non-challenged MOCK and challenged groups (*C. suis* challenged, *C. suis* challenged + vaccinated and *C. suis* challenged + Tri Adjuvant vaccinated) was assessed using DESeq2. Significance of the canonical pathway was assessed using Fisher's exact test. All multiple testing was adjusted by Benjamini-Hochberg.

Ensemble Gene ID	Gene Symbol	Gene Name	General Function	Log2 Fold Change	Adjusted p value
ENSSSCG00000026842	CDH18	cadherin 18	adhesion	6.514001499	0.003218955
ENSSSCG00000000857	IGF1	insulin-like growth factor 1	growth and proliferation	6.495027138	0.002942227
ENSSSCG00000009502	UGGT2	UDP-glucose glycoprotein glucosyltransferase 2	metabolism	6.09677358	0.002983538
ENSSSCG00000027678	CCDC175	coiled-coil Domain Containing 175	structure and trafficking	5.919923343	0.008648947
ENSSSCG00000032365	GPR87	G-protein coupled receptor 87	communication and migration	5.828547485	0.019395021
ENSSSCG00000012002	ROBO2	roundabout guidance receptor 2	proliferation and migration	5.711321741	0.005599321
ENSSSCG00000035000	ABCA16	ATP-binding cassete sub-family A, member 16	molecular transport	5.540309545	0.01728579
ENSSSCG00000016554	MEST	mesoderm specific transcript	metabolism	5.320303203	0.02209914
ENSSSCG00000009217	PKD2	polycystin 2	ion channel	5.213497139	0.024469655
ENSSSCG00000013382	PLEKHA7	pleckstrin homology domain containing A7	adhesion	5.146365546	0.015107422
ENSSSCG00000030877	FRMPD4	FERM and PDZ domain containing 4	scaffolding	5.140995088	0.003574795
ENSSSCG00000017261	ARSG	arylsulfatase G	metabolism	5.121888326	0.015931799
ENSSSCG00000022741	PDGFRB	platelet dervied growth factor receptor beta	growth	5.110208465	0.037526456
ENSSSCG00000034000	SERPINB11L1 [1]	Serpin-like B11	metabolism	5.008991958	0.044098118
ENSSSCG00000007675	EPHB4	ephrin type-B receptor	proliferation	4.81030992	0.041831729
ENSSSCG00000002277	SPTB	spectrin beta	membrane stability	4.795997278	0.018496517
ENSSSCG00000005762	KCNT1	potassium channel subfamily T, member 1	ion channel	4.690706608	0.028148799
ENSSSCG00000003251	NLRP12	NLR family pyrin domain containing 12	inflammation	4.57693532	0.038584841
ENSSSCG00000011485	PTPRG	protein tyrosine phosphatase receptor type G	growth and migration	4.514900161	0.029148929
ENSSSCG00000003789	CTH	cystathionine gamma-lyase	metabolism	4.484348504	0.006405136
ENSSSCG00000016678	NOD1	nucleotide binding oligomerization domain containing 1	inflammation	4.388027764	0.0035279
ENSSSCG00000010626	RBM20	RNA binding motif 20	alternative splicing	4.382216306	0.024142368
ENSSSCG00000039854	TLCD4	TLC domain containing 4	metabolism	4.339526312	0.04830757
ENSSSCG00000036553	SAMD12	sterile alpha motif domain containing 12	DNA binding	4.184921478	0.025461995
ENSSSCG00000032946	HMGN5	high mobility group nueclosome binding domain 5	DNA binding	4.144044731	0.029480236
ENSSSCG00000040967	NACC2	nuclus accumbens-associated protein 2	transcriptional regulation	4.068007871	0.046812872
ENSSSCG00000021562	PLXNA4	plexin A4	cytoskeleton remodeling	4.041299219	0.018980378
ENSSSCG00000009429	TNFSF11	tumor necrosis factor ligand superfamily member 11	inflammation and activation	4.011210923	0.020315766
ENSSSCG00000013147	FAM111B	family with sequence similiarity 111 member B	metabolism	3.941219485	0.016870537
ENSSSCG00000008761	TBC1D19	TBC1 domain family member 19	signaling and metabolism	3.932766694	0.011187952
ENSSSCG00000014625	TRIM3	tripartite motif containing 3	molecular transport	3.87494137	0.025398417
ENSSSCG00000020864	VDR	vitamin D3 receptor	metabolism and inflammation	3.816828275	0.036776221
ENSSSCG00000011353	PFKFB4	6-phosophofructo-2-kinase/fructose-2,6-biphosphatase 4	metabolism	3.81025969	0.018098585
ENSSSCG00000014179	FAM174A	family with sequence similiarity 174 member A	signaling	3.757174913	0.038221344
ENSSSCG00000024065	TMTC2	transmembrane O-mannosyltransferase targeting conditions 2	metabolism	3.749174547	0.040946516
ENSSSCG00000032086	ZNF583	zinc finger protein 583	transcriptional regulation	3.721583593	0.007057135
ENSSSCG00000035258	RABL3	member of RAS oncogene family like 3	signaling	3.700079683	0.002271332
ENSSSCG00000037475	CTSG	cathepsin G	inflammation	3.581407665	0.024589968
ENSSSCG00000015808	ADAM9	disintegrin and metalloproteinase domain-containg protien 9	adhesion	3.426658472	0.018098585
ENSSSCG00000011755	NCEH1	neutral cholesterol ester hydrolase 1	metabolism	3.407326519	0.008197997
ENSSSCG00000037420	TMEM170B	transmembrane protein 170B	signaling	3.37910639	0.049163621
ENSSSCG00000022131	KCTD6	potassium channel tetramerization domain containg 6	signaling	3.359860673	0.020781425
ENSSSCG00000031847	RBM28	RNA binding motif 28	transcriptional regulation	3.336667366	0.012149562
ENSSSCG00000012172	ACOT9	acyl-CoA thioesterase 9	metabolism	3.315946983	0.032564652

Supplementary Table S1 (CONTINUATION). Blood $CD4^+$ T cell total mRNAs profiled using RNA-seq. The pairwise differential gene expression analysis between non-challenged MOCK and challenged groups (*C. suis* challenged, *C. suis* challenged + vaccinated and *C. suis* challenged + Tri Adjuvant vaccinated) was assessed using DESeq2. Significance of the canonical pathway was assessed using Fisher's exact test. All multiple testing was adjusted by Benjamini-Hochberg.

Ensemble Gene ID	Gene Symbol	Gene Name	General Function	Log2 Fold Change	Adjusted p value
ENSSSCG00000013861	SLC35E1	solute carrier family 35 member E1	molecular transport	3.314660992	0.00877453
ENSSSCG00000038493	PFDN1	prefolding subunit 1	molecular transport	3.263456994	0.026294999
ENSSSCG00000035193	MRPS23	mitochondrial ribosomal protein S23	survival	3.162095174	0.048396984
ENSSSCG00000037325	UBIAD1	ubiA prenyltransferase domain containing 1	metabolism	3.127636805	0.027705123
ENSSSCG00000005011	NEMF	nuclear export mediator factor	molecular transport	3.113457185	0.004908871
ENSSSCG00000002305	EXD2	exonuclease 3'-5' domain containing 2	DNA repair	3.088641479	0.032943414
ENSSSCG00000015892	PSMD14	proteasome 26S subunit, non-ATPase 14	protein degradation	3.054264429	0.016268598
ENSSSCG00000033162	UBAC1	ubiquitin-associated domain-containing 1	protein degradation	3.025612433	0.0122442
ENSSSCG00000009193	SMARCAD1	SWI/SNF-related, matrix-associated actin-dependent regulator of chromatin, subfamily A, containing DEAD/H Box 1	DNA binding	3.001023959	0.002894647
ENSSSCG00000016226	FARSB	phenylalanyl-tRNA synthetase beta chain	metabolism	2.994310907	0.00371746
ENSSSCG00000012131	MOSPD2	motile sperm domain containing 2	metabolism	2.9913784	0.006024667
ENSSSCG00000009305	GTF3A	general transcription factor 3A	transcription	2.987510154	0.036921829
ENSSSCG00000028345	ZNF33B	zing finger protein 33B	signaling and metabolism	2.966858443	0.015945452
ENSSSCG00000004946	ZWILCH	zwilch kinetochore protein	proliferation	2.92507877	0.036921829
ENSSSCG00000032580	MGST1	microsomal glutathione s-transferase 1	metabolism	2.89902142	0.039963149
ENSSSCG00000000844	NFYB	nuclear transcription factor Y subunit beta	transcriptional regulation	2.893050892	0.019602372
ENSSSCG00000002525	TRAF3	TNF receptor associated factor 3	signaling and inflammation	2.885270408	0.029148929
ENSSSCG00000032919	ATG4B	autophagy related 4B cysteine peptidase	autophagy	2.821028399	0.032943414
ENSSSCG00000002937	ZNF420	zing finger protein 420	signaling and metabolism	2.793284015	0.039273246
ENSSSCG00000020885	NUS1	nuclear undecaprenyl pyrophosphate synthetae 1	metabolism	2.769905114	0.02991454
ENSSSCG00000005507	PSMD5	proteasome 26S subunit, non-ATPase 5	protein degradation	2.758698463	0.048977939
ENSSSCG00000005587	NEK6	NIMA related kinase 6	signaling and proliferation	2.717168935	0.04243732
ENSSSCG00000000964	LMF2	lipase maturation factor 2	metabolism	2.685857445	0.031616857
ENSSSCG00000003506	PINK1	PTEN induced kinase 1	signaling	2.662957517	0.045979115
ENSSSCG00000010949	DAPK1	death associated protein kinase 1	signaling and surival	2.635847767	0.029957851
ENSSSCG00000012424	ABCB7	ATP-binding cassete sub-family B, member 7	molecular transport	2.494990364	0.015843827
ENSSSCG00000033295	EIF2S1	eukaryotic translation initiation factor 2 subunit alpha	protein synthesis	2.474632908	0.009531644
ENSSSCG00000011162	LARP4B	La ribonucleoprotein 4B	DNA binding	2.454986159	0.044627204
ENSSSCG00000001667	ZNF318	zing finger protein 318	signaling and metabolism	2.449922752	0.046620743
ENSSSCG00000015590	FLVCR1	feline leukemia virus subgroup C receptor-related 1	molecular transport	2.396401517	0.038596864
ENSSSCG00000013347	PRMT3	protein arginine methyltransferase 3	metabolism	2.357566489	0.033986845
ENSSSCG00000036790	AKAP7	A-kinase anchoring protein	signaling	2.356699873	0.037294235
ENSSSCG00000038895	DCTN6	dynactin subunit 6	molecular transport	2.345543214	0.031545264
ENSSSCG00000033154	ARL6IP5	ADP ribosylation factor like GTPase 6 interacting protein 5	signaling	2.341746948	0.012797427
ENSSSCG00000006346	ATF6	activating transcription factor 6	transcription	2.309316884	0.033964553
ENSSSCG00000002844	PHKB	phosphorylase kinase regulatory subunit beta	signaling	2.294356394	0.01654099
ENSSSCG00000010874	ADSS	adenylsuccinate synthase 2	metabolism	2.272571211	0.031666077
ENSSSCG00000004576	RORA	RAR related orphan recetor A	transcriptional regulation	2.240683079	0.017383661
ENSSSCG00000040954	CSTF3	cleavage stimulation factor subunit 3	transcriptional regulation	2.19786242	0.039135766
ENSSSCG00000004999	MIS18BP1	MIS18 binding protein	DNA binding	2.178375045	0.03583276
ENSSSCG00000011833	DLG1	discs large MAGUK scaffold protein 1	signaling	2.003275128	0.027896597
ENSSSCG00000032357	APPL1	adaptor protein, phosphotyrosine interacting with PH domain and leucine zipper 1	proliferation	1.92155645	0.037191961
ENSSSCG00000002701	MON1B	MON1 homolog B	molecular transport	1.772512299	0.048396984
ENSSSCG00000033115	IFNAR1	interferon alpha and beta subunit 1	signaling and inflammation	1.572971046	0.017506452
ENSSSCG00000006553	UBAP2L	Ubiquitin-associated protein 2 L	protein degradation	1.177037687	0.039579458

[1] no human ortholog

IV. *CHLAMYDIA TRACHOMATIS* LIFE CYCLE AND INNATE IMMUNE RESPONSE DURING INFECTION IN PORCINE OVIDUCT EPITHELIAL CELLS

Amanda Amaral[1,2], Bryan Mcqueen[3], Kim Bellingham-Johnstun[4], Caroline Laplante[4] and Tobias Käser[1,2,*]

[1] Department of Population Health and Pathobiology, College of Veterinary Medicine, North Carolina State University, 1060 William Moore Drive, Raleigh, NC 27607, USA
[2] Comparative Medicine Institute, North Carolina State University, 1060 Willian Moore Drive, Raleigh, NC 27607, USA
[3] Department of Microbiology and Immunology, University of North Carolina, 125 Mason Farm Road, Chapel Hill, NC 27599, USA
[4] Department of Molecular Biomedical Sciences, College of Veterinary Medicine, North Carolina State University, 1060 William Moore Drive, Raleigh, NC 27607, USA

* Correspondence: tekaeser@ncsu.edu; +1-919-513-6352

Abstract: *Chlamydia trachomatis (C. trachomatis)* is the most prevalent bacterial sexually transmitted disease in the world. Untreated infections can lead to ectopic pregnancy and infertility. Swine is a powerful biomedical animal model due to its similarities to humans from both a physiological and immunological perspective. Although the host-pathogen interactions between *C. trachomatis* and genital tract epithelial cells in mice and humans are well-understood, its pathogenesis in swine remains poorly characterized. Therefore, the main goal of this study was to provide a detailed analysis of *C. trachomatis* infection in porcine oviduct epithelial cells (pOECs) and the induced innate immune response. Here, we infected isolated pOECs with *C. trachomatis* and determined the timeline of infection by confocal microscopy, flow cytometry, and qPCR. In addition, the immune response of pOECs was studied using NanoString gene expression. Our results indicate that, similar to what is observed in human genital tract cells, *C. trachomatis* completes its life cycle in pOECs within 48 hours and that infection induced an increased mRNA expression of the chemokines CXCL10, CXCL11, CCL20 and RANTES, and the interferon-regulated genes MX1, MX2 and CMPK2. These similarities

support that primary pOECs represent an excellent cell culture model to study the pathogenesis and innate immune response of genital *C. trachomatis* infections.

Keywords: *Chlamydia trachomatis*; porcine oviduct epithelial cell; life cycle; innate immune response.

1. Introduction

Chlamydia trachomatis (C. trachomatis) is the most prevalent bacterial sexually transmitted disease worldwide [1]. In many cases, patients remain asymptomatic and therefore do not receive treatment [167]. Untreated *C. trachomatis* infections can reach the upper genital tract and infect the Fallopian tubes, leading to increased probability of ectopic pregnancy and infertility [6]. Although chlamydia can cause these serious reproductive problems, there is still no vaccine available.

The development of an effective vaccine against *C. trachomatis* requires improvement in the knowledge about the infection process and the host pathogen interactions. It is already known that chlamydia is an intracellular bacterium with a biphasic life cycle characterized by two forms of chlamydia particles – infectious, non-replicative elementary bodies (EBs), and non-infectious, replicative reticulate bodies (RBs) [18]. Furthermore, the *Chlamydia trachomatis* developmental cycle has been well described in mice [24,25] and humans cells [26-30] and nicely summarized over the years [18,31-33]: The EB infects the host cells, mainly epithelial cells, in an endosome called “initial body”. Within the first 2 hours post infection (hpi), the EB differentiates into an RB. Thereafter, the RB divides by binary fission in an “inclusion” [33]; the RB associates with the inclusion membrane and re-differentiates into EBs, which are released from the host cells by lysis or extrusion around 40-48 hpi [18]. The infected epithelial cells react with an innate immune

response including the production of immune effectors like chemokines and cytokines for the recruitment and activation of immune cells against infection [57,168]. Rank et al. [57] demonstrated that endocervical infection with *C. muridarum* induces cervical mRNA expression of chemokines such as CCL20, RANTES, CXCL10 and CXCL11 within the first 24 hours following endocervical infection in mice. Most importantly, Poston et al. [56] demonstrated that the cervical cytokines CXCL10, CXCL11, and RANTES are associated with the increased risk of reinfection with C. trachomatis in women. Furthermore, a recent study has shown an increase in mRNA expression of RANTES, CXCL10 and CXCL11 from apical secretions of primary human Fallopian epithelial cells 48 hours post infection with *C. trachomatis* [168]. In contrast to the data from mice and humans, *C. trachomatis* pathogenesis is less studied in swine – another important animal model.

Swine is a powerful biomedical animal model: Swine have a similar organ's size, physiology, immune system, and hormonal reproductive cycle to humans [14-16]. Swine are also natural host to *C. suis* – a close relative to *C. trachomatis* [13]. Based on these advantages, swine greatly contributed to the study of human *C. trachomatis* infections [105]. But while most *in vivo* studies using pigs or minipigs focused on *C. trachomatis* vaccination [75,76,96,97,128-130,169] or the analysis of the adaptive immune response to *C. trachomatis* [71], pigs have rarely been used for *in vitro* studies on chlamydia pathogenesis and host-pathogen interactions. This lack of *in vitro* studies in pigs represents a great underutilization of another big advantage of pigs – the vast access to porcine blood and genital tract tissue. The pig is used as a food animal and porcine blood and genital tracts are by-products of meat production. Thus, primary immune and other tissue cells can be collected at nearly no cost at slaughter plants and without the need to sacrifice

animals for research. This is a strong advantage in accordance with the 3R principle – replacement, refinement, and reduction [17].

Guseva et al. used this free access and the similarities of pigs with humans to study the hormonal influence on *C. trachomatis* infections in primary cultures of porcine genital tract epithelial cells [170]. They showed that *C. trachomatis* can infect epithelial cells isolated from the porcine cervix, uterus and uterine horns; and they concluded that "primary swine genital epithelia cultured ex vivo appear to be an excellent cell model for dissecting the hormonal modulation of several aspects of chlamydial pathogenesis and infection". Nevertheless, detailed studies on the life cycle and pathogenesis of *C. trachomatis* in porcine genital tract epithelial cells and their immune response are lacking. In addition, Guseva et al. studied *C. trachomatis* infection in epithelial cells isolated from the cervix, uterus and uterine horns but not in porcine oviduct epithelial cells (pOECs) – the counterparts to human Fallopian tubes, the main site of *C. trachomatis* pathology.

Therefore, the goal of this study was not only to provide a detailed analysis of *C. trachomatis* infection but also to study the induced innate immune response in infected pOECs. To that end, pOECs were isolated and infected with *C. trachomatis*. Infection was followed by confocal microscopy, flow cytometry, and qPCR. In addition, the immune response of pOECs was studied using NanoString gene expression covering 31 of the most strongly altered immune genes within *C. trachomatis* infected women (personal communication). Our results indicate that *C. trachomatis* completes its life cycle in pOECs within 48 hours, which corresponds to their life cycle in human cells [29,30]. Furthermore, *C. trachomatis* infection of pOECs induced an immune response dominated by an increased expression of the chemokines CXCL10, CXCL11, CCL20 and RANTES, and the interferon-regulated genes MX1, MX2 and CMPK2. This data

demonstrates similarities of the *C. trachomatis* life cycle and the induced immune response between murine, human, and porcine genital tract epithelial cells. These similarities contribute to the validation of the pOECs as a cell culture model for mechanistic studies into *C. trachomatis* infection and immunity in genital tract epithelial cells.

2. Materials and Methods

2.1. Porcine oviduct epithelial cells isolation and culture

For pOECs isolation, porcine oviducts were collected from six sows at a local slaughterhouse (City Packing/Neese's Sausage Co., Burlington, NC, USA) immediately after slaughter. Oviducts were washed with 1x phosphate buffered saline (PBS, Corning, NY, USA) containing 1X antibiotic-antimycotic (anti-anti, Corning), opened to expose the epithelial layer and cut in pieces of approximately 1 cm. Oviduct pieces were then added into a tube with 20 ml of cell isolation media composed of DMEM/F-12 media (Corning), 1x anti-anti, dispase (v/v 1:200,Corning), and pancreatin (v/w 1:83, MP Biomedicals, Irvine, California, USA). The tissue was incubated at 4°C overnight with continued shaking.

After incubation, the lumen of the oviduct pieces was gently scraped with a scalpel blade to isolate the epithelial cells. Scraped cells and isolation media was collected into a tube and the solution was neutralized with fetal bovine serum (FBS, v/v 1:2, VWR, Radnor, PA, USA). Cells were then centrifuged at 600g for 5 minutes at 4°C and pellet was resuspended with acutase (v/v 1:3, Corning). The cell solution was then incubated at 37°C for a total of 30 minutes, with agitation after 15 minutes. Cells were centrifuged at 600g for 5min at 4°C and pellet was resuspended in 20ml of pOECs media composed of DMEM/F-12 media, 1X anti-anti, 5% FBS,

0.0025% epidermal growth factor (EGF, Corning, REF: 354001), and 0.1% insulin, transferrin, selenium (ITS, Corning).

Cell suspension was then seeded in T-75 flasks (Sarstedt, Nümbrecht, Germany) at the density of 8 x 10^6 cells/flask and incubated at 37°C until about 70-80% confluency (about 48 hours). After incubation, cells were washed twice with 1x PBS and trypsinized with 0.25% trypsin (Corning) for about 15 minutes at 37°C. Trypsinization was stopped with pOECs media. Cells were transferred to a tube and centrifuged at 500g for 8 minutes at 4°C. Next, cell pellet was resuspended in freezing media composed of 50% DMEM/F-12 media, 40% FBS, and 10% dimethyl sulfoxide (DMSO, Corning), and stored at -80°C.

For pOECs culture, frozen pOECs were thawed, washed with DMEM/F-12 media, resuspended in pOECs media, and seeded in 24-well plates (Corning, REF 3337) in the presence or absence of poly-D-lysine coated coverslips at the density of 2 x 10^5 cells/well. The coverslips were used to facilitate confocal microscopy analysis of *C. trachomatis* infection in pOECs. Cells were then incubated at 37°C until about 70-80% confluency (about 24 hours).

2.2. *Chlamydia trachomatis*

The *C. trachomatis* serovar E strain Bour (ATCC VR-348B) was propagated in HeLa cells using standard technique [139] and purified as previously described [140]. Bacteria were titrated on HeLa cells as previously described [141].

2.3. *Chlamydia trachomatis* infection of porcine oviduct epithelial cells

After culture for about 24 hours, pOECs were infected with *C. trachomatis* (MOI 0.5) for 6, 12, 24, 36, 48, and 72 hours post-infection (hpi). For each time point, non-infected pOECs

were used as controls. Cell culture supernatants were collected at each time point and stored at −20°C until used to determine the release of *C. trachomatis* particles via qPCR.

2.4. Fluorescence confocal microscopy

C. trachomatis infection in pOECs were evaluated via fluorescence confocal microscopy as previously described [140]. Briefly, cells were washed with 1x PBS, fixed and permeabilized with methanol (Millipore-Sigma, USA), and stained with: i) anti-chlamydia antibody clone ACI (LSBio, USA) and the secondary anti-mouse IgG3-Alexa 488 antibody (Southern Biotech, USA); ii) anti-claudin 4 antibody (Abcam, Cambridge, USA) and the secondary anti-rabbit polyclonal-Alexa 555 (Southern Biotech, USA); iii) 4',6-diamidino-2-phenylindole (Tocris, USA). Fluorescence images were acquired with a Nikon Eclipse Ti microscope equipped with a 100×/numerical aperture (NA) 1.49 HP Apo TIRF objective (Nikon), a CSU-X1 (Yokogawa) confocal spinning-disk system, 405/488/561/647 nm solid state lasers, and an electron-multiplying cooled charge-coupled device camera (EMCCD IXon 897, Andor Technology). The Nikon Element software was used for acquisition.

2.5. Flow cytometry

C. trachomatis life cycle in pOECs were also monitored via flow cytometry as previously described [140]. Briefly, cells were washed with 1x PBS, trypsinized and stained with Live/Dead Near infra-red. Next, cells were fixed and permeabilized with Fix/Perm kit (eBiosciences, USA), and then stained with anti-chlamydia antibody clone ACI and the secondary anti-mouse IgG3-Alexa 488 antibody (Southern Biotech). Cells were recorded on a Cytoflex flow cytometer using the CytExpert software (Beckman Coulter, USA). Data analysis was performed with FlowJo

version 10.5.3 (FLOWJO LLC). The gating hierarchy used for this analysis is shown in Supplementary Figure S1. The *C. trachomatis* gate was set based on non-infected control cells.

2.6. Detection of chlamydia via qPCR

DNA from pOECs supernatant were used to measure the chlamydia shedding via Taqman qPCR assay. Prior to performing the qPCR, DNA was isolated from pOECs supernatant as previously described [140]. Primers and probe for chlamydia used in this study were previously design [140]: i) Fwd primer: CCTAAGTTGAGGCGTAACTG, ii) Rv primer: GCCTACTAACCGTTCTCATC, iii) Probe: FAM-TTAAGCACGCGGACGATTGGAAGA-TAMRA. A total of 5µl DNA was mixed to 7.5µl of KAPA PROBE Fast qPCR Master (KAPA Biosystems, USA), 0.3µl of each primer, 0.3µl of probe (10µM), and 1.6µl of nuclease free water. qPCR conditions were as follow: 95°C for 3 minutes, followed by 40 cycles with denaturation at 95°C for 10 seconds and annealing/elongation for 30 seconds at 60°C. The Taqman qPCR was run on a qTOWER3G qPCR machine (Analytik Jena, Germany). A standard curve of chlamydia gBlocks (IDT® Integrated DNA Technologies, USA) was included on every plate to determine the number of chlamydia particles.

2.7. NanoString

The innate immune response of pOECs to *C. trachomatis* infection was monitored using NanoString gene expression analysis (NanoString Technologies, Inc., USA). At each time point, pOECs were washed with 500µl of 1x PBS/well and 500 µl of Trizol (TRIzol LS Reagent, Invitrogen, USA) was added into each well. Total RNA isolation using Trizol was preformed according to the manufacturer's instructions. RNA was eluted in 20 µl nuclease-free water and RNA purity and quantity were determined using a Nanodrop 1000 (Thermo Fisher).

The mRNA expression of immune parameters was then measured via NanoString nCounter platform by calculating the mRNA fold change between *C. trachomatis* infected and non-infected pOECs. mRNA input was normalized based on Nanonodrop value to 100 ng and processed according to the nCounter MAX/FLEX System User Manual (NanoString Inc., MAN-C0035-07). Briefly, normalized mRNA was hybridized with biotin-labeled capture probes and fluorescently labeled reporter probes for 19 hours at 65°C. Following hybridization, samples were transferred into a NanoString cartridge and loaded onto the nCounter Prep Station instrument set on high sensitivity. Next, cartridge was transferred into the nCounter Digital Analyzer instrument, where excess capture probe and reporter probe were removed, and hybridized mRNAs were immobilized for imaging (555 fields of view). The panel of genes investigated are listed in Table 1. Following image acquisition, mRNA counts were analyzed using nSolver analysis software.

2.8. Statistical analysis

For the NanoString gene expression analysis, data was analyzed by NanoString n solver (nSolver 4.0 Analysis Software, Inc., Seattle, WA, USA), which make comparisons between infected and non-infected cells using two-tailed t test. For the rest of the data, statistical analyses were performed by GraphPad Prism (GraphPad 8.0 Software, Inc., La Jolla, CA, USA)using repeated-measures one-way ANOVA with hours post infection as the one factor, and post hoc multiple comparisons using Tukey's test. Differences were defined significant (*) for $p < 0.05$.

3. Results

The goal of this study was to determine the *C. trachomatis* life cycle and the innate immune response in pOECs. For that end, pOECs were infected with *C. trachomatis* for 0, 6, 12, 24, 36, 48, and 72 hours, and chlamydia infection was determined via a combination of fluorescence confocal microscopy and flow cytometry (Figure 1). In addition, the innate immune response was determined via NanoString gene expression analysis (Figures 2, and 3).

3.1. *Chlamydia trachomatis* life cycle in pOECs

Chlamydia infection was first determined by fluorescence confocal microscopy. Confocal micrographs showed that *C. trachomatis* had entered pOECs by 6hpi (Figure 1A). At this early stage of infection, the inclusions were small and distributed across the cell cytoplasm. By 24hpi, inclusion bodies were much larger and localized next to the nucleus. At 36 hpi, the inclusions had further increased in size with visible increase in fluorescence intensity, indicating an increase in the density of chlamydial bodies. While the inclusion further grew over time, at 72hpi, there was a decrease in the inclusion bodies fluorescence intensity, indicating a lower density of *C. trachomatis* bodies (Figure 1A).

We also used flow cytometry to corroborate these results (Figure 1B and 1C). At 6hpi, 44% (median) of pOECs were infected with *C. trachomatis* (Figure 1C). The frequency of infected cells stayed relatively constant with a non-significant decline towards the end of this study's time kinetic. Within infected cells, the median fluorescence intensity (MFI), which indicates the content of *C. trachomatis* particles per cell, increased ~15% from 6 to 36 hpi and then declined ~16% from 36 to 72 hpi (Figure 1C).

In addition to monitoring the *C. trachomatis* life cycle in the pOECs, we monitored the release of *C. trachomatis* from pOECs into the supernatant (Figure 1D and 1E). First, we

extracted DNA from the *C. trachomatis*-infected pOECs supernatants and quantified the chlamydia genome copy numbers by qPCR (Figure 1D). While no chlamydia genome copies could be detected prior to inoculation (0 hpi), we detected a median genome copy number of 30 with a range from 19 to 81 at 6 hpi. The median genome copy numbers were statically the same until 36 hpi. By 48 and 72 hpi, the median chlamydia genome copy numbers increased significantly to 187 and 393, respectively. To corroborate these *C. trachomatis* genome copy number data, we used the cell culture supernatants from the *C. trachomatis*-infected pOECs to infect HeLa cells; and we measured the *C. trachomatis* infection of HeLa by flow cytometry (Figure 1E). From 6 to 36 hpi, there was 5-11% of infection; and at 48 hpi, this percentage increased to 17%. By 72 hpi, the infection rate significantly increased to 37%. This data confirm that *C. trachomatis* can infect pOECs and complete its life cycle after ~48 hpi.

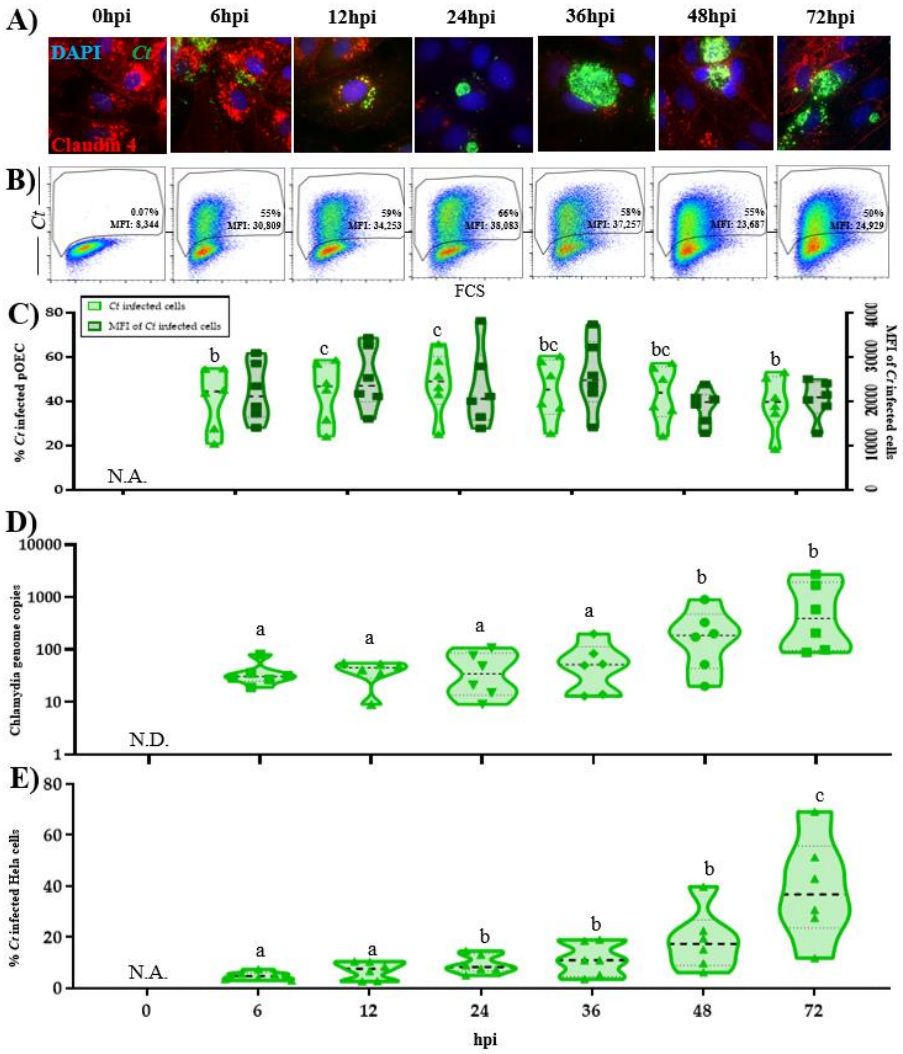

Figure 1. Time kinetic of *Chlamydia trachomatis* (*Ct)* infection in porcine oviduct epithelial cells (pOECs). pOECs were infected with *Ct* (MOI 0.5) and *Ct* multiplication within the cells and release was analyzed after 0, 6, 12, 24, 36, 48, and 72 hours post-infection (hpi) by (A) fluorescence confocal microscopy, (B to D) flow cytometry, and qPCR (E). (A) Cells were fixed and permeabilized with ice-cold methanol and stained for: i) *Ct* using an FITC-conjugated anti-chlamydial LPS antibody (green), ii) claudin 4 as a counterstain (red), and iii) DNA using 4,6-diamidino-2-phenylindole (DAPI, blue). (B) Cells were also trypsinized, fixed and permeabilized, and stained for *Ct* via indirect immunostaining for flow cytometry. Results show the size of the cells (FSC, x-axis) vs the *Ct*-content in the cells (*Ct*, y-axis). The percentage of infected cells and the median fluorescence intensity (MFI) of *Ct* are indicated. (C) The gate of *Ct* infected cells in panel B was used to calculate the percentage of infected cells (light green, left y-axis) and MFI (dark green, right y-axis). (D) Cell supernatant was used to monitor the release of *Ct* particles by measuring chlamydia DNA content via qPCR. N.D.: non detected. (E) The release of *Ct* particles was also monitored by measuring viable chlamydia particles via flow cytometry. Values for individual pigs, medians, and 25/75 percentiles are shown. Comparisons were made using one-way ANOVA test and Tukey's post-test. The time points (hpi) with different letters are significant different ($p < 0.05$).

3.2. Innate immune response of pOECs to *Chlamydia trachomatis* infection

To investigate the innate immune response of pOECs to *C. trachomatis* infection, mRNA from non-infected and infected cells were tested for the expression of 31 immune related molecules (personal communication) via NanoString gene expression analysis (Table 1).

Table 1. Gene regulation induced by *Chlamydia trachomatis* infection in porcine oviduct epithelial cells (pOECs). mRNA fold changes between *Chlamydia trachomatis* infected and non-infected pOECs was calculated via NanoString at 6, 12, 24, 36, and 48 hours post infection (hpi). Data was analyzed by NanoString n solver software by comparing gene counts between neg and pos samples. Gray cells indicate significance of $p < 0.05$ using a two-tailed t test.

Gene	6hpi	12hpi	24hpi	36hpi	48hpi	*Average by gene*
ADAMTS9	1.83	1.42	1.73	1.12	-1.37	0.95
CCL20	2.80	2.43	5.16	3.83	3.82	3.61
CCL4	5.49	3.07	2.91	1.86	2.53	3.17
CMPK2	1.20	1.47	2.32	2.59	1.98	1.91
CSF3	1.60	1.93	1.64	1.37	1.26	1.56
CXCL10	1.59	3.86	7.95	4.50	2.30	4.04
CXCL11	1.18	1.97	4.81	3.45	1.90	2.66
CXCL8	1.18	-1.01	1.12	1.50	1.99	0.96
CXCL9	-1.15	-1.28	1.11	-1.20	1.02	-0.30
EBI3	-1.08	-1.23	1.36	1.12	1.14	0.26
Flt-3L	-1.01	1.14	1.04	1.14	1.28	0.72
HERC5	1.09	1.35	1.89	1.93	1.70	1.59
ICAM1	1.28	1.23	1.30	1.36	1.20	1.27
IL-1 alpha	1.36	1.21	1.24	1.18	1.44	1.29
IL-10	-1.23	1.03	-1.41	-1.29	-1.39	-0.86
IL-15	1.06	1.52	1.60	1.39	1.11	1.34
IL-16	-1.03	1.22	-1.02	1.14	1.05	0.27
IL-1RA	1.02	1.39	1.49	1.03	1.29	1.24
IL-6	1.28	1.26	1.70	1.58	1.49	1.46
IL-7	1.17	1.21	1.85	1.84	1.37	1.49
MMP-2	1.06	-1.11	1.30	1.18	-1.03	0.28
MMP-9	1.23	1.09	-1.11	1.09	1.43	0.75
MX1	1.11	1.39	2.31	2.53	1.98	1.86
MX2	1.38	2.12	3.49	2.66	1.74	2.28
NEURL3	-1.06	-1.19	-1.08	-1.36	1.12	-0.71
OAS2	1.11	1.30	1.92	2.40	1.84	1.71
RANTES	1.60	2.88	5.42	7.42	4.08	4.28
SAA2	-2.55	1.08	-1.20	-1.39	1.02	-0.61
TGF-b	1.05	-1.08	1.09	-1.03	-1.14	-0.22
TNF-alpha	-1.13	-1.16	1.73	-1.23	-1.42	-0.64
VEGF	1.08	1.06	1.21	1.00	-1.04	0.66
Average by hpi	0.80	0.95	1.75	1.43	1.15	

mRNA fold changes between *Chlamydia trachomatis* infected (pos) and non-infected (neg) highlighted in gray indicates significance of $p < 0.05$ using a two-tailed t test.

C. trachomatis infection induced the highest mRNA upregulation compared with non-infected pOECs at 24 hpi (Table 1), which is also the time point with the highest frequency of infected cells (Figure 1C). Within the 31 investigated genes, the highest mRNA fold changes were detected for the interferon regulated genes MX1, MX2, and CMPK2, and for the chemokines CCL20, RANTES, CXCL10, and CXCL11 (Figures 2 and 3, respectively). Although CCL4 had high mRNA fold change (average of 3.17), this chemokine was not considered for analysis because it had a low gene count in NanoString (maximum of 25 counts at 6hpi, Supplementary Table S1).

For the interferon regulated genes, *C. trachomatis* infection induced a significant increase in the MX1 and MX2 mRNA fold change (between ~ 2 and 3.5) at 12, 24 and 36hpi, while CMPk2 mRNA fold change increased between 36 and 48 hpi to around 2.6 and 2, respectively (Figure 2). For the chemokines, there was a significant increase in the CXCL10 mRNA fold change at 24hpi (7.95) and in CXCL11 at 36hpi (3.45) (Figure 3). In addition, a significant increase in the CCL20 mRNA fold change was observed at 6, 24, 36, and 48hpi, with the pick at 24 hpi (5.16). *C. trachomatis* infection also induced a significant increase in RANTES mRNA fold change between 24 hpi and 48hpi, with the highest fold change at 36hpi (7.42).

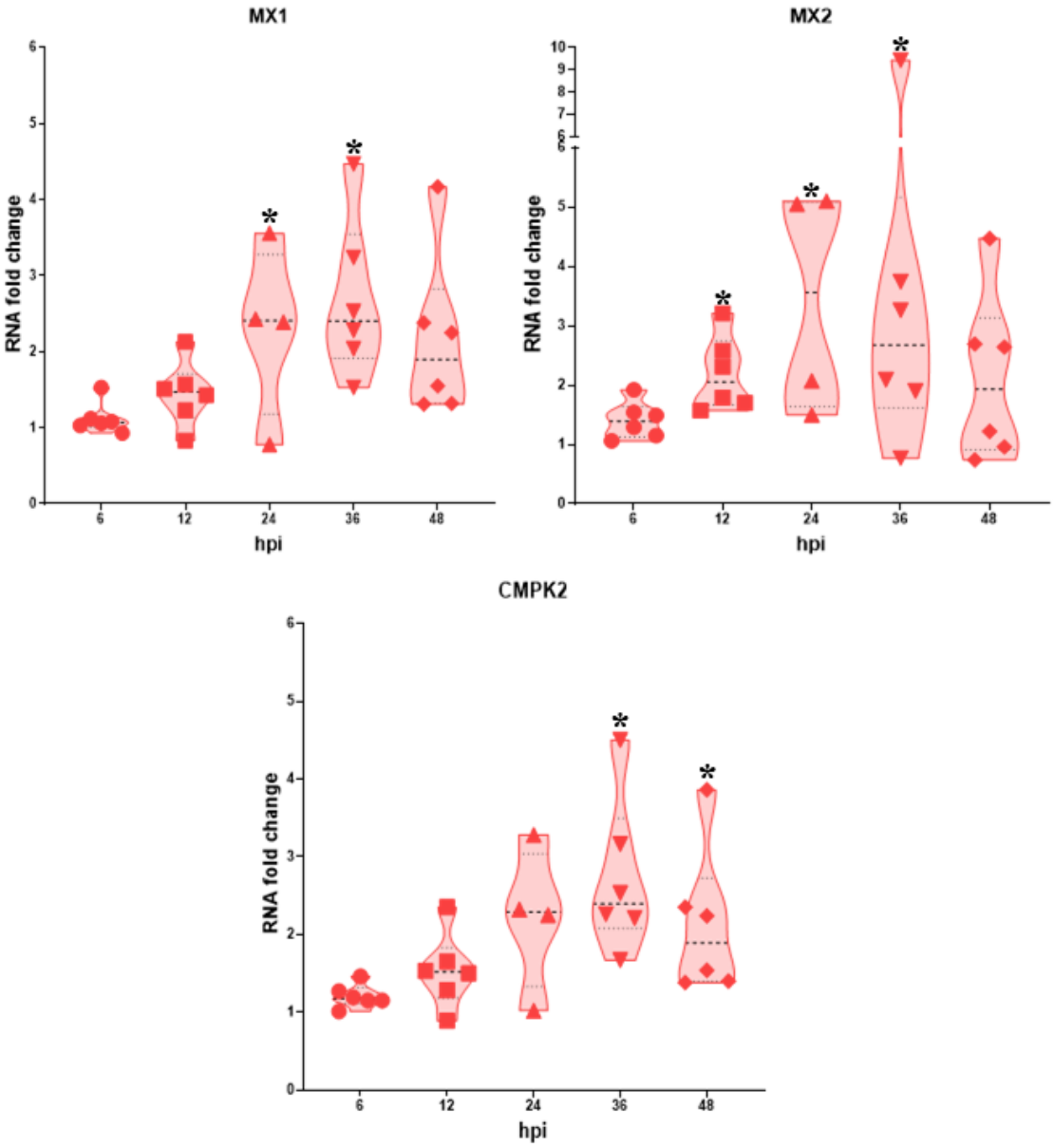

Figure 2. Interferon regulated genes mRNA fold changes in porcine oviduct epithelial cells (pOECs). mRNA fold changes between *Chlamydia trachomatis* infected and non-infected pOECs was calculated via NanoString at 6, 12, 24, 36, and 48 hours post infection (hpi). Values for individual pigs, medians, and 25/75 percentiles are shown. Data comparisons between non-infected and infected cells were performed by the NanoString n solver software using a two-tailed t-test. *$p < 0.05$.

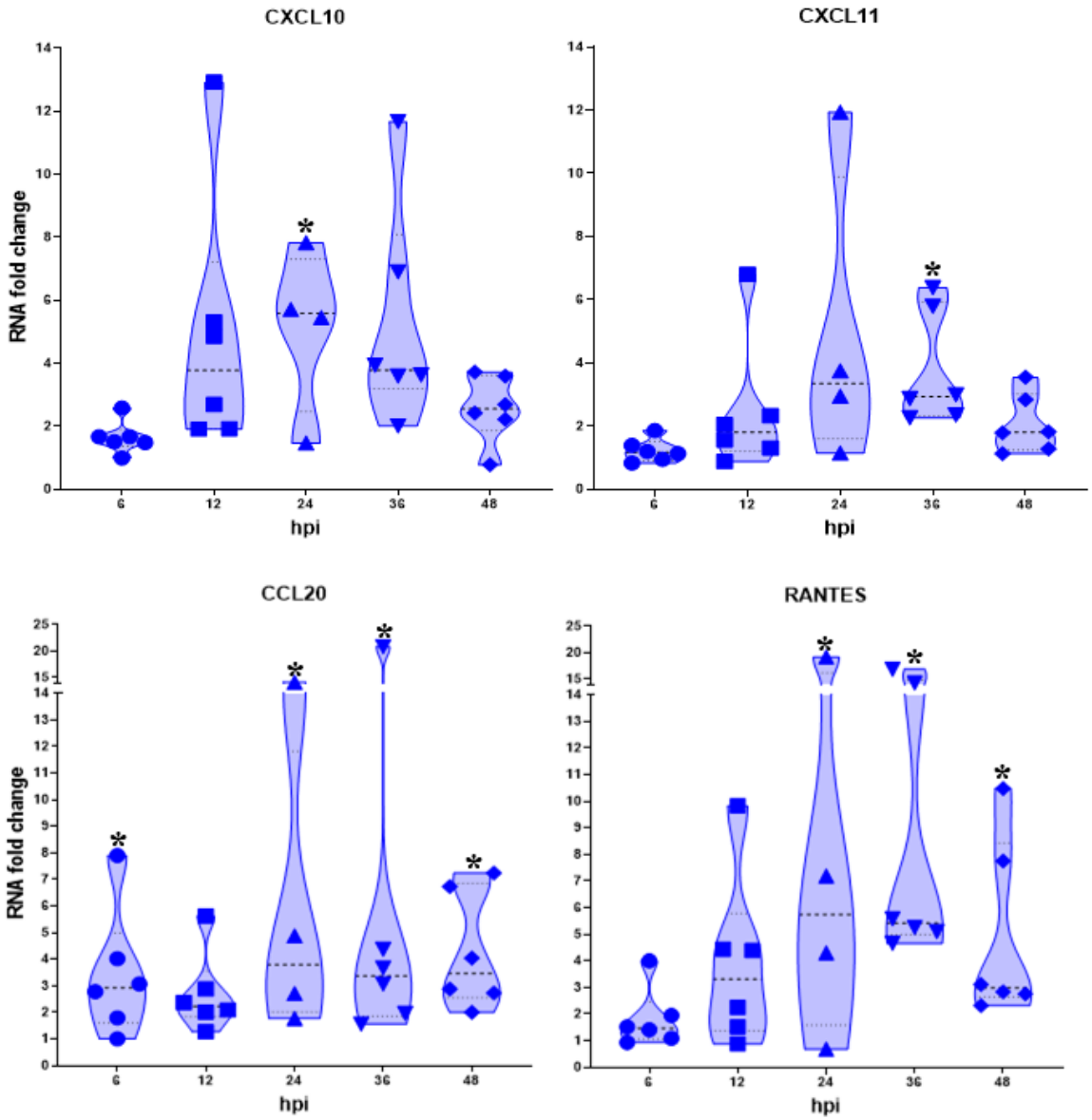

Figure 3. Chemokine mRNA fold changes in porcine oviduct epithelial cells (pOECs). mRNA fold changes between *Chlamydia trachomatis* infected and non-infected pOECs were calculated via NanoString at 6, 12, 24, 36, and 48 hours post infection (hpi). Values for individual pigs, medians, and 25/75 percentiles are shown. Data comparisons between non-infected and infected cells were performed by the NanoString n solver software using a two-tailed t-test. *$p < 0.05$.

4. Discussion and conclusions

While *C. trachomatis* infection in porcine genital tract epithelial cells has been previously described [170], this study provides a detailed analysis of the life cycle of *C. trachomatis* in pOECs, the counterpart of human Fallopian tube epithelial cells. To facilitate the utilization of the relevant pig model for *C. trachomatis* pathogenesis and innate immune response analysis, we characterized the life cycle of *C. trachomatis* in pOECs as well as the induced innate immune response.

4.1. *Chlamydia trachomatis* life cycle in pOECs

Using confocal microscopy and flow cytometry, we demonstrated that *C. trachomatis* can complete its life cycle in pOECs: Infection takes place within the first six hours of inoculation, chlamydial load peaks ~24 hpi and while the inclusion continues to grow until 72 hpi, chlamydial load actually decreases at the later time points probably due to the extrusion of chlamydial EBs (Figure 1 A-C). This timeline is in accordance with the developmental cycle of *C. trachomatis* in human cells [18,31-33].

To ensure that the completion of the *C. trachomatis* life cycle leads to the release of infectious chlamydial EBs, we analyzed the presence of *C. trachomatis* in the supernatants of these cultures not only by qPCR but also by using the supernatants to infect HeLa cells. Our results show that the chlamydia genome copy numbers in the supernatants of *C. trachomatis*-infected pOECs increased starting at 48 hpi (Figure 1D). Therefore, using these supernatants to infect HeLa cells not only confirmed the release of *C. trachomatis* particles after 48 hpi, but also demonstrated that the released particles were indeed infectious EBs (Figure 1E). The start of the release of infectious EBs starting ~48 hpi is also in accordance with the timeline described in human cells [18,31-33].

In summary, our results demonstrate that *C. trachomatis* completes its life cycle in pOECs with the release of infectious EBs within 48 hours. This timeline corresponds to the developmental cycle of *C. trachomatis* in human cells [29,30]; and it supports the use of the pOECs to study *C. trachomatis* mechanisms of infection.

4.2. Innate immune response of pOECs to *Chlamydia trachomatis* infection

To investigate the innate immune response against *C. trachomatis* in pOECs, we isolated mRNA from non-infected and infected cells over time and measured the expression of 31 genes related with chlamydia infection (personal communication) via NanoString gene expression (Table 1). Compared with non-infected cells, infected cells have a significant increase in the mRNA expression of interferon regulated genes (Figure 2), and chemokines (Figures 3).

C. trachomatis infection induced a significant increase in the mRNA expression of the interferon regulated genes MX1, MX2, and CMPK2 (Figure 2). As in our study, *in vitro* studies using murine genital tract epithelial cells have shown that *C. muridarum* infection upregulates the mRNA expression of MX1 and MX2 *[171]*. MX proteins are GTPases found in almost all vertebrates and best known for its anti-virus activities [172]. Multiple studies have demonstrated an effect of Mx protein in pathogen replication by interference with transcription and translation [172]. In addition, human studies have indicated a role of MX1 and MX2 in ocular *C. trachomatis* infection by showing their upregulation in the ocular conjunctiva of humans infected with *C. trachomatis [173]*. Although no studies have demonstrated the effect of MX proteins in chlamydia infection, it is possible that the upregulation of MX1 and MX2 observed in this *in vitro* study was an attempt of the pOECs to limit chlamydia replication. Studies using murine genital tract epithelial cells have also shown an upregulation of CMPK2 mRNA upon *C. muridarum* infection [174]. CMPK2 is an enzyme that supplies deoxyribonucleotides for the

synthesis of mitochondrial DNA (mtDNA) [175]. Furthermore, it has been demonstrated that LPS induces murine macrophage CMPK2-dependent mtDNA synthesis, which enables the activation of the pattern recognition receptor NLRP3 inflammasome [176]. Therefore, we can speculate that CMPK2 could also play a role in chlamydia infection in our pOECs by inducing the activation of NLRP3 inflammasome via chlamydia LPS.

Chlamydia infection also induced a significant mRNA upregulation of the chemokines CCL20, RANTES, CXCL10, and CXCL11 (Table 1 and Figure 3). Our results show an upregulation of CXCL10 and CCL20 at 24 hpi, and CXCL11 at 36 hpi. These results are in accordance with Rank et al. [57], who demonstrated that endocervical infection with *C. muridarum* induces an upregulation of CXCL10, CXCL11, and CCL20 mRNA in the mouse cervix at 24 hpi. CXCL10 and CXCL11 are part of the family of high homology chemokines that binds to the CXCR3 chemokine receptor, while CCL20 binds to its receptor CCR6, both receptors expressed in T cells [177,178]. Furthermore, there was an increase in RANTES mRNA fold change between 24 and 48 hpi (Figure 3). RANTES (or CCL5) binds to its receptor CCR5, also expressed in T cells [179]. This chemokine has also shown to be upregulated in the culture supernatant of primary human Fallopian tube epithelial cells infected with *C. trachomatis* for 48 hour [168]. In addition, Olive et al. [165] showed that CXCR3 and CCR5 are both required for T cell mediated protection against *C. trachomatis* infection in the murine genital mucosa. In summary, these chemokines have an important function in the chlamydia infection immune response: to attract T cells to the site of infection. This function explains their production by chlamydia infected cells including *C. trachomatis*-infected pOECs: These chemokines shall attract T cells into the genital tract to start the adaptive immune response against *C. trachomatis*, especially by IFN-γ producing tissue-homing CD4 T cells – the main adaptive immune

responders against genital *C. trachomatis* infection [70,180,181]. We did not detect a significant RNA upregulation in some cytokines frequently associated with chlamydia infection, such as IL-6, IL-8, and TNF-a. Similarly, these same cytokines were also not upregulated in primary human Fallopian tube epithelial cells after 48 hpi with *C. trachomatis [168]*. Therefore, our data reflects findings of both, murine *in vivo* models as well as human *ex vivo* and *in vitro* models; and hence, they justify the use of pOECs to study the innate immune response to genital *C. trachomatis* infection.

In conclusion, our results demonstrate that *C. trachomatis* can complete its life cycle in pOECs with the release of infectious EBs. In addition, both the *C. trachomatis* life cycle and innate immune response in pOECs resemble their counterparts in the murine model as well as in human genital *C. trachomatis* infections. Based on these similarities, primary pOECs represent an excellent model to study the pathogenesis and innate immune response of genital *C. trachomatis* infections.

Supplementary figure and table:

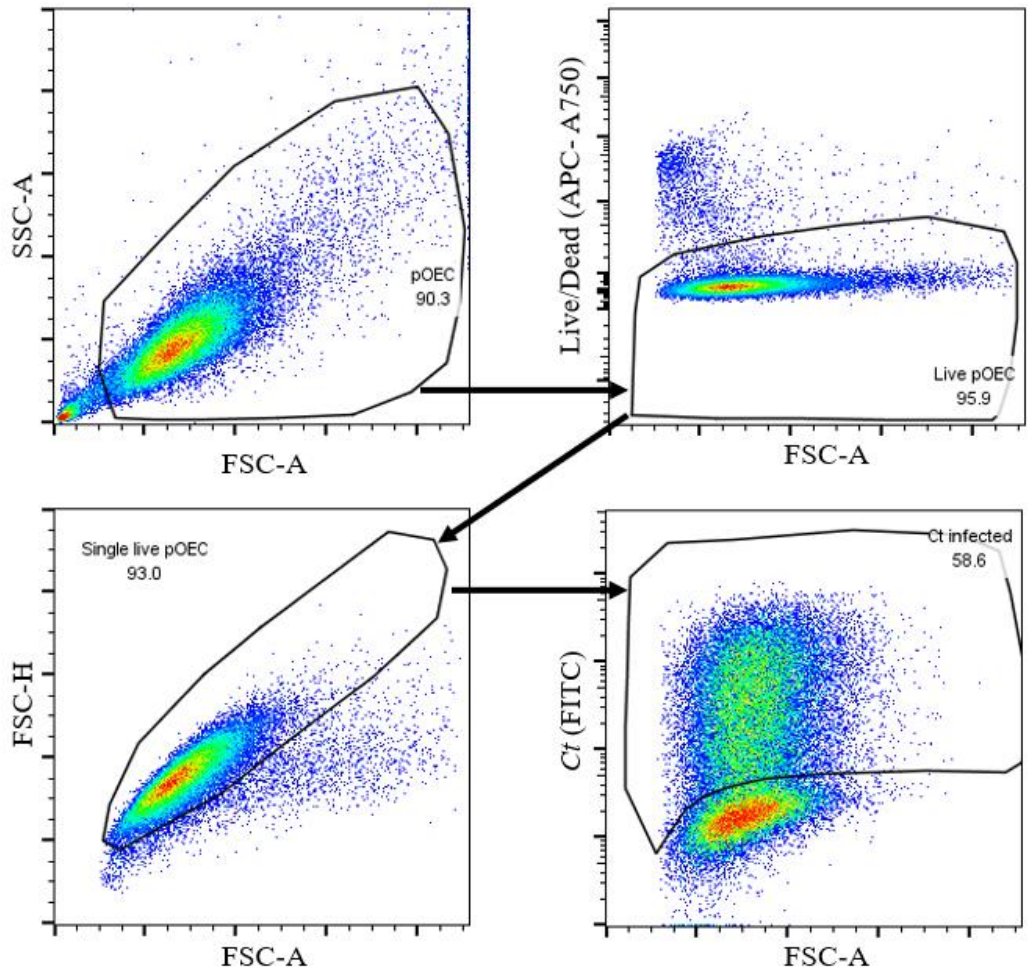

Supplementary Figure S1. Gating hierarchy for *Chlamydia trachomatis* (*Ct*) infection analysis via flow cytometry. Porcine oviduct epithelial cells (pOECs) were infected with *Ct* (MOI 0.5) for 0, 6, 12, 24, 36, 48, and 72 hours post infection. Cells were trypsinized, fixed and permeabilized, and stained for *Ct* via indirect immunostaining for flow cytometry. pOECs were identified by cell size (FSC-A) and granularity (SSC-A). Live cells were then identified by a gate on Live/Dead Near infra-red staining. Next, doublets were excluded by an FSC-A (area)/FSC-H (height) gate. *Ct* infected pOECs were identified via FITC-conjugated anti-chlamydial LPS antibody. Gating is based on non-infected control cells.

Supplementary Table S1. Chlamydia immune related gene count and fold change in porcine oviduct epithelial cells. mRNA fold change between *Chlamydia trachomatis* infected (pos) and non-infected (neg) porcine oviduct epithelial cells was calculated via NanoString at 6, 12, 24, 36, and 48 hours (h) post infection. Data was analyzed by NanoString n solver software by comparing gene counts between neg and pos samples. Gray cells indicates significance of $p < 0.05$ using a two-tailed t test.

Gene	6h pos	6h neg	Fold change	P value 6h	12h pos	12h neg	Fold change	P value 12h	24h pos	24h neg	Fold change	P value 24h	36h pos	36h neg	Fold change	P value 36h	48h pos	48h neg	Fold change	P value 48h
ADAMTS9	3.83	2.09	1.83	0.14	4.05	2.85	1.42	0.18	4.21	2.43	1.73	0.12	4.40	3.91	1.12	0.71	2.34	3.22	-1.37	0.42
CCL20	131.31	46.85	2.80	0.00	45.49	18.75	2.43	0.06	96.37	18.68	5.16	0.01	95.71	25.01	3.83	0.01	94.66	24.80	3.82	0.01
CCL4	25.07	4.56	5.49	0.00	12.90	4.20	3.07	0.02	11.03	3.79	2.91	0.04	11.03	5.92	1.86	0.01	5.95	2.35	2.53	0.05
CMPK2	2214.58	1848.02	1.20	0.27	2075.65	1409.90	1.47	0.09	2265.32	975.54	2.32	0.02	1824.59	705.20	2.59	0.00	1459.81	736.82	1.98	0.04
CSF3	16.57	10.38	1.60	0.11	13.86	7.17	1.93	0.01	14.65	8.94	1.64	0.14	18.13	13.26	1.37	0.28	18.50	14.67	1.26	0.06
CXCL10	989.90	624.11	1.59	0.21	656.52	170.26	3.86	0.05	1306.71	164.33	7.95	0.04	693.40	154.08	4.50	0.07	354.58	153.93	2.30	0.33
CXCL11	121.75	102.77	1.18	0.67	145.42	73.77	1.97	0.20	242.91	50.48	4.81	0.10	164.15	47.63	3.45	0.03	99.61	52.33	1.90	0.28
CXCL8	13008.71	10978.23	1.18	0.51	18026.86	18218.18	-1.01	0.97	14067.17	12594.78	1.12	0.68	11538.16	7695.53	1.50	0.16	7910.43	3974.95	1.99	0.01
CXCL9	20.08	23.18	-1.15	0.18	17.78	22.69	-1.28	0.15	25.90	23.33	1.11	0.52	22.39	26.96	-1.20	0.34	23.40	22.95	1.02	0.91
EBI3	5.97	6.44	-1.08	0.81	6.50	8.00	-1.23	0.40	9.44	6.92	1.36	0.09	8.97	8.03	1.12	0.58	7.04	6.15	1.14	0.65
Flt-3L	19.44	19.57	-1.01	0.96	16.95	14.88	1.14	0.22	17.11	16.52	1.04	0.86	20.13	17.66	1.14	0.54	19.03	14.89	1.28	0.17
HERC5	2086.67	1907.40	1.09	0.42	2350.44	1735.31	1.35	0.04	2424.81	1282.31	1.89	0.01	2129.95	1101.70	1.93	0.00	1765.67	1040.31	1.70	0.02
ICAM1	964.51	756.18	1.28	0.17	711.89	576.75	1.23	0.30	741.03	571.64	1.30	0.26	808.21	594.12	1.36	0.02	767.80	637.62	1.20	0.23
IL-1 alpha	575.69	421.99	1.36	0.01	534.35	442.03	1.21	0.21	551.51	446.34	1.24	0.22	550.82	466.80	1.18	0.20	573.02	398.16	1.44	0.01
IL-10	2.08	2.56	-1.23	0.63	1.99	1.92	1.03	0.91	1.17	1.65	-1.41	0.23	1.58	2.03	-1.29	0.55	1.22	1.69	-1.39	0.25
IL-15	77.25	72.68	1.06	0.75	126.43	83.09	1.52	0.11	219.30	136.80	1.60	0.01	187.75	135.45	1.39	0.09	193.21	174.77	1.11	0.63
IL-16	6.24	6.42	-1.03	0.94	7.12	5.85	1.22	0.38	8.61	8.76	-1.02	0.95	7.03	6.17	1.14	0.70	9.35	8.87	1.05	0.80
IL-1RA	22.02	21.60	1.02	0.89	23.40	16.90	1.39	0.07	28.56	19.23	1.49	0.02	31.60	30.69	1.03	0.89	46.92	36.43	1.29	0.31
IL-6	216.63	169.36	1.28	0.47	222.50	176.70	1.26	0.56	285.41	168.08	1.70	0.26	256.86	162.46	1.58	0.15	236.57	158.44	1.49	0.15
IL-7	36.49	31.23	1.17	0.32	32.48	26.86	1.21	0.31	50.96	27.49	1.85	0.02	49.34	26.74	1.84	0.08	40.87	29.74	1.37	0.15
MMP-2	368.09	347.19	1.06	0.75	278.45	309.55	-1.11	0.65	278.92	215.32	1.30	0.39	214.37	181.27	1.18	0.49	235.06	243.25	-1.03	0.89
MMP-9	26.88	21.85	1.23	0.67	17.38	15.88	1.09	0.83	10.86	12.01	-1.11	0.87	10.10	9.23	1.09	0.82	9.89	6.89	1.43	0.21
MX1	9379.78	8438.14	1.11	0.41	9657.67	6927.36	1.39	0.10	9238.90	4001.03	2.31	0.03	7679.56	3037.33	2.53	0.01	5610.78	2836.02	1.98	0.05
MX2	413.07	299.10	1.38	0.05	146.88	69.23	2.12	0.00	194.74	55.76	3.49	0.01	113.99	42.89	2.66	0.04	83.76	48.26	1.74	0.20
NEURL3	1.18	1.25	-1.06	0.78	1.06	1.26	-1.19	0.11	1.01	1.10	-1.08	0.25	1.05	1.43	-1.36	0.43	1.27	1.13	1.12	0.53
OAS2	2556.12	2308.47	1.11	0.73	2106.88	1615.02	1.30	0.44	1660.46	864.58	1.92	0.20	1706.04	712.33	2.40	0.05	1362.67	739.31	1.84	0.17
RANTES	95.47	59.58	1.60	0.09	99.99	34.66	2.88	0.05	224.87	41.48	5.42	0.02	192.52	25.94	7.42	0.00	118.92	29.17	4.08	0.00
SAA2	3.36	8.56	-2.55	0.02	7.37	6.84	1.08	0.77	4.84	5.81	-1.2	0.63	4.27	5.95	-1.39	0.20	4.64	4.57	1.02	0.96
TGF-b	1181.15	1123.74	1.05	0.86	791.91	856.27	-1.08	0.83	518.21	475.19	1.09	0.84	415.12	426.45	-1.03	0.93	447.65	512.29	-1.14	0.61
TNF-alpha	7.76	8.74	-1.13	0.53	7.82	9.04	-1.16	0.54	10.27	5.95	1.73	0.07	7.1	8.73	-1.23	0.69	5.62	7.95	-1.42	0.24
VEGF	2192.06	2037.22	1.08	0.51	1888.03	1788.25	1.06	0.69	2264.86	1874.13	1.21	0.21	2253.5	2244.13	1	0.98	2739.96	2848.92	-1.04	0.83

mRNA fold changes between *Chlamydia trachomatis* infected (pos) and non-infected (neg) highlighted in gray indicates significance of $p < 0.05$ using a two-tailed t test.

V. *CHLAMYDIA TRACHOMATIS* DECREASES EXPRESSION OF THE TIGHT JUNCTION PROTEIN CLAUDIN-4 IN PORCINE OVIDUCT EPITHELIAL CELLS

Amanda Amaral[1,2], Bryan Mcqueen[3], Kim Bellingham-Johnstun[4], Caroline Laplante[4] and Tobias Käser[1,2,*]

[1] Department of Population Health and Pathobiology, College of Veterinary Medicine, North Carolina State University, 1060 William Moore Drive, Raleigh, NC 27607, USA
[2] Comparative Medicine Institute, North Carolina State University, 1060 Willian Moore Drive, Raleigh, NC 27607, USA
[3] Department of Microbiology and Immunology, University of North Carolina, 125 Mason Farm Road, Chapel Hill, NC 27599, USA
[4] Department of Molecular Biomedical Sciences, College of Veterinary Medicine, North Carolina State University, 1060 William Moore Drive, Raleigh, NC 27607, USA

* Correspondence: tekaeser@ncsu.edu; +1-919-513-6352

Abstract: In the genital tract, epithelial cells create a permeability barrier essential to prevent pathogens inducing sexually transmitted diseases (STD) from entering the host. Claudins are integral structural components of tight junctions and play a key role in the permeability barrier of epithelial cells. *Chlamydia trachomatis (C. trachomatis)* is the most prevalent bacteria STD worldwide and, once it infects the Fallopian tube epithelial cells, can lead to infertility. Chlamydia infections are also associated with an increase in HIV shedding and transmission. However, it is not fully understood how chlamydia infection can cause an increase in HIV infection. Studies have shown that *C. trachomatis* can induce an alteration in the expression of tight junction proteins claudin 1-4 in epithelial cells and decrease cell barrier function. Here, we investigate the effect of *C. trachomatis* infection on the expression of the tight junction protein claudin-4 in the porcine oviduct epithelial cells, the counterpart of human Fallopian tube epithelial cells. Our results show that *C. trachomatis* infection reduces the localization of claudin-4 at the tight junction, which could in turn explain the increased susceptibility of *C. trachomatis* patients to HIV infection.

Keywords: *Chlamydia trachomatis*; claudin-4; tight junction; porcine oviduct epithelial cell

1. Introduction

Epithelial cells are an essential part of the innate immune system, acting as a physical permeability barrier between the inside and the outside of the body and protecting against pathogens [36,38]. These cells adhere to each other at their lateral membranes by intercellular junctions such as the tight junction [38], large protein complexes located at the apicolateral domains of the cells immediately basal to adherents junctions. Claudins are important membrane proteins found in the tight junctions of all epithelial cells [38]. Furthermore, claudins are an integral structural component of the tight junctions and play a key role in the permeability of epithelial cells [38]. In the genital tract, epithelial cells are essential to prevent pathogens inducing sexually transmitted diseases (STD) from entering the host [36].

Chlamydia trachomatis (C. trachomatis) is the most prevalent bacteria STD worldwide [1]. This bacteria can ascend to the upper genital tract and infect columnar epithelial cells of the Fallopian tube, leading to ectopic pregnancy and infertility [6]. Furthermore, chlamydia infection has been shown to alter tight junction formation and disturb epithelial integrity in other models [40,41]. For example, *Chlamydia muridarum* infection has shown to alter the composition of tight junction proteins such as claudins 1-4 in mouse oviduct epithelial cells, the counterpart of human Fallopian tube epithelial cells [40]. Additionally, it has been demonstrated that *C. trachomatis* can decrease claudin-4 RNA expression in human uterine epithelial cell line [41]. Most importantly, this decrease in tight junction protein expression was associated with a decrease in the barrier function of tight junction [41].

Moreover, studies have shown that chlamydia infections are associated with an increased HIV shedding in the female reproductive tract and may facilitate HIV transmission [42-45].

However, it is not fully understood how chlamydia infection can lead to this increase in HIV infection. Therefore, the main goal of the present study is to investigate if *C. trachomatis* infection can decrease the expression of the tight junction protein claudin-4 in the cell membrane. To accomplish our goal, porcine oviduct epithelial cells were infected with *C. trachomatis* and claudin-4 expression in the cells was evaluated. Our results show that *C. trachomatis* infection reduces the claudin-4 expression in the cell membrane. This reduced claudin-4 cell membrane expression could in turn explain the increased susceptibility of *C. trachomatis* patients to HIV infection.

2. Materials and Methods

2.1. Porcine oviduct epithelial cells isolation and culture

For porcine oviduct cells (pOECs) isolation, porcine oviducts were collected from six sows at a local slaughterhouse (City Packing/Neese's Sausage Co., Burlington, NC, USA) immediately after slaughter. Oviducts were washed with 1x phosphate buffered saline (PBS, Corning, NY, USA) containing 1X antibiotic-antimycotic (anti-anti, Corning), opened to expose the epithelial layer and cut in pieces of about 1 cm. Oviduct pieces were then added into a tube with 20 ml of cell isolation media composed of DMEM/F-12 media (Corning), 1x anti-anti, dispase (v/v 1:200,Corning), and pancreatin (v/w 1:83, MP Biomedicals, Irvine, California, USA). The tissue was incubated at 4°C overnight with continued shaking.

After incubation, the lumen of the oviduct pieces was gently scraped with a scalpel blade to isolate the epithelial cells. Scraped cells and isolation media was collected into a tube and the solution was neutralized with fetal bovine serum (FBS, v/v 1:2, VWR, Radnor, PA, USA). Cells were then centrifuged at 600g for 5 minutes at 4°C and pellet was resuspended with acutase (v/v

1:3, Corning). The cell solution was then incubated at 37°C for a total of 30 minutes, with agitation after 15 minutes. Cells were centrifuged at 600g for 5min at 4°C and pellet was resuspended in 20ml of pOECs media composed of DMEM/F-12 media, 1X anti-anti, 5% FBS, 0.0025% epidermal growth factor (EGF, Corning, REF: 354001), and 0.1% insulin, transferrin, selenium (ITS, Corning).

Cell suspension was then seeded in T-75 flasks (Sarstedt, Nümbrecht, Germany) at the density of 8 x 10^6 cells/flask and incubated at 37°C until about 70-80% confluency (about 48 hours). After incubation, cells were washed twice with 1x PBS and trypsinized with 0.25% trypsin (Corning) for about 15 minutes at 37°C. Trypsinization was stopped with pOECs media. Cells were transferred to a tube and centrifuged at 500g for 8 minutes at 4°C. Next, cell pellet was resuspended in freezing media composed of 50% DMEM/F-12 media, 40% FBS, and 10% dimethyl sulfoxide (DMSO, Corning), and stored at -80°C.

For pOECs culture, frozen pOECs were thawed, washed with DMEM/F-12 media, resuspended in pOECs media, and seeded in 24-well plates (Corning, REF 3337) in the presence or absence of poly-D-lysine coated coverslips at the density of 2 x 10^5 cells/well. Cells were then incubated at 37°C until about 70-80% confluency (about 24 hours).

2.2. *Chlamydia trachomatis*

The *Chlamydia trachomatis* serovar E strain Bour (ATCC VR-348B) was propagated in HeLa cells using standard technique [139] and purified as previously described [140]. Bacteria was titrated on HeLa cells as previously described [141].

2.3. *Chlamydia trachomatis* infection of porcine oviduct epithelial cells

After culture for about 24 hours, pOECs were infected with *C. trachomatis* (MOI 0.5) for 0, 6, 12, 24, 36, 48, and 72 hours post-infection. For each time point, non-infected pOECs were also cultured as controls.

2.4. NanoString

Claudin-4 RNA expression in pOECs during *C. trachomatis* infection was evaluated using NanoString (NanoString Technologies, Inc., USA). To do that, pOECs were washed with 500µl of 1x PBS/well and 500 µl of Trizol (TRIzol LS Reagent, Invitrogen, USA) was added into each well. Total RNA isolation using Trizol was done according to the supplier. RNA was eluted in 20 µl nuclease-free water and RNA quality and quantity were determined using a Nanodrop 1000 (Thermo Fisher).

Claudin-4 RNA expression was then measured via NanoString by calculating the RNA fold change between *C. trachomatis* infected and non-infected pOECs. RNA input was normalized based on Nanonodrop value to 100 ng and processed according to the nCounter MAX/FLEX System User Manual (NanoString Inc., MAN-C0035-07). Briefly, normalized RNA was hybridized with biotin-labeled capture probes and fluorescently labeled reporter probes for 19 hours at 65°C. Following hybridization, samples were transferred into a NanoString cartridge and loaded onto the nCounter Prep Station instrument set on high sensitivity. Next, cartridge was transferred into the nCounter Digital Analyzer instrument, where excess capture probe and reporter probe were removed, and hybridized mRNAs were immobilized for imaging (555 fields of view). Following image acquisition, mRNA counts were analyzed using nSolver analysis software v4.0 (NanoString Inc.).

2.5. Flow cytometry

Claudin-4 protein expression in pOECs during *C. trachomatis* infection was evaluated using flow cytometry. Cells were washed with 1x PBS, trypsinized and stained with Live/Dead Near infra-red. Next, cells were fixed and permeabilized with Fix/Perm kit (eBiosciences, USA), and then stained first with the primary antibodies anti-chlamydia antibody clone ACI (LSBio, USA) and anti-claudin-4 antibody (Abcam, Cambridge, USA), and then with the secondary antibodies anti-mouse IgG3-Alexa 488 antibody (Southern Biotech, USA) and anti-rabbit polyclonal-Alexa 555 (Southern Biotech, USA). Cells were recorded on a Cytoflex flow cytometer using the CytExpert software (Beckman Coulter, USA). Data analysis was performed with FlowJo version 10.5.3 (FLOWJO LLC). The gating hierarchy used for this analysis is shown in Supplementary Figure S1.

2.6. Fluorescence confocal microscopy

Cell membrane claudin-4 protein expression in pOECs during *C. trachomatis* infection was also evaluated using fluorescence confocal microscopy. Briefly, cells were washed with 1x PBS, fixed and permeabilized with methanol (Millipore-Sigma, USA), and stained with: 1) primary antibodies anti-chlamydia antibody clone ACI (LSBio) and anti-claudin-4 (Abcam); 2) secondary antibodies: anti-mouse IgG3-Alexa 488 (Southern Biotech) and anti-rabbit polyclonal-Alexa 555 (Southern Biotech); 3) 4',6-diamidino-2-phenylindole (DAPI) (Tocris, USA).

For the cell membrane claudin-4 staining evaluation during *C. trachomatis* infection, fluorescence images were acquired with a Nikon Eclipse Ti microscope equipped with a 100×/numerical aperture (NA) 1.49 HP Apo TIRF objective (Nikon), a CSU-X1 (Yokogawa) confocal spinning-disk system, 405/488/561/647 nm solid state lasers, and an electron-multiplying cooled charge-coupled device camera (EMCCD IXon 897, Andor Technology). The

Nikon Element software was used for acquisition. By using Fiji, image stacks were summed, and brightness/contrast was adjusted to a minimum of 9,493 and a maximum of 87,853.2. After claudin-4 staining images were taken, images were evaluated by four independent investigators by giving a score to the claudin-4 staining from 0 to 3, where 0 was absence and 3 was the strongest staining.

2.7. Statistical analysis

For the NanoString gene expression analysis, data was analyzed by NanoString n solver (nSolver 4.0 Analysis Software, Inc., Seattle, WA, USA), which make comparisons between infected and non-infected cells using two-tailed t test. For the rest of the data, statistical analyses were performed by GraphPad Prism (GraphPad 8.0 Software, Inc., La Jolla, CA, USA) using repeated-measures one-way ANOVA with hours post infection as the one factor, and post hoc multiple comparisons using Tukey's test. Differences were defined significant (*) for $p < 0.05$.

3. Results

The goal of this study was to evaluate if *C. trachomatis* infection can decrease the expression of the tight junction protein claudin-4 in the pOECs. To accomplish this goal, pOECs were infected with *C. trachomatis* (MOI 0.5) for 0, 6, 12, 24, 36, 48, and 72 hpi. The overall claudin-4 expression in pOECs were evaluated via NanoString (Figure 1) and flow cytometry (Figure 2), while the cell membrane claudin-4 expression was evaluated via confocal microscopy (Figure 3).

We first evaluated if chlamydia infection affects the overall claudin-4 expression in pOECs. Claudin-4 RNA expression was access via NanoString by calculating the RNA fold change between *C. trachomatis* infected and non-infected pOECs. As shown in Figure 1, there

was no significant change in claudin-4 RNA expression between infected and non-infected cells in any of the time points evaluated, with the RNA fold change ranging from 0.68 to 1.24. After evaluating the claudin-4 overall RNA expression, we also evaluated its overall protein expression. Median fluorescence intensity (MFI) of claudin 4 was measured via flow cytometry. There was no significant change in claudin-4 MFI between chlamydia infected and non-infected pOECs (Figure 2). In summary, these results show that *C. trachomatis* infection does not affect the overall claudin-4 expression in both RNA and protein levels.

Next, we evaluated if chlamydia infection can affect the cell membrane claudin-4 expression in pOECs (Figure 3). Cells were stained for claudin-4 and protein expression was evaluated via fluorescence confocal microscope. As *C. trachomatis* infection progressed, as indicated by the increase in chlamydia inclusion size (Figure 3A), the expression of claudin-4 changed over the time (Figure 3B). There was a stronger claudin-4 expression in the cell membrane at the beginning of the infection (0, 6, and 12 hpi), followed by a decrease in expression during the middle of infection (24 and 36 hpi). As observed in Figure 3B, this decrease in cell membrane claudin-4 expression was accompanied by a co-localization of the chlamydia inclusion and claudin-4 protein. Finally, at the end of the infection (48 and 72 hpi), it was observed an increase of the cell membrane claudin-4 expression (Figure 3A and 3B).

In order to quantify the observations on the cell membrane claudin-4 expression, claudin 4 staining images of infected and non-infected pOECs were visually evaluated by two independent investigators by giving a score to the claudin 4 staining from 0 to 3, where 0 is absence and 3 is the strongest staining. We first evaluated the difference between infected and non-infected cells for each time point (Figure 3C) and confirmed that there was a significant decrease in claudin-4 expression in infected cells at 24 and 36 hpi. We also observed that,

compared with non-infected cells, claudin-4 expression in infected cells increased at 48 hpi and decrease at 72 hpi. After confirming a significant difference in cell membrane claudin 4 expression between infected and no-infected cells, we next evaluated if claudin-4 expression in infected cells is significantly altered over time (Figure 3D). Initially, claudin-4 expression decreased from 6 to 12 hpi and then stayed the same until 36 hpi. At 48 hpi, the expression of claudin-4 went back to similar levels as observed at 6 hpi, and then was increased at 72 hpi (Figure 3C). These results show chlamydia infection can indeed affect the cell membrane claudin-4 expression in pOECs and that this effect changes over time.

All together, these results demonstrate that, although *C. trachomatis* infection does not affect the overall claudin-4 expression on pOECs, infection leads to cell membrane claudin-4 expression alterations during the chlamydia infection timeline investigated (0 to 72 hpi).

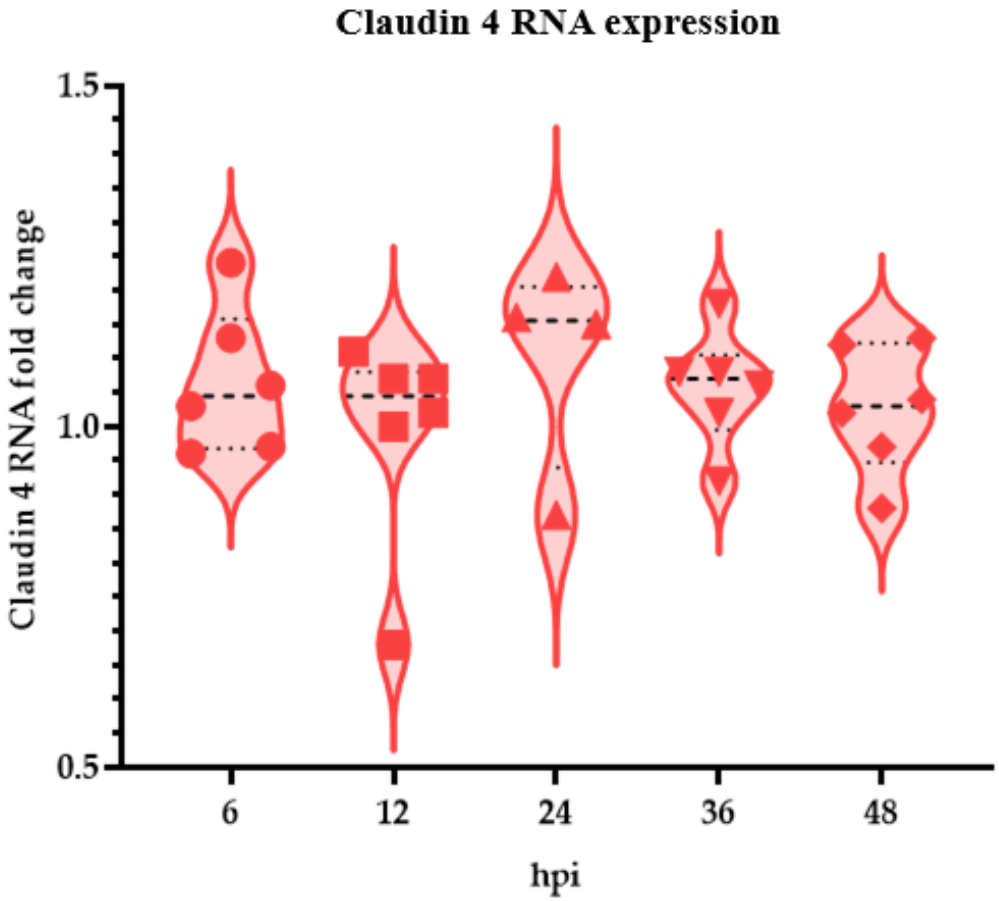

Figure 1. *Claudin 4* RNA fold change in porcine oviduct epithelial cells (pOECs). pOECs were infected with *Chlamydia trachomatis (Ct)* (MOI 0.5) for 0, 6, 12, 24, 46, 48, and 72 hours post infection (hpi). RNA was then isolated, and claudin 4 RNA expression was measured via NanoString by calculating the RNA fold change between *Ct* infected and non-infected pOECs. Values for individual pigs, medians, and 25/75 percentiles are shown. Data was analyzed by NanoString n solver software, which make comparisons between infected and non-infected cells using two-tailed t test.

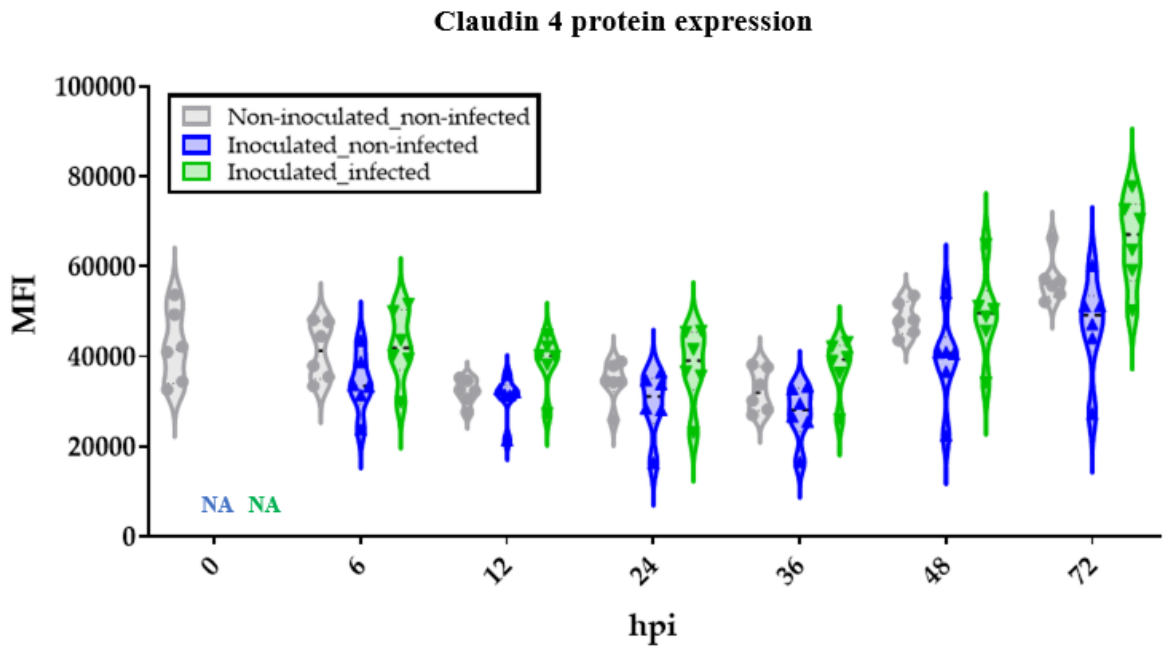

Figure 2. Median fluorescence intensity (MFI) of claudin-4 in porcine oviduct epithelial cells (pOECs). pOECs were inoculated with *Chlamydia trachomatis (Ct)* (MOI 0.5) or media (non-inoculated) for 0, 6, 12, 24, 46, 48, and 72 hours post infection (hpi). Cells were then trypsinized, fixed and permeabilized, and stained for *Ct* to determine if cells were infected and claudin-4 via indirect immunostaining for flow cytometry. Values for individual pigs, medians, and 25/75 percentiles are shown. Comparisons were made using two-way ANOVA test and Sidak's post-test. *$p < 0.05$.

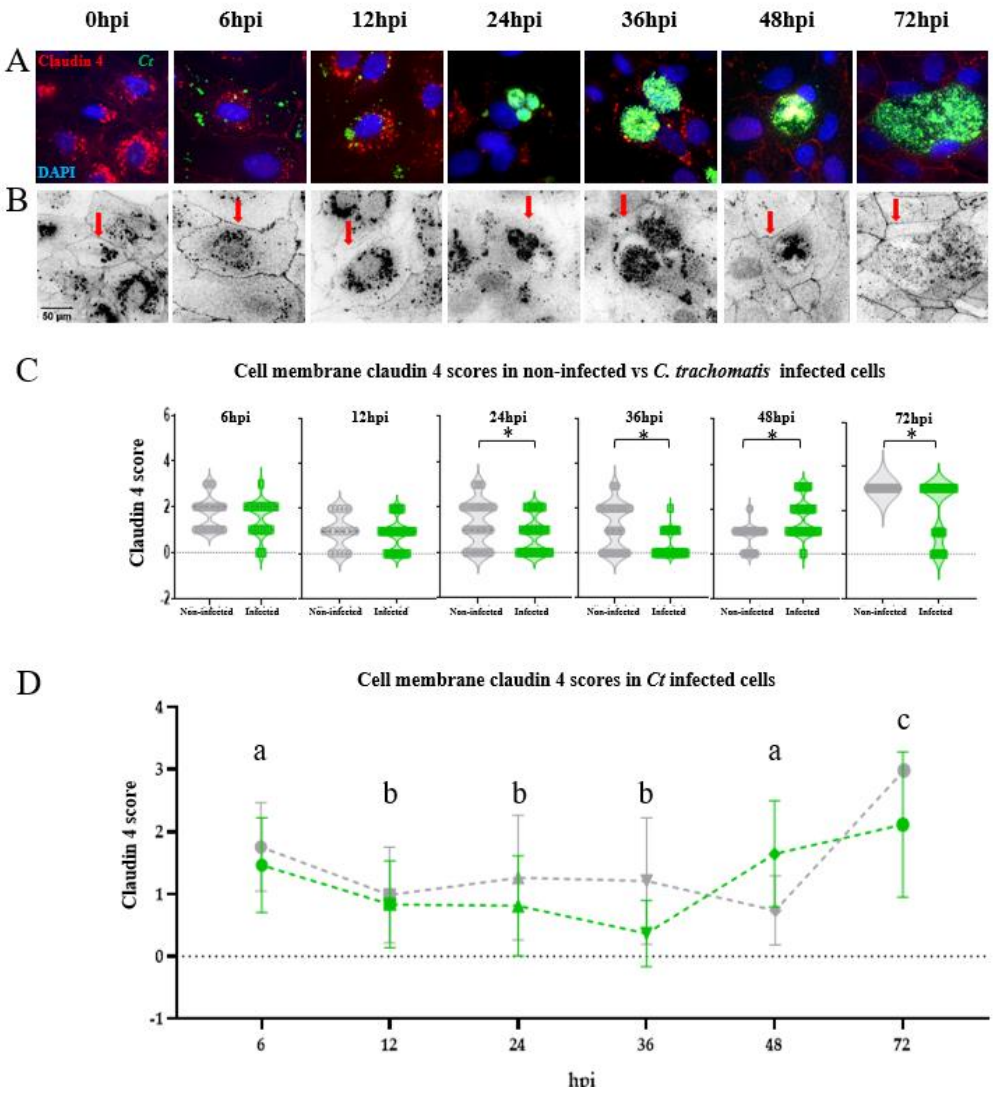

Figure 3. Cell membrane Claudin-4 staining evaluation during *Chlamydia trachomatis* (*Ct)* infection in porcine oviduct epithelial cells (pOECs). pOECs were infected with *Ct* (MOI 0.5) for 0, 6, 12, 24, 36, 48, and 72 hours post infection (hpi). A) Cells were then fixed and permeabilized with methanol and stained for: i) claudin-4 (red), ii) *Ct* using an FITC-conjugated anti-chlamydia LPS antibody (green), and iii) DNA using 4,6-diamidino-2-phenylindole (DAPI, blue). Claudin-4 expression was analyzed by fluorescence confocal microscopy. B) Same images from panel A with claudin-4 staining in black for a better claudin-4 staining visualization, as indicated with the red arrows. Next, claudin-4 staining images were visually evaluated by two independent investigators by giving a score to the claudin-4 staining from 0 to 3, where 0 is absence and 3 is the strongest staining. C) Claudin-4 staining in pOECs membrane in *Ct* infected and non-infected cells at 6, 36, and 72 hpi. Values for individual pigs, medians, and 25/75 percentiles are shown. Comparisons between *Ct* non-infected and infected cells were made using unpaired t test. *$p < 0.05$. D) Cell membrane claudin-4 staining in pOECs in *Ct* infected and non-infected cells at different hpi. Mean and standard deviation are shown. Comparisons between hpi withing infected cells were made using one-way ANOVA test and Tukey's post-test. *$p < 0.05$.

4. Discussion and conclusions

Claudins are an important structural component of the tight junctions and play a key role in the permeability of epithelial cells [38]. In the genital tract, epithelial cells are essential to prevent pathogens inducing STD from entering the host [36]. *C. trachomatis* is the most prevalent bacteria STD worldwide [1], and genital chlamydia infections have demonstrated to be associated with an increase in HIV shedding and transmission [42-45]. Nevertheless, it is not fully understood how chlamydia can aid with HIV infection. Since it is known that chlamydia infections can induce an alteration in expression of claudins (1-4) in epithelial cells and decrease cell barrier function, we hypothesized that *C. trachomatis* infection will lead to a decrease in claudin-4 expression in pOECs, the counterpart of human Fallopian tube epithelial cells.

In the present study, although there was no change in the overall claudin-4 RNA and protein expression in pOECs infected with *C. trachomatis* compared with non-infected cells (Figures 1 and 2), there was a decrease in the cell membrane claudin-4 protein expression between 24 and 36 hpi (Figure 3). Other studies have also shown the effect of chlamydia infection on important proteins of the tight junction. For example, Prozialeck et al. [39] showed that infection of primary human cervical epithelial cells with *C. trachomatis* for 24 hours caused a disruption in cell-cell contact, as indicated by a marked loss of cell membrane N-cadherin protein, a component of the adherens intercellular junctions in epithelial cells [37]. Additionally, it has been demonstrated that *C. trachomatis* can decrease claudin-4 RNA expression in human uterine epithelial cell line and that this decrease in tight junction protein expression is associated with a decrease in the barrier function of tight junction, as demonstrated by a decrease in transepithelial electrical resistance [41]. Collectively, these findings suggest that the decrease in the pOECs membrane claudin-4 expression caused by chlamydia infection observed in this study

could be associated with an impairment of the epithelial barrier function. This impairment in the epithelial barrier could result in an increase in the STD pathogens such as HIV from entering the host.

Additionally, the decrease in cell membrane claudin-4 expression in *C. trachomatis* infected cells at 12, 24, and 36 hpi (Figure 3D) was accompanied by an increase in in the claudin-4 expression on the same location as the chlamydia inclusions (Figure 3B). Hence, the reduction of cell membrane claudin-4 expression could be induced by the internalization of this protein to the *C. trachomatis* inclusion, which may facilitate host structural rearrangements required for inclusion enlargement.

In conclusion, our study shows that while *C. trachomatis* infection does not interfere with the overall claudin-4 RNA expression and protein production, the infection reduces the claudin-4 expression in the cell membrane. The reduction in claudin-4 cell membrane expression is likely induced by the internalization of this protein to the *C. trachomatis* inclusion. Furthermore, the *C. trachomatis*-induced reduction of the membrane expression of the tight junction molecule claudin-4 can represent a relevant pathway by which *C. trachomatis* decreases the genital tract epithelial barrier function. In turn, this could contribute to the increased susceptibility of *C. trachomatis* patients to HIV infection.

Supplementary figure:

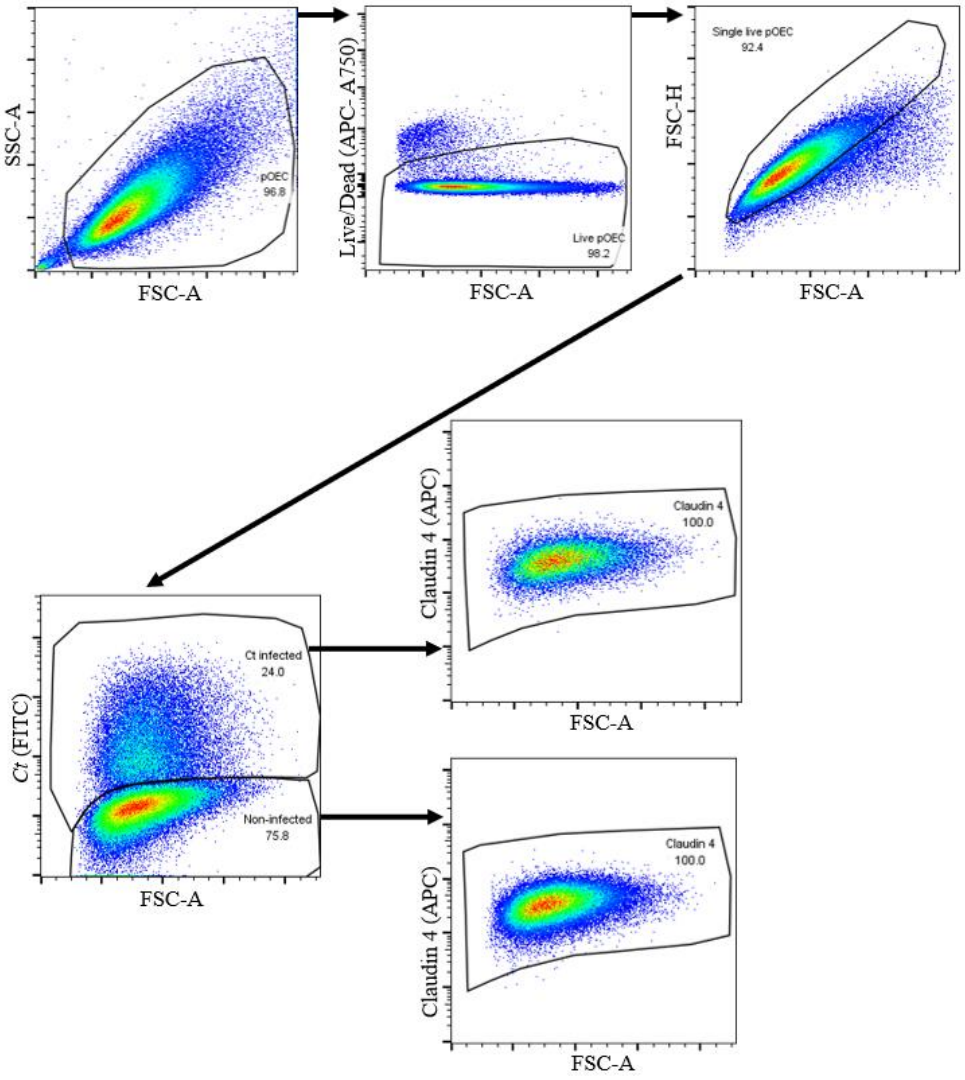

Supplementary Figure S1. Gating hierarchy for claudin 4 protein expression during *Chlamydia trachomatis* (*Ct*) infection via flow cytometry. Porcine oviduct epithelial cells (pOECs) were infected with *Ct* (MOI 0.5) for 0, 6, 12, 24, 36, 48, and 72 hours post infection. Cells were trypsinized, fixed and permeabilized, and stained for *Ct* via indirect immunostaining for flow cytometry. pOECs were identified by cell size (FSC-A) and granularity (SSC-A). Live cells were then identified by a gate on Live/Dead Near infra-red staining. Next, doublets were excluded by an FSC-A (area)/FSC-H (height) gate. *Ct* infected pOECs were identified via chlamydia marker (*Ct* - FITC) and claudin 4 expression via claudin 4 marker (Claudin 4 - APC). Gating is based on the relevant fluorescent minus one (FMO) controls.

VI. CONCLUSIONS AND FUTURE DIRECTIONS

Although the pig has been used as an animal model for chlamydia vaccine development, the pig is still under-utilized for some of their advantages such as: The high prevalence of chlamydia in outbred pig populations, making the pig a great animal to model phase III clinical trials for genital *C. trachomatis* vaccines; the vast access to porcine genital tract tissue, enabling the isolation of large amounts of pOECs – the counterparts of human Fallopian tube epithelial cells, the main target cell of *C. trachomatis*. Therefore, the overall purpose of this PhD project was to optimize the outbred *C. suis* pre-exposed pig model of human genital *C. trachomatis* infection and we did that by performing an *in vivo* vaccine trial with *C. suis* pre-exposed outbred pigs (section III), and *in vitro* studies with *C. trachomatis* and pOECs (section IV).

In section III, we have demonstrated that outbred pigs pre-exposed with *C. suis* can be used as an animal model for genital chlamydia vaccine development. We can follow the infection by determining vaginal chlamydia load via qPCR and analyze the humoral and cellular immune response via ELISA and flow cytometry, respectively. With the increasing interest of the swine industry on *C. suis* infections in pigs, we next want to evaluate our UV-inactivate *C. suis* vaccine in the control of reproductive problems in pigs. Furthermore, we also want to develop a *C. trachomatis* vaccine and test in our pig model.

In section IV, we investigated the *C. trachomatis* life cycle and the induced innate immune response in primary porcine oviduct epithelial cells (pOECs). We found that both the *C. trachomatis* life cycle and innate immune response in primary pOECs resemble their counterpart in the human Fallopian tube epithelial cells *C. trachomatis* infection, indicating that this *in vitro* cell model can be an excellent model to study the pathogenesis and innate immune response of genital *C. trachomatis* infections. Since IFN-γ is a key cytokine in the response against *C.*

trachomatis in humans, to further establish our porcine *in vitro* cell model, we next want to verify if porcine cells use the IDO/tryptophan pathway to limit the growth of chlamydia as observed in human cells.

The experiments from section V explored a potential mechanism of chlamydia pathogenesis: The *C. trachomatis* induction of downregulation of the tight junction protein claudin-4. Our overall hypothesis is that, by downregulating the expression of the tight junction protein claudin 4, *C. trachomatis* infection can affect epithelial cell barrier function, and increase the susceptibility to HIV infection. We have demonstrated that, although chlamydia infection does not induce a decrease in the overall claudin-4 mRNA or protein expression, it does induce a downregulation of membrane-bound claudin-4. We are currently investigating if this decrease in cell membrane claudin-4 corresponds with a decrease in tight junctions by using transmission electronic microscope. Our next step is to: i) investigate the molecular mechanisms leading to *C. trachomatis*-induced downregulation of membrane-bound CLDN-4; ii) determine if this downregulation of claudin 4 will result in an increase in cell permeability, and iii) investigate if this increase in cell permeability will, in turn, result in an increase in HIV trafficking throw the epithelial cells.

Collectively, the work of this dissertation has added new knowledge to improve the use of outbred *C. suis* pre-exposed pigs as models of human genital *C. trachomatis* infection. This knowledge will hopefully accelerate the development of an effective *C. trachomatis* vaccine, resulting in the improvement of health of many people worldwide, including in the USA and North Carolina.

VII. REFERENCES

1. Newman, L.; Rowley, J.; Vander Hoorn, S.; Wijesooriya, N.S.; Unemo, M.; Low, N.; Stevens, G.; Gottlieb, S.; Kiarie, J.; Temmerman, M. Global Estimates of the Prevalence and Incidence of Four Curable Sexually Transmitted Infections in 2012 Based on Systematic Review and Global Reporting. *PLoS One* **2015**, *10*, 1-17, doi:10.1371/journal.pone.0143304.
2. Prevention, C.f.D.C.a. Sexually Transmitted Disease Surveillance 2018. Services, U.S.D.o.H.a.H., Ed. Atlanta, 2019; 10.15620/cdc.79370.
3. Centers of Disease Control and Prevention. Chlamydia - CDC fact sheet (detailed). Availabe online: https://www.cdc.gov/std/chlamydia/stdfact-chlamydia-detailed.htm (accessed on
4. O'Connell, C.M.; Ferone, M.E. Chlamydia trachomatis Genital Infections. *Microb Cell* **2016**, *3*, 390-403, doi:10.15698/mic2016.09.525.
5. Vasilevsky, S.; Greub, G.; Nardelli-Haefliger, D.; Baud, D. Genital Chlamydia trachomatis: understanding the roles of innate and adaptive immunity in vaccine research. *Clin Microbiol Rev* **2014**, *27*, 346-370, doi:10.1128/CMR.00105-13.
6. Darville, T.; Hiltke, T.J. Pathogenesis of genital tract disease due to Chlamydia trachomatis. *J Infect Dis* **2010**, *201 Suppl 2*, S114-125, doi:10.1086/652397.
7. Phillips, S.; Quigley, B.L.; Timms, P. Seventy Years of Chlamydia Vaccine Research - Limitations of the Past and Directions for the Future. *Front Microbiol* **2019**, *10*, 70, doi:10.3389/fmicb.2019.00070.
8. Brunham, R.C.; Rappuoli, R. Chlamydia trachomatis control requires a vaccine. *Vaccine* **2013**, *31*, 1892-1897, doi:10.1016/j.vaccine.2013.01.024.
9. De Clercq, E.; Kalmar, I.; Vanrompay, D. Animal models for studying female genital tract infection with Chlamydia trachomatis. *Infect Immun* **2013**, *81*, 3060-3067, doi:10.1128/IAI.00357-13.
10. Carlin, J.M.; Weller, J.B. Potentiation of Interferon-Mediated Inhibition of Chlamydia Infection by Interleukin-1 in Human Macrophage Cultures. *Infection and Immunity* **1995**, *63*, 1870–1875.
11. Roshick, C.; Wood, H.; Caldwell, H.D.; McClarty, G. Comparison of gamma interferon-mediated antichlamydial defense mechanisms in human and mouse cells. *Infect Immun* **2006**, *74*, 225-238, doi:10.1128/IAI.74.1.225-238.2006.
12. Thomas, S.R.; Mohr, D.; Stocker, R. Nitric Oxide Inhibits Indoleamine 2,3Dioxygenase Activitiyn Interferon-y Primed Mononuclear Phagocyte. *The Journal of Biological Chemestry* **1994**, *269*, 14457-14464.
13. Longbottom, D.; Coulter, L.J. Animal Chlamydioses and Zoonotic Implications. *Journal of Comparative Pathology* **2003**, *128*, 217-244, doi:10.1053/jcpa.2002.0629.
14. Meurens, F.; Summerfield, A.; Nauwynck, H.; Saif, L.; Gerdts, V. The pig: a model for human infectious diseases. *Trends Microbiol* **2012**, *20*, 50-57, doi:10.1016/j.tim.2011.11.002.
15. Lossi, L.; D'Angelo, L.; De Girolamo, P.; Merighi, A. Anatomical features for an adequate choice of experimental animal model in biomedicine: II. Small laboratory rodents, rabbit, and pig. *Ann Anat* **2016**, *204*, 11-28, doi:10.1016/j.aanat.2015.10.002.

16. Lorenzen, E.; Follmann, F.; Jungersen, G.; Agerholm, J.S. A review of the human vs. porcine female genital tract and associated immune system in the perspective of using minipigs as a model of human genital Chlamydia infection. *Vet Res* **2015**, *46*, 1-13, doi:10.1186/s13567-015-0241-9.
17. MacArthur Clark, J. The 3Rs in research: a contemporary approach to replacement, reduction and refinement. *Br J Nutr* **2018**, *120*, S1-S7, doi:10.1017/S0007114517002227.
18. Brunham, R.C.; Rey-Ladino, J. Immunology of Chlamydia infection: implications for a Chlamydia trachomatis vaccine. *Nat Rev Immunol* **2005**, *5*, 149-161, doi:10.1038/nri1551.
19. Caldwell, H.D.; Kromhout, J.; Schachter, J. Purification and Partial Characterization of the Major Outer Membrane Protein of Chlamydia trachomatis. *Infection and Immunity* **1981**, *31*, 1161-1176.
20. Fadel, S.; Eley, A. Chlamydia trachomatis OmcB protein is a surface-exposed glycosaminoglycan-dependent adhesin. *J Med Microbiol* **2007**, *56*, 15-22, doi:10.1099/jmm.0.46801-0.
21. Swanson, K.A.; Taylor, L.D.; Frank, S.D.; Sturdevant, G.L.; Fischer, E.R.; Carlson, J.H.; Whitmire, W.M.; Caldwell, H.D. Chlamydia trachomatis polymorphic membrane protein D is an oligomeric autotransporter with a higher-order structure. *Infect Immun* **2009**, *77*, 508-516, doi:10.1128/IAI.01173-08.
22. Olsen, A.W.; Follmann, F.; Erneholm, K.; Rosenkrands, I.; Andersen, P. Protection Against Chlamydia trachomatis Infection and Upper Genital Tract Pathological Changes by Vaccine-Promoted Neutralizing Antibodies Directed to the VD4 of the Major Outer Membrane Protein. *J Infect Dis* **2015**, *212*, 978-989, doi:10.1093/infdis/jiv137.
23. Olsen, A.W.; Lorenzen, E.K.; Rosenkrands, I.; Follmann, F.; Andersen, P. Protective Effect of Vaccine Promoted Neutralizing Antibodies against the Intracellular Pathogen Chlamydia trachomatis. *Front Immunol* **2017**, *8*, 1652, doi:10.3389/fimmu.2017.01652.
24. Lyons, J.M.; Ito, J.I., Jr.; Pena, A.S.; Morre, S.A. Differences in growth characteristics and elementary body associated cytotoxicity between Chlamydia trachomatis oculogenital serovars D and H and Chlamydia muridarum. *J Clin Pathol* **2005**, *58*, 397-401, doi:10.1136/jcp.2004.021543.
25. Phillips, D.M.; Burillo, C.A. Ultrastructure of the murine cervix following infection with Chlamydia trachomatis. *Tissue & Cell* **1998**, *30*, 446-452.
26. Belland, R.J.; Zhong, G.; Crane, D.D.; Hogan, D.; Sturdevant, D.; Sharma, J.; Beatty, W.L.; Caldwell, H.D. Genomic transcriptional profiling of the developmental cycle of Chlamydia trachomatis. *Proceedings of the National Academy of Sciences of the United States of America* **2003**, *100*, 8478-8483.
27. Cortina, M.E.; Ende, R.J.; Bishop, R.C.; Bayne, C.; Derre, I. Chlamydia trachomatis and Chlamydia muridarum spectinomycin resistant vectors and a transcriptional fluorescent reporter to monitor conversion from replicative to infectious bacteria. *PLoS One* **2019**, *14*, e0217753, doi:10.1371/journal.pone.0217753.
28. Lee, J.K.; Enciso, G.A.; Boassa, D.; Chander, C.N.; Lou, T.H.; Pairawan, S.S.; Guo, M.C.; Wan, F.Y.M.; Ellisman, M.H.; Sutterlin, C., et al. Replication-dependent size reduction precedes differentiation in Chlamydia trachomatis. *Nat Commun* **2018**, *9*, 45, doi:10.1038/s41467-017-02432-0.

29. Mathews, S.A.; Volp, K.M.; Timms, P. Development of a quantitative gene expression assay for Chlamydia trachomatis identifed temporal expression of c factors. *FEBS Letters* **1999**, *458*, 354-358.
30. Shaw, E.I.; Dooley, C.A.; Fischer, E.R.; Scidmore, M.A.; Fields, K.A.; Hackstadt, T. Three temporal classes of gene expression during the Chlamydia trachomatis developmental cycle. *Molecular Microbiology* **2000**, *37*, 913-925.
31. Abdelrahman, Y.M.; Belland, R.J. The chlamydial developmental cycle. *FEMS Microbiol Rev* **2005**, *29*, 949-959, doi:10.1016/j.femsre.2005.03.002.
32. Bastidas, R.J.; Elwell, C.A.; Engel, J.N.; Valdivia, R.H. Chlamydial intracellular survival strategies. *Cold Spring Harb Perspect Med* **2013**, *3*, a010256, doi:10.1101/cshperspect.a010256.
33. Elwell, C.; Mirrashidi, K.; Engel, J. Chlamydia cell biology and pathogenesis. *Nat Rev Microbiol* **2016**, *14*, 385-400, doi:10.1038/nrmicro.2016.30.
34. Subbarayal, P.; Karunakaran, K.; Winkler, A.C.; Rother, M.; Gonzalez, E.; Meyer, T.F.; Rudel, T. EphrinA2 receptor (EphA2) is an invasion and intracellular signaling receptor for Chlamydia trachomatis. *PLoS Pathog* **2015**, *11*, e1004846, doi:10.1371/journal.ppat.1004846.
35. Hybiske, K.; Stephens, R.S. Mechanisms of host cell exit by the intracellular bacterium Chlamydia. *Proceedings of the National Academy of Sciences of the United States of America* **2007**, *104*, 11430-11435.
36. Amjadi, F.; Salehi, E.; Mehdizadeh, M.; Aflatoonian, R. Role of the innate immunity in female reproductive tract. *Adv Biomed Res* **2014**, *3*, 1, doi:10.4103/2277-9175.124626.
37. Dolat, L.; Valdivia, R.H. A renewed tool kit to explore Chlamydia pathogenesis: from molecular genetics to new infection models. *F1000Res* **2019**, *8*, doi:10.12688/f1000research.18832.1.
38. Gunzel, D.; Yu, A.S. Claudins and the modulation of tight junction permeability. *Physiol Rev* **2013**, *93*, 525-569, doi:10.1152/physrev.00019.2012.
39. Prozialeck, W.C.; Fay, M.J.; Lamar, P.C.; Pearson, C.A.; Sigar, I.; Ramsey, K.H. Chlamydia trachomatis disrupts N-cadherin-dependent cell-cell junctions and sequesters beta-catenin in human cervical epithelial cells. *Infect Immun* **2002**, *70*, 2605-2613, doi:10.1128/iai.70.5.2605-2613.2002.
40. Kumar, R.; Gong, H.; Liu, L.; Ramos-Solis, N.; Seye, C.I.; Derbigny, W.A. TLR3 deficiency exacerbates the loss of epithelial barrier function during genital tract Chlamydia muridarum infection. *PLoS One* **2019**, *14*, e0207422, doi:10.1371/journal.pone.0207422.
41. Mukura, L.R.; Hickey, D.K.; Rodriguez-Garcia, M.; Fahey, J.V.; Wira, C.R. Chlamydia trachomatis regulates innate immune barrier integrity and mediates cytokine and antimicrobial responses in human uterine ECC-1 epithelial cells. *Am J Reprod Immunol* **2017**, *78*, doi:10.1111/aji.12764.
42. Galvin, S.R.; Cohen, M.S. The role of sexually transmitted diseases in HIV transmission. *Nat Rev Microbiol* **2004**, *2*, 33-42, doi:10.1038/nrmicro794.
43. Ghys, P.D.; Fransen, K.; Diallo, M.O.; Ettiègne-Traoré, V.; Coulibaly, I.; Yeboué, K.M.; Kalish, M.L.; Maurice, C.; Whitaker, J.P.; Greenberg, A.E., et al. The associations between cervicovaginal HIV shedding, sexually transmitted diseases and immunosuppression in female sex workers in Abidjan, Côte d'Ivoire. *AIDS* **1997**, *11*, F85–F93.

44. Johnson, L.F.; Lewis, D.A. The effect of genital tract infections on HIV-1 shedding in the genital tract: a systematic review and meta-analysis. *Sex Transm Dis* **2008**, *35*, 946-959, doi:10.1097/OLQ.0b013e3181812d15.
45. Plummer, F.A.; Simonsen, J.N.; Cameron, D.W.; Ndinya-Achola, J.O.; Kreiss, J.K.; Gakinya, M.N.; Waiyaki, P.; Cheang, M.; Piot, P.; Ronald, A.R., et al. Cofactors in Male-Female Sexual Transmission of Human Immunodeficiency Virus Type 1. *The Journal of Infectious Diseases* **1991**, *163*, 233-239.
46. Torrone, E.; Papp, J.; Weinstock, H. Prevalence of Chlamydia trachomatis genital infection among persons aged 14–39 years — United States, 2007–2012. *MMWR Morbidity and Mortality Weekly Report* **2014**, *63*, 834-838.
47. Geisler, W.M. Duration of untreated, uncomplicated Chlamydia trachomatis genital infection and factors associated with chlamydia resolution: a review of human studies. *J Infect Dis* **2010**, *201 Suppl 2*, S104-113, doi:10.1086/652402.
48. Geisler, W.M.; Lensing, S.Y.; Press, C.G.; Hook, E.W., 3rd. Spontaneous resolution of genital Chlamydia trachomatis infection in women and protection from reinfection. *J Infect Dis* **2013**, *207*, 1850-1856, doi:10.1093/infdis/jit094.
49. Menon, S.; Timms, P.; Allan, J.A.; Alexander, K.; Rombauts, L.; Horner, P.; Keltz, M.; Hocking, J.; Huston, W.M. Human and Pathogen Factors Associated with Chlamydia trachomatis-Related Infertility in Women. *Clin Microbiol Rev* **2015**, *28*, 969-985, doi:10.1128/CMR.00035-15.
50. Szabo, K.A.; Ablin, R.J.; Singh, G. Matrix metalloproteinases and the immune response. *Clinical and Applied Immunology Reviews* **2004**, *4*, 295-319, doi:10.1016/j.cair.2004.02.001.
51. Stephens, R.S. The cellular paradigm of chlamydial pathogenesis. *TRENDS in Microbiology* **2003**, *11*, 44-51.
52. Poston, T.B.; Gottlieb, S.L.; Darville, T. Status of vaccine research and development of vaccines for Chlamydia trachomatis infection. *Vaccine* **2017**, 10.1016/j.vaccine.2017.01.023, doi:10.1016/j.vaccine.2017.01.023.
53. Ochiel, D.O.; Fahey, J.V.; Ghosh, M.; Haddad, S.N.; Wira, C.R. Innate Immunity in the Female Reproductive Tract: Role of Sex Hormones in Regulating Uterine Epithelial Cell Protection Against Pathogens. *Curr Womens Health Rev* **2008**, *4*, 102-117, doi:10.2174/157340408784246395.
54. Darville, T.; O'Neill, J.M.; Andrews, C.W., Jr.; Nagarajan, U.M.; Stahl, L.; Ojcius, D.M. Toll-like receptor-2, but not Toll-like receptor-4, is essential for development of oviduct pathology in chlamydial genital tract infection. *J Immunol* **2003**, *171*, 6187-6197, doi:10.4049/jimmunol.171.11.6187.
55. Heine, H.; Muller-Loennies, S.; Brade, L.; Lindner, B.; Brade, H. Endotoxic activity and chemical structure of lipopolysaccharides from Chlamydia trachomatis serotypes E and L2 and Chlamydophila psittaci 6BC. *Eur J Biochem* **2003**, *270*, 440-450, doi:10.1046/j.1432-1033.2003.03392.x.
56. Poston, T.B.; Lee, D.E.; Darville, T.; Zhong, W.; Dong, L.; O'Connell, C.M.; Wiesenfeld, H.C.; Hillier, S.L.; Sempowski, G.D.; Zheng, X. Cervical Cytokines Associated With Chlamydia trachomatis Susceptibility and Protection. *J Infect Dis* **2019**, *220*, 330-339, doi:10.1093/infdis/jiz087.
57. Rank, R.G.; Lacy, H.M.; Goodwin, A.; Sikes, J.; Whittimore, J.; Wyrick, P.B.; Nagarajan, U.M. Host chemokine and cytokine response in the endocervix within the first

developmental cycle of Chlamydia muridarum. *Infect Immun* **2010**, *78*, 536-544, doi:10.1128/IAI.00772-09.
58. Rasmussen, S.J.; Eckmann, L.; Quayle, A.J.; Shen, L.; Zhang, Y.; Anderson, D.J.; Fierer, J.; Stephens, R.S.; Kagnoff, M.F. Secretion of Proinflammatory Cytokines by Epithelial Cells in Response to Chlamydia Infection Suggests a Central Role for Epithelial Cells in Chlamydial Pathogenesis. *The Journal of Clinical Investigation* **1997**, *99*, 77–87.
59. Beatty, W.L.; Belanger, T.A.; Desai, A.A.; Morrison, R.P.; Byrne, G.I. Tryptophan depletion as a mechanism of gamma interferon-mediated chlamydial persistence. *Infection and Immunity* **1994**, *62*, 3705-3711.
60. Caldwell, H.D.; Wood, H.; Crane, D.; Bailey, R.; Jones, R.B.; Mabey, D.; Maclean, I.; Mohammed, Z.; Peeling, R.; Roshick, C., et al. Polymorphisms in Chlamydia trachomatis tryptophan synthase genes differentiate between genital and ocular isolates. *Journal of Clinical Investigation* **2003**, *111*, 1757-1769, doi:10.1172/jci17993.
61. Murphy, K.; Weaver, C. The Adaptative Immune Response. In *Janeway's Immunobiology*, Ninth ed.; Garland Science: New York, 2017; pp. 345-398.
62. Karunakaran, K.P.; Yu, H.; Jiang, X.; Chan, Q.W.T.; Foster, L.J.; Johnson, R.M.; Brunham, R.C. Discordance in the Epithelial Cell-Dendritic Cell Major Histocompatibility Complex Class II Immunoproteome: Implications for Chlamydia Vaccine Development. *J Infect Dis* **2020**, *221*, 841-850, doi:10.1093/infdis/jiz522.
63. Su, B.H.; Messer, R.; Whitmire, W.; Fischer, E.; Portis, J.C.; Caldwell, H.D. Vaccination against chlamydial genital tract infection after immunization with dendritic cells pulsed ex vivo with nonviable Chlamydiae. *The Journal of Experimental Medicine* **1998**, *188*, 809–818.
64. Wizel, B.; Nystrom-Asklin, J.; Cortes, C.; Tvinnereim, A. Role of CD8(+)T cells in the host response to Chlamydia. *Microbes Infect* **2008**, *10*, 1420-1430, doi:10.1016/j.micinf.2008.08.006.
65. Roan, N.R.; Starnbach, M.N. Antigen-specific CD8+ T cells respond to Chlamydia trachomatis in the genital mucosa. *J Immunol* **2006**, *177*, 7974-7979, doi:10.4049/jimmunol.177.11.7974.
66. Rank, R.G.; Soderberg, L.S.F.; Barron, A.L. Chronic chlamydial genital infection in congenitally athymic nude mice. *Infection and Immunity* **1885**, *48*, 847-849.
67. Igietseme, J.U.; Magee, D.M.; Williams, D.M.; Rank, R.G. Role for CD8+ T cells in antichlamydial immunity defined by chlamydia-specific T-lymphocyte clones. *Infection and Immunity* **1994**, *62*, 5195-5197.
68. Helble, J.D.; Mann, A.O.; Starnbach, M.N. Antigen-specific memory and naive CD4+ T cells following secondary Chlamydia trachomatis infection. *PLoS One* **2020**, *15*, e0240670, doi:10.1371/journal.pone.0240670.
69. Morrison, S.G.; Morrison, R.P. In situ analysis of the evolution of the primary immune response in murine Chlamydia trachomatis genital tract infection. *Infection and Immunity* **2000**, *68*, 2870–2879.
70. Morrison, R.P.; Feilzer, K.; Tumas, D.B. Gene knockout mice establish a primary protective role for major histocompatibility complex class II-restricted responses in Chlamydia trachomatis genital tract infection. *Infection and Immunity* **1995**, *63*, 4661–4668.
71. Käser, T.; Pasternak, J.A.; Delgado-Ortega, M.; Hamonic, G.; Lai, K.; Erickson, J.; Walker, S.; Dillon, J.R.; Gerdts, V.; Meurens, F. Chlamydia suis and Chlamydia

trachomatis induce multifunctional CD4 T cells in pigs. *Vaccine* **2017**, *35*, 91-100, doi:10.1016/j.vaccine.2016.11.050.
72. Johansson, M.; Schön, K.; Ward, M.; Lycke, N. Genital tract infection with Chlamydia trachomatis fails to induce protective immunity in gamma interferon receptor-deficient mice despite a strong local immunoglobulin A response. *Infection and Immunity* **1997**, *65*, 1032–1044.
73. Helble, J.D.; Gonzalez, R.J.; Von Andrian, U.H.; Starnbacha, M.N. Gamma Interferon Is Required for Chlamydia Clearance but Is Dispensable for T Cell Homing to the Genital Tract. *American Society for Microbiology* **2020**, *11*, 1-11.
74. Stary, G.; Olive, A.; Radovic-Moreno, A.F.; Gondek, D.; Alvarez, D.; Basto, P.A.; Perro, M.; Vrbanac, V.D.; Tager, A.M.; Shi, J., et al. A mucosal vaccine against Chlamydia trachomatis generates two waves of protective memory T cells. *Science* **2015**, *348*, 1-32, doi:10.1126/science.aaa8205.
75. Erneholm, K.; Lorenzen, E.; Boje, S.; Olsen, A.W.; Jungersen, G.; Jensen, H.E.; Cassidy, J.P.; Andersen, P.; Agerholm, J.S.; Follmann, F. Genital Infiltrations of CD4(+) and CD8(+) T Lymphocytes, IgA(+) and IgG(+) Plasma Cells and Intra-Mucosal Lymphoid Follicles Associate With Protection Against Genital Chlamydia trachomatis Infection in Minipigs Intramuscularly Immunized With UV-Inactivated Bacteria Adjuvanted With CAF01. *Front Microbiol* **2019**, *10*, 1-10, doi:10.3389/fmicb.2019.00197.
76. Lorenzen, E.; Follmann, F.; Boje, S.; Erneholm, K.; Olsen, A.W.; Agerholm, J.S.; Jungersen, G.; Andersen, P. Intramuscular Priming and Intranasal Boosting Induce Strong Genital Immunity Through Secretory IgA in Minipigs Infected with Chlamydia trachomatis. *Front Immunol* **2015**, *6*, 1-12, doi:10.3389/fimmu.2015.00628.
77. Akande, V.A.; Hunt, L.P.; Cahill, D.J.; Caul, E.O.; Ford, W.C.; Jenkins, J.M. Tubal damage in infertile women: prediction using chlamydia serology. *Hum Reprod* **2003**, *18*, 1841-1847, doi:10.1093/humrep/deg347.
78. Morrison, S.G.; Su, H.; Caldwell, H.D.; Morrison, R.P. Immunity to murine Chlamydia trachomatis genital tract reinfection involves B cells and CD4+ T Cells but Not CD8+ T Cells. *Infection and Immunity* **2000**, *68*, 6979–6987.
79. Morrison, S.G.; Morrison, R.P. A predominant role for antibody in acquired immunity to chlamydial genital tract reinfection. *Journal of Immunology* **2005**, *175*, 7536–7542.
80. Rank, R.G.; Batteiger, B.E. Protective Role of Serum Antibody in Immunity to Chlamydial Genital Infection. *American Society for Microbiology* **1989**, *57*, 299-301.
81. Brunham, R.C.; C., K.; Cles, L.; Holmes, K.K. Correlation of Host Immune Response with Quantitative Recovery of Chlamydia trachomatis from the Human Endocervix. *American Society for Microbiology* **1983**, *39*, 1491-1494.
82. Cotter, T.W.; Meng, Q.; Shen, Z.; Zhang, Y.; Su, H.; Caldwell, H.D. Protective Efficacy of Major Outer Membrane Protein-Specific Immunoglobulin A (IgA) and IgG Monoclonal Antibodies in a Murine Model of Chlamydia trachomatis Genital Tract Infection. *American Society for Microbiology* **1995**, *63*, 4704–4714.
83. Murphy, K.; Weaver, C. The Humoral Immune Response. In *Janeway's Immunobiology*, Ninth ed.; Garland Science: New York, 2017; pp. 400-421.
84. Moore, T.; Ekworomadu, C.O.; Eko, F.O.; MacMillan, L.; Ramey, K.; Ananaba, G.A.; Patrickson, J.W.; Nagappan, P.R.; Lyn, D.; Black, C.M., et al. Fc receptor–mediated antibody regulation of T cell immunity against intracellular pathogens. *The Journal of Infectious Diseases* **2003**, *188*, 617–624.

85. Peeling, R.; Maclean, I.W.; Brunham, R.C. In vitro neutralization of Chlamydia trachomatis with monoclonal antibody to an epitope on the major outer membrane protein. *Infection and Immunity* **1984**, *46*, 484-488.
86. Beagley, K.W.; Gockel, C.M. Regulation of innate and adaptive immunity by the female sex hormones oestradiol and progesterone. *FEMS Immunology & Medical Microbiology* **2003**, *38*, 13-22, doi:10.1016/s0928-8244(03)00202-5.
87. Berry, A.; Hall, J.V. The complexity of interactions between female sex hormones and Chlamydia trachomatis infections. *Curr Clin Microbiol Rep* **2019**, *6*, 67-75, doi:10.1007/s40588-019-00116-5.
88. Lorenzen, E.; Follmann, F.; Secher, J.O.; Goericke-Pesch, S.; Hansen, M.S.; Zakariassen, H.; Olsen, A.W.; Andersen, P.; Jungersen, G.; Agerholm, J.S. Intrauterine inoculation of minipigs with Chlamydia trachomatis during diestrus establishes a longer lasting infection compared to vaginal inoculation during estrus. *Microbes Infect* **2017**, *19*, 334-342, doi:10.1016/j.micinf.2017.01.008.
89. De Winter, P.J.J.; Verdonck, M.; De Kruif, A.; Devriese, L.A.; Haesebrouck, F. Endometritis and vaginal discharge in the sow. *Animal Reproduction Science* **1992**, *28*, 51-58.
90. Quispe Calla, N.E.; Vicetti Miguel, R.D.; Mei, A.; Fan, S.; Gilmore, J.R.; Cherpes, T.L. Dendritic cell function and pathogen-specific T cell immunity are inhibited in mice administered levonorgestrel prior to intranasal Chlamydia trachomatis infection. *Sci Rep* **2016**, *6*, 37723, doi:10.1038/srep37723.
91. Wolf, J.; Bruno, S.; Eichberg, M.; Jannat, R.; Rudo, S.; VanRheenen, S.; Coller, B.A. Applying lessons from the Ebola vaccine experience for SARS-CoV-2 and other epidemic pathogens. *NPJ Vaccines* **2020**, *5*, 51, doi:10.1038/s41541-020-0204-7.
92. Leroux-Roels, G.; Bonanni, P.; Tantawichien, T.; Zepp, F. Vaccine development. *Perspectives in Vaccinology* **2011**, *1*, 115-150, doi:10.1016/j.pervac.2011.05.005.
93. Gerdts, V.; Wilson, H.L.; Meurens, F.; van Drunen Littel-van den Hurk, S.; Wilson, D.; Walker, S.; Wheler, C.; Townsend, H.; Potter, A.A. Large animal models for vaccine development and testing. *ILAR J* **2015**, *56*, 53-62, doi:10.1093/ilar/ilv009.
94. Karunakaran, K.P.; Yu, H.; Jiang, X.; Chan, Q.; Moon, K.M.; Foster, L.J.; Brunham, R.C. Outer membrane proteins preferentially load MHC class II peptides: implications for a Chlamydia trachomatis T cell vaccine. *Vaccine* **2015**, *33*, 2159-2166, doi:10.1016/j.vaccine.2015.02.055.
95. Korsholm, K.S.; Petersen, R.V.; Agger, E.M.; Andersen, P. T-helper 1 and T-helper 2 adjuvants induce distinct differences in the magnitude, quality and kinetics of the early inflammatory response at the site of injection. *Immunology* **2010**, *129*, 75-86, doi:10.1111/j.1365-2567.2009.03164.x.
96. Boje, S.; Olsen, A.W.; Erneholm, K.; Agerholm, J.S.; Jungersen, G.; Andersen, P.; Follmann, F. A multi-subunit Chlamydia vaccine inducing neutralizing antibodies and strong IFN-gamma(+) CMI responses protects against a genital infection in minipigs. *Immunol Cell Biol* **2016**, *94*, 185-195, doi:10.1038/icb.2015.79.
97. Nguyen, N.; Olsen, A.W.; Lorenzen, E.; Andersen, P.; Hvid, M.; Follmann, F.; Dietrich, J. Parenteral vaccination protects against transcervical infection with Chlamydia trachomatis and generate tissue-resident T cells post-challenge. *NPJ Vaccines* **2020**, *5*, 7, doi:10.1038/s41541-020-0157-x.

98. Goldman, J.M.; Murr, A.S.; Cooper, R.L. The rodent estrous cycle: characterization of vaginal cytology and its utility in toxicological studies. *Birth Defects Res B Dev Reprod Toxicol* **2007**, *80*, 84-97, doi:10.1002/bdrb.20106.
99. Haley, P.J. Species differences in the structure and function of the immune system. *Toxicology* **2003**, *188*, 49-71, doi:10.1016/s0300-483x(03)00043-x.
100. Mestas, J.; Hughes, C.C. Of mice and not men: differences between mouse and human immunology. *J Immunol* **2004**, *172*, 2731-2738, doi:10.4049/jimmunol.172.5.2731.
101. Dawson, H.D.; Loveland, J.E.; Pascal, G.; Gilbert, J.G.R.; Uenishi, H.; Mann, K.M.; Sang, Y.; Zhang, J.; Carvalho-Silva, D.; Hunt, T., et al. Structural and functional annotation of the porcine immunome. *BMC Genomics* **2013**, *14*, 1-16.
102. McIntosh, E.D.G. Development of vaccines against the sexually transmitted infections gonorrhoea, syphilis, Chlamydia, herpes simplex virus, human immunodeficiency virus and Zika virus. *Ther Adv Vaccines Immunother* **2020**, *8*, 2515135520923887, doi:10.1177/2515135520923887.
103. Kari, L.; Whitmire, W.M.; Olivares-Zavaleta, N.; Goheen, M.M.; Taylor, L.D.; Carlson, J.H.; Sturdevant, G.L.; Lu, C.; Bakios, L.E.; Randall, L.B., et al. A live-attenuated chlamydial vaccine protects against trachoma in nonhuman primates. *J Exp Med* **2011**, *208*, 2217-2223, doi:10.1084/jem.20111266.
104. Abraham, S.; Juel, H.B.; Bang, P.; Cheeseman, H.M.; Dohn, R.B.; Cole, T.; Kristiansen, M.P.; Korsholm, K.S.; Lewis, D.; Olsen, A.W., et al. Safety and immunogenicity of the chlamydia vaccine candidate CTH522 adjuvanted with CAF01 liposomes or aluminium hydroxide: a first-in-human, randomised, double-blind, placebo-controlled, phase 1 trial. *The Lancet Infectious Diseases* **2019**, *19*, 1091-1100, doi:10.1016/s1473-3099(19)30279-8.
105. Käser, T.; Renois, F.; Wilson, H.L.; Cnudde, T.; Gerdts, V.; Dillon, J.R.; Jungersen, G.; Agerholm, J.S.; Meurens, F. Contribution of the swine model in the study of human sexually transmitted infections. *Infect Genet Evol* **2017**, *66*, 346-360, doi:10.1016/j.meegid.2017.11.022.
106. Buse, E.; Zöller, M.; Van Esch, E. The Macaque Ovary, with Special Reference to the Cynomolgus Macaque (Macaca fascicularis). *Toxicologic Pathology* **2008**, *36*, 24S-66S, doi:10.1177/0192623308327407.
107. Van Esch, E.; Cline, J.M.; Buse, E.; Wood, C.E.; de Rijk, E.P.C.T.; Weinbauer, G.F. Summary Comparison of Female Reproductive System in Human and the Cynomolgus Monkey (Macaca fascicularis). *Toxicologic Pathology* **2008**, *36*, 171S-172S, doi:10.1177/0192623308327415.
108. D'Hooghe, T.M.; Nyachieo, A.; Chai, D.C.; Kyama, C.M.; Spiessens, C.; Mwenda, J.M. Reproductive research in non-human primates at Institute of Primate Research in Nairobi, Kenya (WHO Collaborating Center): a platform for the development of clinical infertility services? *ESHRE Monographs* **2008**, *2008*, 102-107, doi:10.1093/humrep/den164.
109. Hafez, E.S.E.; Jaszczak, S. Comparative Anatomy and Histology of the Cervix Uteri in Non-Human Primates. *Primates* **1972**, *13*, 297-316
110. Wood, C.E. Morphologic and Immunohistochemical Features of the Cynomolgus Macaque Cervix. *Toxicologic Pathology* **2008**, *36*, 119S-129S, doi:10.1177/0192623308326094.
111. Messaoudi, I.; Estep, R.; Robinson, B.; Wong, S.W. Nonhuman Primate Models of Human Immunology. *Antioxidants and Redox signaling* **2011**, *14*, 261-273.

112. Burudi, E.M.; Marcondes, M.C.; Watry, D.D.; Zandonatti, M.; Taffe, M.A.; Fox, H.S. Regulation of indoleamine 2,3-dioxygenase expression in simian immunodeficiency virus-infected monkey brains. *J Virol* **2002**, *76*, 12233-12241, doi:10.1128/jvi.76.23.12233-12241.2002.
113. Drenzek, J.G.; Breburda, E.E.; Burleigh, D.W.; Bondarenko, G.I.; Grendell, R.L.; Golos, T.G. Expression of indoleamine 2,3-dioxygenase in the rhesus monkey and common marmoset. *Journal of Reproductive Immunology* **2008**, *78*, 125–133.
114. Bell, J.D.; Bergin, I.L.; Schmidt, K.; Zochowski, M.K.; Aronoff, D.M.; Patton, D.L. Nonhuman primate models used to study pelvic inflammatory disease caused by Chlamydia trachomatis. *Infect Dis Obstet Gynecol* **2011**, *2011*, 1-7, doi:10.1155/2011/675360.
115. Patton, D.L.; Cosgrove Sweeney, Y.T.; Paul, K.J. A summary of preclinical topical microbicide vaginal safety and chlamydial efficacy evaluations in a pigtailed macaque model. *Sex Transm Dis* **2008**, *35*, 889-897, doi:10.1097/OLQ.0b013e31817dfdb8.
116. Haggerty, C.L.; Gottlieb, S.L.; Taylor, B.D.; Low, N.; Xu, F.; Ness, R.B. Risk of sequelae after Chlamydia trachomatis genital infection in women. *J Infect Dis* **2010**, *201 Suppl 2*, S134-155, doi:10.1086/652395.
117. Kari, L.; Whitmire, W.M.; Crane, D.D.; Reveneau, N.; Carlson, J.H.; Goheen, M.M.; Peterson, E.M.; Pal, S.; de la Maza, L.M.; Caldwell, H.D. Chlamydia trachomatis native major outer membrane protein induces partial protection in nonhuman primates: implication for a trachoma transmission-blocking vaccine. *J Immunol* **2009**, *182*, 8063-8070, doi:10.4049/jimmunol.0804375.
118. Schautteet, K.; Vanrompay, D. Chlamydiaceae infections in pig. *Veterinary Research* **2011**, *42*, 1-10.
119. Rypula, K.; Kumala, A.; Ploneczka-Janeczko, K.; Lis, P.; Karuga-Kuzniewska, E.; Dudek, K.; Calkosinski, I.; Kuznik, P.; Chorbinski, P. Occurrence of reproductive disorders in pig herds with and without Chlamydia suis infection - statistical analysis of breeding parameters. *Anim Sci J* **2018**, *89*, 817-824, doi:10.1111/asj.13000.
120. Senger, P.L. The organization and function of the female reproductive system In *Pathways to Pregnancy and Parturition*, Third ed.; Senger, P.L., Ed. Current Conceptions Washington, 2012; pp. 10-43.
121. Vanrompay, D.; Hoang, T.Q.; De Vos, L.; Verminnen, K.; Harkinezhad, T.; Chiers, K.; Morre, S.A.; Cox, E. Specific-pathogen-free pigs as an animal model for studying Chlamydia trachomatis genital infection. *Infect Immun* **2005**, *73*, 8317-8321, doi:10.1128/IAI.73.12.8317-8321.2005.
122. Howard, C.; Friedman, D.L.; Leete, J.K.; Christensen, M.L. Correlation of the Percent of Positive Chlamydia trachomatis Direct Fluorescent Antibody Detection Tests with the Adequacy of Specimen Collection. *Diagnostic Microbiology and Infectious Disease* **1991**, *14*, 233-237.
123. Miessen, K.; Sharbatia, S.; Einspaniera, R.; Schoena, J. Modelling the porcine oviduct epithelium: A polarized in vitro system suitable for long-term cultivation. *Theriogenology* **2011**, *76*, 900–910, doi:10.1016/j.theriogenology.2011.04.021.
124. Takamatsu, H.H.; Denyer, M.S.; Stirling, C.; Cox, S.; Aggarwal, N.; Dash, P.; Wileman, T.E.; Barnett, P.V. Porcine gammadelta T cells: possible roles on the innate and adaptive immune responses following virus infection. *Vet Immunol Immunopathol* **2006**, *112*, 49-61, doi:10.1016/j.vetimm.2006.03.011.

125. Rahman, K.S.; Darville, T.; Russell, A.N.; O'Connell, C.M.; Wiesenfeld, H.C.; Hillier, S.L.; Chowdhury, E.U.; Juan, Y.C.; Kaltenboeck, B. Discovery of Human-Specific Immunodominant Chlamydia trachomatis B Cell Epitopes. *mSphere* **2018**, *3*, doi:10.1128/mSphere.00246-18.
126. Rahman, K.S.; Darville, T.; Wiesenfeld, H.C.; Hillier, S.L.; Kaltenboeck, B. Mixed Chlamydia trachomatis Peptide Antigens Provide a Specific and Sensitive Single-Well Colorimetric Enzyme-Linked Immunosorbent Assay for Detection of Human Anti-C. trachomatis Antibodies. *mSphere* **2018**, *3*, 1-20, doi:10.1128/mSphere.00484-18.
127. Wirthgen, E.; Tuchscherer, M.; Otten, W.; Domanska, G.; Wollenhaupt, K.; Tuchscherer, A.; Kanitz, E. Activation of indoleamine 2,3-dioxygenase by LPS in a porcine model. *Innate Immun* **2014**, *20*, 30-39, doi:10.1177/1753425913481252.
128. Schautteet, K.; Stuyven, E.; Cox, E.; Vanrompay, D. Validation of the Chlamydia trachomatis genital challenge pig model for testing recombinant protein vaccines. *J Med Microbiol* **2011**, *60*, 117-127, doi:10.1099/jmm.0.024448-0.
129. Schautteet, K.; Stuyven, E.; Beeckman, D.S.; Van Acker, S.; Carlon, M.; Chiers, K.; Cox, E.; Vanrompay, D. Protection of pigs against Chlamydia trachomatis challenge by administration of a MOMP-based DNA vaccine in the vaginal mucosa. *Vaccine* **2011**, *29*, 1399-1407, doi:10.1016/j.vaccine.2010.12.042.
130. Schautteet, K.; De Clercq, E.; Jonsson, Y.; Lagae, S.; Chiers, K.; Cox, E.; Vanrompay, D. Protection of pigs against genital Chlamydia trachomatis challenge by parenteral or mucosal DNA immunization. *Vaccine* **2012**, *30*, 2869-2881, doi:10.1016/j.vaccine.2012.02.044.
131. De Clercq, E.; Devriendt, B.; Yin, L.; Chiers, K.; Cox, E.; Vanrompay, D. The immune response against Chlamydia suis genital tract infection partially protects against re-infection. *Veterinary Research* **2014**, *45*, 1-12.
132. Erneholm, K.; Lorenzen, E.; Boje, S.; Olsen, A.W.; Andersen, P.; Cassidy, J.P.; Follmann, F.; Jensen, H.E.; Agerholm, J.S. Genital tract lesions in sexually mature Gottingen minipigs during the initial stages of experimental vaginal infection with Chlamydia trachomatis serovar D. *BMC Vet Res* **2016**, *12*, 200, doi:10.1186/s12917-016-0793-6.
133. Singh, K.; Mehta, S. The clinical development process for a novel preventive vaccine: An overview. *J Postgrad Med* **2016**, *62*, 4-11, doi:10.4103/0022-3859.173187.
134. Holmgren, J.; Svennerholm, A.M. Vaccines against mucosal infections. *Curr Opin Immunol* **2012**, *24*, 343-353, doi:10.1016/j.coi.2012.03.014.
135. Garg, R.; Babiuk, L.; van Drunen Littel-van den Hurk, S.; Gerdts, V. A novel combination adjuvant platform for human and animal vaccines. *Vaccine* **2017**, *35*, 4486-4489, doi:10.1016/j.vaccine.2017.05.067.
136. Lizarraga, D.; Carver, S.; Timms, P. Navigating to the most promising directions amid complex fields of vaccine development: a chlamydial case study. *Expert Rev Vaccines* **2019**, *18*, 1323-1337, doi:10.1080/14760584.2019.1698954.
137. Li, L.X.; McSorley, S.J. B cells enhance antigen-specific CD4 T cell priming and prevent bacteria dissemination following Chlamydia muridarum genital tract infection. *PLoS Pathog* **2013**, *9*, 1-10, doi:10.1371/journal.ppat.1003707.
138. De Puysseleyr, K.; De Puysseleyr, L.; H., D.; Geens, T.; Braeckman, L.; Morré, S.A.; Cox, E.; Vanrompay, D. Evaluation of the presence and zoonotic transmission of Chlamydia suis in a pig slaughterhouse. *BMC Infectious Diseases* **2014**, *14*, 1-6.

139. Scidmore, M.A. Cultivation and Laboratory Maintenance of Chlamydia trachomatis. *Current Protocols in Microbiology* **2005**.
140. Käser, T.; Cnudde, T.; Hamonic, G.; Rieder, M.; Pasternak, J.A.; Lai, K.; Tikoo, S.K.; Wilson, H.L.; Meurens, F. Porcine retinal cell line VIDO R1 and Chlamydia suis to modelize ocular chlamydiosis. *Vet Immunol Immunopathol* **2015**, *166*, 95-107, doi:10.1016/j.vetimm.2015.06.003.
141. Käser, T.; Pasternak, J.A.; Hamonic, G.; Rieder, M.; Lai, K.; Delgado-Ortega, M.; Gerdts, V.; Meurens, F. Flow cytometry as an improved method for the titration of Chlamydiaceae and other intracellular bacteria. *Cytometry A* **2016**, *89*, 451-460, doi:10.1002/cyto.a.22822.
142. Ramirez, A.; Karriker, L.A. Herd Evaluation. In *Diseases of Swine*, 10th ed.; J., Z.J., A., K.L., A., R., J., S.K., W., S.G., Eds. Wiley-Blackwell: Ames, Iowa, 2012; p. 10.
143. Andrews, S. FastQC: a quality control tool for high throughput sequence data. Availabe online: https://www.bioinformatics.babraham.ac.uk/projects/fastqc/ (accessed on 24 May 2020).
144. Aronesty, E. Comparison of Sequencing Utility Programs. *The Open Bioinformatics Journal* **2013**, *7*, 1-8.
145. Dobin, A.; Davis, C.A.; Schlesinger, F.; Drenkow, J.; Zaleski, C.; Jha, S.; Batut, P.; Chaisson, M.; Gingeras, T.R. STAR: ultrafast universal RNA-seq aligner. *Bioinformatics* **2013**, *29*, 15-21, doi:10.1093/bioinformatics/bts635.
146. Love, M.I.; Huber, W.; Anders, S. Moderated estimation of fold change and dispersion for RNA-seq data with DESeq2. *Genome Biol* **2014**, *15*, 550, doi:10.1186/s13059-014-0550-8.
147. Navarro, M.N.; Feijoo-Carnero, C.; Arandilla, A.G.; Trost, M.; Cantrell, D.A. Protein kinase D2 is a digital amplifier of T cell receptor-stimulated diacylglycerol signaling in naive CD8(+) T cells. *Sci Signal* **2014**, *7*, ra99, doi:10.1126/scisignal.2005477.
148. Spitaler, M.; Emslie, E.; Wood, C.D.; Cantrell, D. Diacylglycerol and protein kinase D localization during T lymphocyte activation. *Immunity* **2006**, *24*, 535-546, doi:10.1016/j.immuni.2006.02.013.
149. von Essen, M.R.; Kongsbak, M.; Schjerling, P.; Olgaard, K.; Odum, N.; Geisler, C. Vitamin D controls T cell antigen receptor signaling and activation of human T cells. *Nat Immunol* **2010**, *11*, 344-349, doi:10.1038/ni.1851.
150. Cao, S.; Carlesso, G.; Osipovich, A.B.; Llanes, J.; Lin, Q.; Hoek, K.L.; Khan, W.N.; Ruley, H.E. Subunit 1 of the prefoldin chaperone complex is required for lymphocyte development and function. *J Immunol* **2008**, *181*, 476-484, doi:10.4049/jimmunol.181.1.476.
151. Xie, P.; Kraus, Z.J.; Stunz, L.L.; Liu, Y.; Bishop, G.A. TNF receptor-associated factor 3 is required for T cell-mediated immunity and TCR/CD28 signaling. *J Immunol* **2011**, *186*, 143-155, doi:10.4049/jimmunol.1000290.
152. Douglas, R.S.; Gianoukakis, A.G.; Kamat, S.; Smith, T.J. Aberrant expression of the insulin-like growth factor-1 receptor by T cells from patients with Graves' disease may carry functional consequences for disease pathogenesis. *J Immunol* **2007**, *178*, 3281-3287, doi:10.4049/jimmunol.178.5.3281.
153. Lee, S.E.; Chung, W.J.; Kwak, H.B.; Chung, C.H.; Kwack, K.B.; Lee, Z.H.; Kim, H.H. Tumor necrosis factor-alpha supports the survival of osteoclasts through the activation of Akt and ERK. *J Biol Chem* **2001**, *276*, 49343-49349, doi:10.1074/jbc.M103642200.

154. Wang, R.; Zhang, L.; Zhang, X.; Moreno, J.; Celluzzi, C.; Tondravi, M.; Shi, Y. Regulation of activation-induced receptor activator of NF- k B ligand (RANKL) expression in T cells. *European Journal of Immunology* **2002**, *32*, 1090–1098.
155. Ellis, G.I.; Zhi, L.; Akundi, R.; Bueler, H.; Marti, F. Mitochondrial and cytosolic roles of PINK1 shape induced regulatory T-cell development and function. *Eur J Immunol* **2013**, *43*, 3355-3360, doi:10.1002/eji.201343571.
156. Cohen, C.J.; Crome, S.Q.; MacDonald, K.G.; Dai, E.L.; Mager, D.L.; Levings, M.K. Human Th1 and Th17 cells exhibit epigenetic stability at signature cytokine and transcription factor loci. *J Immunol* **2011**, *187*, 5615-5626, doi:10.4049/jimmunol.1101058.
157. Miao, T.; Symonds, A.L.J.; Singh, R.; Symonds, J.D.; Ogbe, A.; Omodho, B.; Zhu, B.; Li, S.; Wang, P. Egr2 and 3 control adaptive immune responses by temporally uncoupling expansion from T cell differentiation. *J Exp Med* **2017**, *214*, 1787-1808, doi:10.1084/jem.20160553.
158. Solt, L.A.; Kumar, N.; Nuhant, P.; Wang, Y.; Lauer, J.L.; Liu, J.; Istrate, M.A.; Kamenecka, T.M.; Roush, W.R.; Vidovic, D., et al. Suppression of TH17 differentiation and autoimmunity by a synthetic ROR ligand. *Nature* **2011**, *472*, 491-494, doi:10.1038/nature10075.
159. Wei, Z.; Li, P.; He, R.; Liu, H.; Liu, N.; Xia, Y.; Bi, G.; Du, Q.; Xia, M.; Pei, L., et al. DAPK1 (death associated protein kinase 1) mediates mTORC1 activation and antiviral activities in CD8(+) T cells. *Cell Mol Immunol* **2019**, 10.1038/s41423-019-0293-2, doi:10.1038/s41423-019-0293-2.
160. Ohland, C.L.; Jobin, C. Microbial activities and intestinal homeostasis: A delicate balance between health and disease. *Cell Mol Gastroenterol Hepatol* **2015**, *1*, 28-40, doi:10.1016/j.jcmgh.2014.11.004.
161. Erneholm, K.; Lorenzen, E.; Boje, S.; Olsen, A.W.; Jungersen, G.; Jensen, H.E.; Cassidy, J.P.; Andersen, P.; Agerholm, J.S.; Follmann, F. Genital Infiltrations of CD4(+) and CD8(+) T Lymphocytes, IgA(+) and IgG(+) Plasma Cells and Intra-Mucosal Lymphoid Follicles Associate With Protection Against Genital Chlamydia trachomatis Infection in Minipigs Intramuscularly Immunized With UV-Inactivated Bacteria Adjuvanted With CAF01. *Frontiers in microbiology* **2019**, *10*, 197, doi:10.3389/fmicb.2019.00197.
162. Barral, R.; Desai, R.; Zheng, X.; Frazer, L.C.; Sucato, G.S.; Haggerty, C.L.; O'Connell, C.M.; Zurenski, M.A.; Darville, T. Frequency of Chlamydia trachomatis-specific T cell interferon-gamma and interleukin-17 responses in CD4-enriched peripheral blood mononuclear cells of sexually active adolescent females. *J Reprod Immunol* **2014**, *103*, 29-37, doi:10.1016/j.jri.2014.01.002.
163. Yu, H.; Karunakaran, K.P.; Kelly, I.; Shen, C.; Jiang, X.; Foster, L.J.; Brunham, R.C. Immunization with live and dead Chlamydia muridarum induces different levels of protective immunity in a murine genital tract model: correlation with MHC class II peptide presentation and multifunctional Th1 cells. *J Immunol* **2011**, *186*, 3615-3621, doi:10.4049/jimmunol.1002952.
164. Rey-Ladino, J.; Ross, A.G.; Cripps, A.W. Immunity, immunopathology, and human vaccine development against sexually transmitted Chlamydia trachomatis. *Hum Vaccin Immunother* **2014**, *10*, 2664-2673, doi:10.4161/hv.29683.

165. Olive, A.J.; Gondek, D.C.; Starnbach, M.N. CXCR3 and CCR5 are both required for T cell-mediated protection against C. trachomatis infection in the murine genital mucosa. *Mucosal Immunol* **2011**, *4*, 208-216, doi:10.1038/mi.2010.58.
166. Roan, N.R.; Gierahn, T.M.; Higgins, D.E.; Starnbach, M.N. Monitoring the T cell response to genital tract infection. *PNAS* **2006**, *103*, 12069–12074.
167. Witkin, S.S.; Minis, E.; Athanasiou, A.; Leizer, J.; Linhares, I.M. Chlamydia trachomatis: the Persistent Pathogen. *Clin Vaccine Immunol* **2017**, *24*, doi:10.1128/CVI.00203-17.
168. McQueen, B.E.; Kiatthanapaiboon, A.; Fulcher, M.L.; Lam, M.; Patton, K.; Powell, E.; Kollipara, A.; Madden, V.; Suchland, R.J.; Wyrick, P., et al. Human Fallopian Tube Epithelial Cell Culture Model To Study Host Responses to Chlamydia trachomatis Infection. *Infection and Immunity* **2020**, *88*, 1-16.
169. Amaral, A.F.; Rahman, K.S.; Kick, A.R.; Cortes, L.M.; Robertson, J.; Kaltenboeck, B.; Gerdts, V.; O'Connell, C.M.; Poston, T.B.; Zheng, X., et al. Mucosal Vaccination with UV-Inactivated Chlamydia suis in Pre-Exposed Outbred Pigs Decreases Pathogen Load and Induces CD4 T-Cell Maturation into IFN-gamma(+) Effector Memory Cells. *Vaccines (Basel)* **2020**, *8*, doi:10.3390/vaccines8030353.
170. Guseva, N.V.; Knight, S.T.; Whittimore, J.D.; Wyrick, P.B. Primary cultures of female swine genital epithelial cells in vitro: a new approach for the study of hormonal modulation of Chlamydia infection. *Infect Immun* **2003**, *71*, 4700-4710, doi:10.1128/iai.71.8.4700-4710.2003.
171. Johnson, R.M.; Kerr, M.S. Modeling the transcriptome of genital tract epithelial cells and macrophages in healthy mucosa versus mucosa inflamed by Chlamydia muridarum infection. *Pathog Dis* **2015**, *73*, ftv100, doi:10.1093/femspd/ftv100.
172. Verhelst, J.; Hulpiau, P.; Saelens, X. Mx proteins: antiviral gatekeepers that restrain the uninvited. *Microbiol Mol Biol Rev* **2013**, *77*, 551-566, doi:10.1128/MMBR.00024-13.
173. Natividad, A.; Freeman, T.C.; Jeffries, D.; Burton, M.J.; Mabey, D.C.; Bailey, R.L.; Holland, M.J. Human conjunctival transcriptome analysis reveals the prominence of innate defense in Chlamydia trachomatis infection. *Infect Immun* **2010**, *78*, 4895-4911, doi:10.1128/IAI.00844-10.
174. Kumar, R.; Derbigny, W.A. TLR3 Deficiency Leads to a Dysregulation in the Global Gene-Expression Profile in Murine Oviduct Epithelial Cells Infected with Chlamydia muridarum. *Int J Microbiol Curr Res* **2018**, *1*, 1-13, doi:10.18689/ijmr-1000101.
175. Xu, Y.; Johansson, M.; Karlsson, A. Human UMP-CMP kinase 2, a novel nucleoside monophosphate kinase localized in mitochondria. *J Biol Chem* **2008**, *283*, 1563-1571, doi:10.1074/jbc.M707997200.
176. Zhong, Z.; Liang, S.; Sanchez-Lopez, E.; He, F.; Shalapour, S.; Lin, X.J.; Wong, J.; Ding, S.; Seki, E.; Schnabl, B., et al. New mitochondrial DNA synthesis enables NLRP3 inflammasome activation. *Nature* **2018**, *560*, 198-203, doi:10.1038/s41586-018-0372-z.
177. Groom, J.R.; Luster, A.D. CXCR3 ligands: redundant, collaborative and antagonistic functions. *Immunol Cell Biol* **2011**, *89*, 207-215, doi:10.1038/icb.2010.158.
178. Lee, A.Y.; Eri, R.; Lyons, A.B.; Grimm, M.C.; Korner, H. CC Chemokine Ligand 20 and Its Cognate Receptor CCR6 in Mucosal T Cell Immunology and Inflammatory Bowel Disease: Odd Couple or Axis of Evil? *Front Immunol* **2013**, *4*, 194, doi:10.3389/fimmu.2013.00194.

179. Sakthivel, S.K.; Singh, U.P.; Singh, S.; Taub, D.D.; Igietseme, J.U.; Lillard, J.W., Jr. CCL5 regulation of mucosal chlamydial immunity and infection. *BMC Microbiol* **2008**, *8*, 136, doi:10.1186/1471-2180-8-136.
180. Bakshi, R.K.; Gupta, K.; Jordan, S.J.; Chi, X.; Lensing, S.Y.; Press, C.G.; Geisler, W.M. An Adaptive Chlamydia trachomatis-Specific IFN-gamma-Producing CD4(+) T Cell Response Is Associated With Protection Against Chlamydia Reinfection in Women. *Front Immunol* **2018**, *9*, 1981, doi:10.3389/fimmu.2018.01981.
181. Gondek, D.C.; Olive, A.J.; Stary, G.; Starnbach, M.N. CD4+ T cells are necessary and sufficient to confer protection against Chlamydia trachomatis infection in the murine upper genital tract. *J Immunol* **2012**, *189*, 2441-2449, doi:10.4049/jimmunol.1103032.